

ON THE APPLICATION OF THE FINITE  
ELEMENT METHOD TO THREE-DIMENSIONAL  
INCOMPRESSIBLE ~~POTENTIAL~~ FLOW.

by

Sedky A. El-Shammaa, B.Sc. (Mech.Eng.)

A Thesis

Submitted to the School of Graduate Studies  
in Partial Fulfilment of the Requirements  
for the Degree  
Master of Engineering.

McMaster University,

August 1975



ON THE APPLICATION OF THE FINITE  
ELEMENT METHOD TO THREE-DIMENSIONAL  
INCOMPRESSIBLE POTENTIAL FLOW.

MASTER OF ENGINEERING  
(Mechanical Engineering)

McMaster University, Hamilton,  
Ontario.

TITLE: On the Application of The Finite Element Method to Three-  
Dimensional Incompressible Potential Flow.

AUTHOR: Sedky A. El-Shammaa, B.Sc. (Mech. Eng.)  
(Cairo University, Cairo, Egypt).

SUPERVISOR: Dr. J.H.T. Wade.

NUMBER OF PAGES: x - 107

SCOPE AND CONTENTS:

This thesis describes the application of the finite element method to three-dimensional potential flow. The flow is assumed to be steady and incompressible. The flow region is simply connected and has complicated geometric boundaries. The boundary condition is of the Neumann type, or mixed Dirichlet-Neumann type. The finite element method presented provides an economical solution for the problem which could be difficult to solve using other methods.

A versatile computer program was developed and used for solving three specific problems of flow around bends. One of the three problems had a known two-dimensional exact solution. The results obtained for this problem are in good agreement with its exact solution. The computer program can be utilized to solve similar problems, subject to the same governing equations and boundary conditions, in related fields such as electrostatics and heat conduction.

## ACKNOWLEDGEMENTS

The author wishes to express his appreciation to Dr. J.H.T. Wade for suggesting the problem for study. The author also wishes to express his sincere gratitude to Dr. J.H.T. Wade and Dr. M.A. Dokainish for their constant guidance and encouragement during this study. The valuable discussions the author had with them throughout the period of this research made it a rewarding learning experience.

The author is grateful to Westinghouse Canada Ltd. for providing a specific  $90^{\circ}$  turbine inlet configuration for the study.

The programming advice of Dr. W. El-Maraghy and the assistance offered by Mr. E. Allam in the preparation of the drawings are gratefully acknowledged.

Thanks are due to Mrs. Peggy Johnstone for typing the manuscript.

The financial support provided by the National Research Council through Grant A.1585 is also acknowledged.

## TABLE OF CONTENTS

	<u>Page</u>
LIST OF ILLUSTRATIONS	
NOMENCLATURE	
CHAPTER 1. INTRODUCTION	1
1.1 Scope of the Study	1
1.2 Literature Survey	2
CHAPTER 2. STATEMENT OF THE PROBLEM	6
2.1 Introduction	6
2.2 Definitions	6
2.3 Approximate Solution of Field Problems	7
2.4 The Finite Element Method	8
2.5 Mathematical Statement of the Problem	9
2.5.1 The Potential Field	9
2.5.2 Boundary Conditions	10
2.5.3 Uniqueness Theorems	11
2.6 The Variational Analogue of the Laplace Equation	12
CHAPTER 3. THE FINITE ELEMENT SOLUTION	13
3.1 The Development of the Finite Element	13
3.2 Equations of the Discretized Region	18
3.3 The Property Matrix of the Tetrahedral Element	22
3.4 The Boundary Conditions (Constraint Vector)	27
3.4.1 The Neumann Boundary Condition	28
3.4.2 The Dirichlet Boundary Condition	33
3.5 Discretization and Assemblage Procedure	33

Table of Contents  
(Cont)

	<u>Page</u>	
3.5.1	Five Tetrahedra Composite Unit	35
3.5.2	Six Tetrahedra Composite Unit	35
3.5.3	Discretization of the Region, Node Identifiers and Node Numbers	38
3.5.4	Assembly of the Finite Element Equations	40
3.5.5	Solution of the System of Equations	41
3.6	The Velocity Field	45
CHAPTER 4.	APPLICATIONS AND RESULTS	48
4.1	Dimensionless Representation of Results	48
4.2	Application 1. Flow around 90° Corner	49
4.3	Application 2. Reducing Bend of Square Cross-Section Base Centred on a Circular Arc.	66
4.4	Application 3. Reducing Bend with a Rectangular Inlet and an Annular Outlet	82
4.5	Concluding Remarks	95
BIBLIOGRAPHY		98
APPENDIX I.	FORMULATION OF A BOUNDARY VALUE PROBLEM IN TERMS OF THE CALCULUS OF VARIATIONS.	100
APPENDIX II.	FLOW CHART OF THE COMPUTER PROGRAM OF THE FINITE ELEMENT SOLUTION	107

## LIST OF ILLUSTRATIONS

<u>Figure</u>	<u>Title</u>	<u>Page</u>
1.	Tetrahedral Element	13
2.	Element with an external face (i,j,m) where q is specified	30
3.	Five-Tetrahedra Composite Unit	36
4.	Six-Tetrahedra Composite Unit	37
5.	Discretization Mesh	39
6.	Layout of Equation Storage in Solution Subroutine	45
7.	Flow around 90° Corner	50
8.	Isometric Configuration	51
9.	Location of Nodal Points on a Horizontal Plane	53
10-15.	Potential Distribution on Horizontal Planes (Five Tetrahedral Scheme)	54 - 59
16-21.	Potential Distribution on Horizontal Planes (Six Tetrahedral Scheme)	60 - 65
22.	Reducing Bend Projections	67
23.	Top View of Discretized Region	68
24-36,	Equi-potential Contour Maps on Sections (I-XIII)	69 - 81
37.	Isometric Configuration (Front-View)	83
38.	Isometric Configuration (Back-View)	84
39.	Reducing Bend Projections	85
40.	Potential Values On Inlet Surface	86
41.	Potential Values On Exit Plane	87
42-54.	Potential Values On Sections (I-XIII)	88 - 94

## NOMENCLATURE

<u>Symbol</u>	<u>Description</u>
$a$	Function of $x, y, z$ (When $a$ is equal to zero, the Cauchy condition reduces to Neumann condition).
$a_i, a_j, a_m, a_n$	Elements in the inverse of the coordinate matrix $[A^e]$
(A)	Row vector $(a_i \ a_j \ a_m \ a_n)$
$b_i, b_j, b_m, b_n$	Elements in the inverse of the coordinate matrix $[A^e]$
(B)	Row vector $(b_i \ b_j \ b_m \ b_n)$
(c)	Coordinate vector $(1 \ x \ y \ z)$
$c_i, c_j, c_m, c_n$	Elements in the inverse of the coordinate matrix $[A^e]$
(C)	Row vector $(c_i \ c_j \ c_m \ c_n)$
$d_i, d_j, d_m, d_n$	Elements in the inverse of the coordinate matrix $[A^e]$
(D)	Row vector $(d_i \ d_j \ d_m \ d_n)$
D	Domain
e	Indicates a tetrahedral element (used as superscript in the analysis).
f	Element in the constraint vector
{F}	Constraint vector
g	Specified value of $\phi$ (or $v$ ) on the boundary
G	Function of $x, y, z$
h	Arbitrary function from the class of admissible functions
[K]	Property Matrix
$\ell$	Total number of tetrahedral elements in the region
$\ell_1$	Number of elements with specified Dirichlet condition
$\ell_2$	Number of elements with specified Neumann condition
$L'$	Characteristic length



Nomenclature  
(cont)

$\hat{n}$	Unit vector normal to the surface
$n_x, n_y, n_z$	Components of $\hat{n}$ in the x, y, and z directions
$\bar{n}$	Total number of nodal points in the region
$\bar{n}_1$	Number of nodal points where the Dirichlet condition is specified
$\bar{n}_2$	Number of nodal points where the Neumann condition is specified
q	Function of x, y and z, that becomes the normal velocity component at the boundaries when $a = 0$
S	Boundary surface
[Sk]	Property matrix of composite unit [8 x 8]
T'	Unit time
v	Function of x, y, and z that becomes the required solution $\phi$
$\bar{v}_p$	Approximate value of v at the nodal point p
V	Volume
x	Cartesian coordinate
$x_j$	A set of independent variables
X	Function of x, y and z
$X_D$	Dirichlet integral
$X_N$	Surface integral on the boundary where Neumann condition is specified
$X(v), X(\phi)$	Functional satisfying extremal condition
y	Cartesian coordinate
Y	Function of x, y and z
z	Cartesian coordinate
Z	Function of x, y and z.

Nomenclature  
(Cont)

$\alpha_k$	$k = 1, 2, 3, 4$ constants determined in terms of $\phi$ at the nodal points of the tetrahedral element
$\{\alpha\}$	Coefficient vector
$\epsilon$	Arbitrary constant
$\phi$	Potential function
$\bar{\phi}_p$	Approximate value of $\phi$ at the nodal point $p$ .
$\{\bar{\phi}\}$	Vector containing the values of $\phi$ at the nodal points.
$\psi$	Stream function

Subscripts

$av$	Average value
$C$	Refers to surface where Cauchy condition applies
$D$	Refers to surface where Dirichlet condition applies
$h$	Refers to points on the boundary where the Dirichlet condition is specified.
$i, j, m, n$	Indicate values corresponding to the nodal points $i, j, m$ and $n$ of the tetrahedral element.
$N$	Refers to surface where Neumann condition applies.
$x, y, z$	Partial differentiation with respect to $x, y$ and $z$ .
$\bar{\phi}_i, \bar{\phi}_j, \bar{\phi}_m, \bar{\phi}_n$	Partial differentiation with respect to $\bar{\phi}_i, \bar{\phi}_j, \bar{\phi}_m$ and $\bar{\phi}_n$ .

Superscripts

$e$	Indicates a set of values belonging to the tetrahedral element
$*$	Indicates a dimensionless quantity

Nomenclature  
(Cont)

Brackets

$( )$	Row vector
$\{ \}$	Column vector
$[ ]$	Matrix
$   $	Determinant
$   \quad   $	Absolute value of a determinant

Abbreviations

Abs.	Absolute value
D	Domain
R	Region
S	Surface
Max.	Maximum
Min.	Minimum.

## CHAPTER 1

### INTRODUCTION

#### 1.1 Scope of the Study

In this study the finite element method is applied to solve the steady, three-dimensional, incompressible potential flow problem in reducing bends of complicated geometry. The potential distribution in the flow region was calculated using a computer program which was developed and used to solve three specific problems.

The three problems are:

1. A test problem with a known two-dimensional solution (Flow around  $90^\circ$  finite corner). The results were compared with the exact solution.
2. A problem of a  $90^\circ$  reducing bend of square cross section base centred on an arc of a circle.
3. A practical problem of defining the flow around a  $90^\circ$  bend having a rectangular inlet and an annular outlet. The bend has application in a ground power unit wherein the inlet flow is taken from a silencer configuration and passed into the annular intake of a turbo-jet engine.

The flow region, in the problems solved, is simply connected with natural (Neumann) type boundary condition, or with mixed Dirichlet-Neumann boundary condition. The formulation allows the solution of problems

with a non-uniform normal velocity component at the inlet and outlet boundaries.

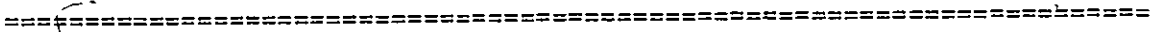
The variational principle was used for the formulation of the finite element solution. The basic finite element is a tetrahedron with a linear shape function.

A modular eight-nodal unit composed of six tetrahedral elements was used, providing an automatic satisfaction to continuity of the discretized region. Also a five tetrahedra composite unit was used in conjunction with the first application and results from both schemes were compared.

The potential was computed at a maximum of 468 nodal points in the flow region, which corresponds to 1800 tetrahedral elements when using the six-tetrahedra composite unit scheme. The resulting system of linear algebraic equations was solved using a direct method of solution and banded symmetric nature of the system property matrix was maintained. The results obtained as compared to the exact solution of the first application are in good agreement.

1.2 Literature Survey

The conventional analytical and finite difference methods of solving two-dimensional potential flow, as well as the complexities of the three-dimensional case, are summarized in reference [1]\*



\*Numbers in square brackets designate references in the Bibliography.

In the first presentation [2] of the finite element application to a field problem, a quasi-harmonic equation was considered for the two-dimensional case, using triangular elements and the method was applied to a torsional problem of known solution and to a steady-state heat conduction problem of an axi-symmetric pressure vessel.

Several years later, the specific application to a potential flow problem followed [3]; where simple triangular elements with a linear shape function were used to solve a problem of flow around a cylinder placed between two parallel walls, and to solve Saint Venant's problem. The solution was obtained utilizing a structural computer program that was developed for the Boeing Company.

De Vries and Norrie [4,5] applied the finite element method to multiple-body potential flow fields, such as aerofoil cascades, with special boundary conditions including moving boundaries and Kutta condition. They also indicated the extension of the method to the solution of Poisson's equation. However, the scope of their study was restricted to two-dimensional flow problems. Later, [6] they presented the superposition technique for the stream function solution. In reference [7] they presented a detailed formulation of the two-dimensional potential flow problem.

Argyris et al. [8] presented straight and curvilinear triangles with edge nodes as well as vertex nodes. The two-dimensional problem was considered using the TRIC and TRIM-like triangular elements, in conjunction with the stream function, which allowed direct and exact satisfaction of the boundary conditions. It was pointed out that if

the same elements were to be used in conjunction with the potential function, the observance of the boundary conditions becomes cumbersome. Therefore other types of elements were introduced for the potential function. No examples were given for the three-dimensional case and the analysis was basically two-dimensional.

Doctors [9] summarized an experimental application of the finite element method to two-dimensional inviscid flow. A test problem of known solution was discussed for the case of velocity specified boundaries and the case of singularity specified boundaries. In the latter case the resulting system of equations was found to have an ill-conditioned matrix.

Udo Meissner [10] presented a mixed finite element model for the potential flow problem, introducing a dual functional of the velocity and the velocity potential. The generalized variational principle was used for solving two problems of the two-dimensional type, including a source flow and finite corner flow.

Carstan and Devos [11] presented a theoretical basis for the application of the finite element technique to a three-dimensional flow problem, for incompressible and compressible fluids. The Reynold's<sup>o</sup> equation was programmed and applied to the particular case of gas lubricated Rayleigh step journal bearing. However, the application of the method was for two-dimensional viscous flow.

Of relevance to the potential flow problems are references on heat conduction and electrostatic field. Zienkiewicz and Parekh [12] used isoparametric elements in a time-stepping solution for a three-

dimensional heat conduction problem. The solution was obtained using a rather crude model of three subdivisions to represent an eighth of a spheroid. Zienkiewicz and Bahrani[13] used a five tetrahedra composite element to obtain the electrostatic potential distribution in an earthed porcelain insulator, and also to obtain the pressure on an accelerating surface of a dam. The two problems solved by the authors have simple geometric boundaries.



## CHAPTER 2

### STATEMENT OF THE PROBLEM

#### 2.1 Introduction

In this chapter the preparation of the problem for the finite element solution is briefly discussed. Some basic definitions are stated and a short introduction of the finite element technique is presented. The mathematical statement of the problem as well as its variational analogue are included.

#### 2.2 Definitions

In a physical problem, whether discrete or continuous, the state of the system can be described by variables, of which a set  $x'_1, x'_2, \dots, x'_n$  (collectively represented by  $x'_j$ ) are independent and a set of  $u_1, u_2, \dots, u_m$  (collectively represented by  $u_i$ ) are dependent. The region of the system is defined by the sets of all possible values that the  $x'_j$  can have. A particular set of allowable values of  $x'_j$  defines a point in the region. If at a point (with the remaining independent variables held constant) one of the  $x'_j$ 's can either be increased or decreased to another allowable value, the point is said to be in the interior of the region. If the variable can be decreased to another allowable value, but an increase gives a value outside the prescribed range, or vice versa, then the point is on the boundary of the region.

Sometimes there is no upper (and/or lower) bound on one or more

more of the independent variables, and in this case the boundary is said to be open. When the independent variables are bounded the boundary is considered closed.

The region will be denoted by R, the domain by D and the boundaries by S, where  $R = D + S$ , meaning that the region includes the domain and its boundaries.

In some cases, the region is internally subdivided by interior boundaries. A region is termed connected if any point in it may be joined to any other point by an infinite number of paths, each of which lies in the region. A circuit, composed of alternative paths between the same two points, is termed reducible if it can be contracted to a point without passing out of the region. A simply connected region is one for which all paths joining any two points are reducible, otherwise it is termed multiply-connected region.

### 2.3 Approximate Solution of Field Problems.

Of the various available approximate methods for solving field problems, those methods in which a trial solution is used are of particular interest. In a field problem of one dependent variable  $\phi$  each of the governing (domain + boundaries) equations can be written generally as:

$$F(\phi) = G(\phi) \tag{2.3.1}$$

where F and G are functions of  $\phi$ .

The solution  $\phi(x_j)$  that satisfies the set of equation (2.3.1) is sought.

The method considered is that in which  $\phi$  is approximated by a trial

solution  $\phi_\mu$  of the linear form:

$$\phi_{\mu} = \sum_{\kappa=1}^M C'_{\kappa} \phi_{\kappa} \quad (2.3.2)$$


where  $\phi_{\kappa}$  are linearly independent selected functions  $\phi_{\kappa}(x'_j)$  existing over  $D + S$  and  $C'_{\kappa}$  are unknown parameters to be determined subsequently. It is understood that equation (2.3.2) can have added to it a term  $\phi_0 (= \phi_0(x'_j))$  if desired.

Most of the methods that use a trial function of the form (2.3.2) fall into two groups, namely residual and variational methods. In the variational method, with which the present study is concerned, the desired solution  $\phi(x'_j)$  is known to give an extremum value to some functional  $X(\phi)$ . The substitution of equation (2.3.2) into the functional  $X(\phi)$ , and the requirement that this new functional  $X_{\mu} = X(\phi_{\mu})$  satisfies the extremal conditions, leads to a set of equations from which the approximate solution  $\phi_{\mu}$  is obtained. Alternatively, a variational equation may be used instead of the functional  $X(\phi)$ .

For linear problems, the variational method yields a set of algebraic equations whose solution gives the parameters  $C'_{\kappa}$  of equation (2.3.2). The original problem involving differential equations is thus transformed into inherently simple algebraic equations.

#### 2.4 The Finite Element Method.

A finite element method is one in which the subdivisions of the region into "subdomains", "finite elements" or "cells" is an essential part of the procedure, with some functional representation of the solution being adopted over the element so that the parameters of the representation



become the unknowns of the problem. The finite element method is thus a particular class of discretization procedure by which the original governing equations having infinite degrees of freedom are transformed into approximation equations with finite degrees of freedom. The dependent variable  $\phi$  is represented over an element using element parameters that are the unknowns for which the problem is to be solved.

The key features of the finite element method are:

1. The domain is divided into subdivisions or finite elements usually of the same form and interconnected at nodal points.
2. The trial solution is prescribed (functionally) over the domain in a piecewise fashion, element by element.

Since the true solution is assumed to be continuous, it is an obvious requirement that the trial solution is continuous within the element, and in the limit as the element's size tends to zero to be continuous across the domain, and also continuous across the interelement boundaries in the same limit.

## 2.5 Mathematical Statement of the Problem

In the following section the differential equation and the boundary conditions of the problem are stated as well as the uniqueness theorems related to it.

### 2.5.1 The Potential Field

The potential field  $\phi$  is a point function in the field R. It is single valued and in steady flow is governed by the Laplace equation.

$$\nabla^2 \phi = 0 \tag{2.5.1.1}$$

subject to special boundary conditions on the surface,  $S$ , terminating the region,  $R$ .

The velocity field  $\bar{V}$  is the gradient of the scalar potential  $\phi$

$$\bar{V} = \nabla\phi \quad (2.5.1.2)$$

The continuity equation as applied to the velocity field can be written

$$\nabla \cdot \bar{V} = 0 \quad (2.5.1.3)$$

The irrotationality condition is

$$\nabla \times \bar{V} = 0 \quad (2.5.1.4)$$

From equations (2.5.1.3) and (2.5.1.4) it is seen that the velocity field is a solenoidal irrotational field.

## 2.5.2 Boundary Conditions

There are three types of boundary conditions commonly encountered in the Laplace field problem. They are known as the first, second and third kind, or the Dirichlet, Neumann and Cauchy boundary condition, respectively.

### 1. The Dirichlet Boundary Condition

The value of the potential  $\phi$  is specified at all the points of the boundary  $S$

$$\phi = g \quad \text{on } S \quad (2.5.2.1)$$

### 2. The Neumann Boundary Condition

The normal derivative of the potential is specified on the boundary  $S$

$$\frac{\partial \phi}{\partial n} = p \quad \text{on } S \quad (2.5.2.2)$$

### 3. The Cauchy Boundary Condition

Both the potential and its normal derivative are specified in relation to each other on the boundary

$$\frac{\partial \phi}{\partial n} + a \phi + q = 0 \quad \text{on } S \quad (2.5.2.3)$$

If on each of two or more sections of the boundary a different condition is specified, the problem is said to have mixed boundary condition.

#### 2.5.3 Uniqueness Theorems

For a simply connected domain  $D$  enclosed by a surface  $S$ , the following uniqueness theorems for the Laplace field can be used to determine whether the field equation in  $D$  plus the boundary conditions on  $S$  uniquely describe the phenomena.

1. If the Dirichlet condition is specified everywhere on the boundary, the solution  $\phi$  is uniquely determined.
2. If the Neumann condition is specified on the boundary, the solution is determined except for an additive constant.
3. For the Cauchy condition, the solution is unique if  $a$  is positive.
4. For a mixed Dirichlet-Neumann boundary condition, the solution is unique.

The boundary conditions must be sufficient to constrain the problem to a unique solution, i.e. the problem must be "well posed". The Laplace equation, being of the elliptic type, conditions on all boundaries must be specified.

## 2.6 The Variational Analogue of the Laplace Equation

The variational formulation of the Laplace equation is given in detail in Appendix I.

For the Laplace equation ( $\nabla^2 \phi = 0$ ) with the boundary conditions

$$\phi = g(x, y, z) \quad \text{on } S_D \quad (2.6.1)$$

and

$$\frac{\partial \phi}{\partial n} + a\phi + q = 0 \quad \text{on } S_C \quad (2.6.2)$$

there is a solution

$$\phi = \phi(x, y, z) \quad (2.6.3)$$

given by the function

$$v = v(x, y, z) \quad (2.6.4)$$

that minimizes the functional  $X(v)$ , where

$$X(v) = \int_D \frac{1}{2} \left[ \left( \frac{\partial v}{\partial x} \right)^2 + \left( \frac{\partial v}{\partial y} \right)^2 + \left( \frac{\partial v}{\partial z} \right)^2 \right] dV + \int_{S_C} (qv + \frac{1}{2} av^2) dS_C \quad \dots (2.6.5)$$

In equations (2.6.1), (2.6.2) and (2.6.5).

$D$  - Is the domain of the potential field  $\phi$ .

$S_D$  - That part of the boundary where the Dirichlet condition is specified.

$S_C$  - That part of the boundary where the Cauchy condition is specified.

Either  $S_C$  or  $S_D$  can be zero. Also  $a$  can be zero in which case the Cauchy condition reduces to the Neumann condition, and  $q$  becomes the normal component of velocity to the surface  $S_N$  where the Neumann condition is specified.

## CHAPTER 3

### THE FINITE ELEMENT SOLUTION

#### 3.1 The Development of the Finite Element

The basic element used in this analysis was a tetrahedral element with a linear shape function. In the equations to follow a dash over the symbol  $v$  or  $\phi$  will indicate an approximation.

A global system of coordinates is directly used as one is dealing with a scalar field and the formulation is in terms of global coordinates. The region is divided into  $\bar{n}$  number of elements, corresponding to  $\bar{n}$  number of nodal points;  $1, 2, \dots, p, \dots, \bar{n}$ . The tetrahedron shown in Figure(1) has the nodal point identifiers  $i, j, m$  and  $n$ . The potential  $\phi$  is assumed to have a linear variation in the element

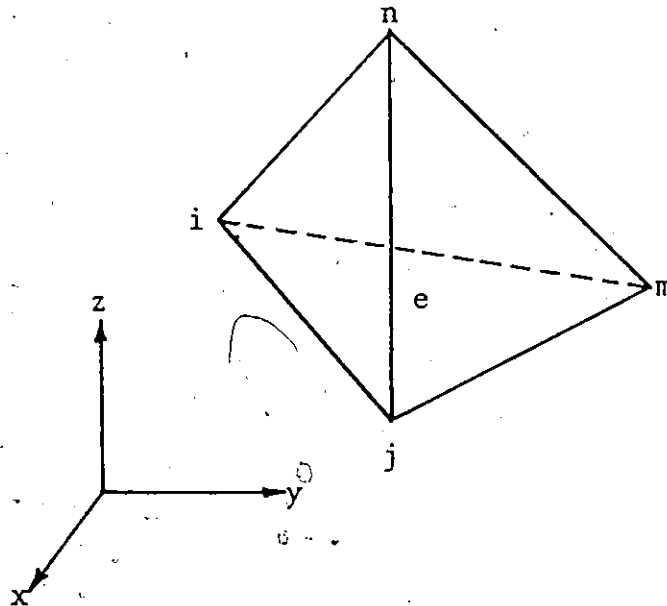


Figure 1. Tetrahedral Element



$$\phi = \alpha_1 + \alpha_2 X + \alpha_3 Y + \alpha_4 Z \quad (3.1.1)$$

where  $\alpha_1$ ,  $\alpha_2$ ,  $\alpha_3$  and  $\alpha_4$  are constants. These constants are to be determined in terms of the values of  $\phi$  at the nodal points of the element;  $\bar{\phi}_i$ ,  $\bar{\phi}_j$ ,  $\bar{\phi}_m$  and  $\bar{\phi}_n$ , and hence

$$\alpha_k = f_k(\bar{\phi}_i, \bar{\phi}_j, \bar{\phi}_m, \bar{\phi}_n) \quad (3.1.2)$$

where  $k = 1, 2, 3, 4$ .

For the four nodal points of the element one can rewrite Equation (3.1.1) by substituting the nodal values of  $\phi$  and the coordinates of each node as follows:

$$\left. \begin{aligned} \bar{\phi}_i &= \alpha_1 + \alpha_2 x_i + \alpha_3 y_i + \alpha_4 z_i & (a) \\ \bar{\phi}_j &= \alpha_1 + \alpha_2 x_j + \alpha_3 y_j + \alpha_4 z_j & (b) \\ \bar{\phi}_m &= \alpha_1 + \alpha_2 x_m + \alpha_3 y_m + \alpha_4 z_m & (c) \\ \bar{\phi}_n &= \alpha_1 + \alpha_2 x_n + \alpha_3 y_n + \alpha_4 z_n & (d) \end{aligned} \right\} (3.1.3)$$

Defining the coordinate vector of a point (c)

$$(c) \equiv (1 \quad x \quad y \quad z) \quad (3.1.4)$$

the coefficient vector  $\{\alpha\}$

$$\{\alpha\} \equiv \begin{Bmatrix} \alpha_1 \\ \alpha_2 \\ \alpha_3 \\ \alpha_4 \end{Bmatrix} \quad (3.1.5)$$

the nodal potential vector of the element  $e$  as

$$\{\bar{\phi}^e\} = \begin{Bmatrix} \bar{\phi}_i \\ \bar{\phi}_j \\ \bar{\phi}_m \\ \bar{\phi}_n \end{Bmatrix} \quad (3.1.6)$$

and the coordinates matrix of the element  $e$

$$[A^e] = \begin{bmatrix} 1 & x_i & y_i & z_i \\ 1 & x_j & y_j & z_j \\ 1 & x_m & y_m & z_m \\ 1 & x_n & y_n & z_n \end{bmatrix} \quad (3.1.7)$$

Equation (3.1.1) can then be written as

$$\phi = (c) \{\alpha\} \quad (3.1.8)$$

Alternatively, Equation (3.1.8) can be written in expanded matrix form as

$$\phi = (1 \ x \ y \ z) \begin{Bmatrix} \alpha_1 \\ \alpha_2 \\ \alpha_3 \\ \alpha_4 \end{Bmatrix} \quad (3.1.9)$$

Also Equation (3.1.3) can be written in a matrix form as

$$\{\bar{\phi}^e\} = [A^e] \{\alpha\} \quad (3.1.10)$$

which can be expanded in the form

$$\begin{Bmatrix} \bar{\phi}_i \\ \bar{\phi}_j \\ \bar{\phi}_m \\ \bar{\phi}_n \end{Bmatrix} = \begin{bmatrix} 1 & x_i & y_i & z_i \\ 1 & x_j & y_j & z_j \\ 1 & x_m & y_m & z_m \\ 1 & x_n & y_n & z_n \end{bmatrix} \begin{Bmatrix} \alpha_1 \\ \alpha_2 \\ \alpha_3 \\ \alpha_4 \end{Bmatrix} \quad (3.1.11)$$

To obtain the coefficients  $\alpha_1, \alpha_2, \alpha_3$  and  $\alpha_4$ , from Equation (3.1.10) one can write

$$\{\alpha\} = [A^e]^{-1} \{\bar{\phi}^e\} \quad (3.1.12)$$

where  $[A^e]^{-1}$  is the inverse of the element's coordinates matrix  $[A^e]$ .

The matrix  $[A^e]^{-1}$  is assumed to have the component form

$$[A^e]^{-1} = \begin{bmatrix} a_i & a_j & a_m & a_n \\ b_i & b_j & b_m & b_n \\ c_i & c_j & c_m & c_n \\ d_i & d_j & d_m & d_n \end{bmatrix} \quad (3.1.13)$$

wherein

$$a_i = \begin{vmatrix} x_j & x_m & x_n \\ y_j & y_m & y_n \\ z_j & z_m & z_n \end{vmatrix} / \det [A^e]$$

$$b_i = - \begin{vmatrix} 1 & 1 & 1 \\ y_j & y_m & y_n \\ z_j & z_m & z_n \end{vmatrix} / \det [A^e]$$

$$c_i = \begin{vmatrix} 1 & 1 & 1 \\ x_j & x_m & x_n \\ z_j & z_m & z_n \end{vmatrix} / \det [A^e]$$

and

$$d_i = - \begin{vmatrix} 1 & 1 & 1 \\ x_j & x_m & x_n \\ y_j & y_m & y_n \end{vmatrix} / \det [A^e]$$

The other constants may similarly be obtained using a cyclic interchange of the subscripts.

Denoting the rows of the matrix  $[A^e]^{-1}$  by (A), (B), (C) and (D) respectively one can write

$$\left. \begin{aligned} (A) &\equiv (a_i \quad a_j \quad a_m \quad a_n) & (a) \\ (B) &\equiv (b_i \quad b_j \quad b_m \quad b_n) & (b) \\ (C) &\equiv (c_i \quad c_j \quad c_m \quad c_n) & (c) \\ (D) &\equiv (d_i \quad d_j \quad d_m \quad d_n) & (d) \end{aligned} \right\} \quad (3.1.14)$$

Hence one can write Equation (3.1.13) using the definition (3.1.14) in the compact form shown below

$$\lambda [A^e]^{-1} = \begin{bmatrix} (A) \\ (B) \\ (C) \\ (D) \end{bmatrix} \quad (3.1.15)$$

Also Equation (3.1.12) can be written in the form

$$\begin{Bmatrix} \alpha_1 \\ \alpha_2 \\ \alpha_3 \\ \alpha_4 \end{Bmatrix} = \begin{bmatrix} a_i & a_j & a_m & a_n \\ b_i & b_j & b_m & b_n \\ c_i & c_j & c_m & c_n \\ d_i & d_j & d_m & d_n \end{bmatrix} \begin{Bmatrix} \bar{\phi}_i \\ \bar{\phi}_j \\ \bar{\phi}_m \\ \bar{\phi}_n \end{Bmatrix} \quad (3.1.16)$$

Substituting the values of  $\{\alpha\}$  obtained from Equation (3.1.12) into Equation (3.1.8) one obtains an expression for  $\phi$  as follows

$$\phi = (c) [A^e]^{-1} \{\bar{\phi}^e\} \quad (3.1.17)$$

Using Equation (3.1.16) and Equation (3.1.9), Equation (3.1.17) can be written in an expanded matrix form as

$$\phi = (1 \quad x \quad y \quad z) \begin{bmatrix} a_i & a_j & a_m & a_n \\ b_i & b_j & b_m & b_n \\ c_i & c_j & c_m & c_n \\ d_i & d_j & d_m & d_n \end{bmatrix} \begin{Bmatrix} \bar{\phi}_i \\ \bar{\phi}_j \\ \bar{\phi}_m \\ \bar{\phi}_n \end{Bmatrix} \quad (3.1.18-a)$$

Further expansion produces the following expression for  $\phi$

$$\begin{aligned} \phi = & (a_i + b_i x + c_i y + d_i z) \bar{\phi}_i \\ & + (a_j + b_j x + c_j y + d_j z) \bar{\phi}_j \\ & + (a_m + b_m x + c_m y + d_m z) \bar{\phi}_m \\ & + (a_n + b_n x + c_n y + d_n z) \bar{\phi}_n \end{aligned} \quad (3.1.18-b)$$

Using the definitions (3.1.14) one can also write

$$\phi = (A)\{\bar{\phi}^e\} + (B)\{\bar{\phi}^e\}x + (C)\{\bar{\phi}^e\}y + (D)\{\bar{\phi}^e\}z \quad \dots\dots\dots (3.1.18-c)$$

Equation (3.1.18) provides the potential  $\phi$  at a point  $(x,y,z)$  within the element  $e$ , in terms of the values of  $\phi$  at the nodal points of the element;  $\bar{\phi}_i$ ,  $\bar{\phi}_j$ ,  $\bar{\phi}_m$  and  $\bar{\phi}_n$ . The values of  $\phi$  at the nodal points remain as the basic unknowns to be determined.

### 3.2 Equations of the Discretized Region

Equation (2.6.5) can be written for a problem having Neumann boundary condition as well as for mixed Dirichlet-Neumann type, with  $a = 0$ , in the form

$$X(v) = \int_D \frac{1}{2} \left[ \left( \frac{\partial v}{\partial x} \right)^2 + \left( \frac{\partial v}{\partial y} \right)^2 + \left( \frac{\partial v}{\partial z} \right)^2 \right] dV + \int_{S_N} q v dS \quad \dots (3.2.1)$$

In Equation (3.2.1)  $S_N$  is the part of the boundary where the Neumann condition is specified, and  $q$  is the normal component of velocity at the boundary. The Dirichlet Integral is defined as

$$X_0 \equiv \int_D \frac{1}{2} \left[ \left( \frac{\partial v}{\partial x} \right)^2 + \left( \frac{\partial v}{\partial y} \right)^2 + \left( \frac{\partial v}{\partial z} \right)^2 \right] dx dy dz \quad (3.2.2)$$

Denoting the second term on the right hand side of Equation (3.2.1) by  $X_N$ , i.e.

$$X_N \equiv \int_{S_N} q v dS \quad (3.2.3)$$

Equation (3.2.1) can be written as follows

$$X(v) = X_0 + X_N \quad (3.2.4)$$

If the Dirichlet integral is carried over an element  $e$  it is denoted by  $X_0^e$ , and for the whole domain one has

$$X_0 = \sum_{e=1}^{\ell} X_0^e \quad (3.2.5)$$

Let there be  $\bar{n}_1$  nodal points on the boundary where the Dirichlet condition is prescribed and  $\bar{n}_2$  nodal points on the boundary where the Neumann condition is prescribed, then

$$X_N = \sum_{\ell_2} X_N^e \quad (3.2.6)$$

where  $\ell_2$  is the number of elements with specified Neumann condition

(sharing the  $\bar{n}_2$  nodal points).

It is clear that  $X(v)$  is a function of all the nodal values  $\bar{v}_p$  ( $p=1,2, \dots, p, \dots, \bar{n}$ ), but as there is  $\bar{n}_1$  specified values of  $\bar{v}_p$  on  $S_D$ , then the functional  $X(v)$  is in fact a function of the nodal values  $\bar{v}_p$  in  $D + S_N$ , (i.e. of  $\bar{n} - \bar{n}_1$  nodal values).

The necessary condition to minimize  $X(v)$  is written

$$\frac{\partial X(v)}{\partial \bar{v}_p} = 0 \quad (3.2.7)$$

where  $p = 1, 2, \dots, p, \dots, \bar{n}$ , excluding the  $\bar{n}_1$  points on  $S_D$ .

Substituting Equation (3.2.2) into Equation (3.2.1) and differentiating with respect to  $\bar{v}_p$  one obtains

$$\left. \begin{aligned} \frac{\partial X(v)}{\partial \bar{v}_p} &= \sum_{e=1}^{\ell} \frac{\partial X_O^e}{\partial \bar{v}_p} + \sum_{e=1}^{\ell_2} \frac{\partial X_N^e}{\partial \bar{v}_p} & (a) \\ &= \sum_{e=1}^{\ell} \frac{\partial X_O^e}{\partial \bar{v}_p} + \int_{S_N} q \frac{\partial v}{\partial \bar{v}_p} dS & (b) \end{aligned} \right\} (3.2.8)$$

Substituting Equation (3.2.8) into the minimization condition of Equation (3.2.7) yields

$$\left. \begin{aligned} \sum_{e=1}^{\ell} \frac{\partial X_O^e}{\partial \bar{v}_p} + \sum_{e=1}^{\ell_2} \frac{\partial X_N^e}{\partial \bar{v}_p} &= 0 & (a) \\ \sum_{e=1}^{\ell} \frac{\partial X_O^e}{\partial \bar{v}_p} + \int_{S_N} q \frac{\partial v}{\partial \bar{v}_p} dS &= 0 & (b) \end{aligned} \right\} (3.2.9)$$

or

From Equation (3.2.9) one can derive  $(\bar{n} - \bar{n}_1)$  equations which are linear algebraic equations in  $(\bar{n} - \bar{n}_1)$  dependent variables

From the prescribed Dirichlet boundary condition on  $S_D$ , another set of  $\bar{n}_1$  equations can be written in the form

$$\bar{v}_h = g_h \quad (3.2.10)$$

The total number of equations is thus  $\bar{n}$ . These equations are to be assembled in a matrix form.

As the solution  $\bar{v}_p$  is to be, in the final analysis, the desired approximate solution for  $\phi$ , therefore  $\bar{\phi}_p$  can be substituted for  $\bar{v}_p$  in Equations (3.2.9) and (3.2.10). After the minimization the resulting  $\bar{n}$  linear algebraic equations will have the matrix form

$$[K] \{\bar{\phi}\} + \{F\} = \{0\} \quad (3.2.11)$$

The matrix  $[K]$  is termed the System Property Matrix, while the vector  $\{F\}$  will be termed the Constraint Vector.

The purpose of the analysis in the following sections is to formulate the matrix  $[K]$  from the tetrahedral element property matrix  $[K^e]$ . In a similar fashion the system constraint vector  $\{F\}$  will be assembled from the element constraint vector  $\{F^e\}$ . The basic Equations (3.2.7), (3.2.9) and (3.2.10) are used in the formulation of  $[K]$  and  $\{F\}$ . The assemblage of the  $(\bar{n} - \bar{n}_1)$  equations given by Equation (3.2.9-b) and the  $\bar{n}_1$  equations given by (3.2.10) is to be written in the form of Equation (3.2.11).



### 3.3 The Property Matrix of the Tetrahedral Element

Consider the minimization of the Dirichlet integral in Equation (3.2.9)

$$\frac{\partial X_0}{\partial \bar{v}_p} = \sum_{e=1}^{\ell} \frac{\partial X_0^e}{\partial \bar{v}_p} \quad (3.3.1)$$

excluding  $\bar{n}_1$  points on  $S_D$ .

As mentioned in section (3.2) the solution  $\bar{v}_p$  is the desired approximate solution of  $\phi$ , then substituting  $\bar{\phi}_p$  for  $\bar{v}_p$  in Equation (3.3.1) one has

$$\frac{\partial X_0}{\partial \bar{\phi}_p} = \sum_{e=1}^{\ell} \frac{\partial X_0^e}{\partial \bar{\phi}_p} \quad (3.3.2)$$

excluding  $\bar{n}_1$  points on  $S_D$ .

The problem at this stage reduces to the calculation of  $(\partial X_0 / \partial \bar{\phi}_p)$  for those elements that have the node  $p$  as a common vertex since the contribution from all other elements is zero [14]. However, the observation of the elements sharing the node  $p$ , in a three-dimensional problem, is a cumbersome task because there is an average of 24 elements sharing one node. Therefore, in this analysis, the formulation of the problem in terms of  $(\partial X_0 / \partial \bar{\phi}_p)$  for each node [4,6,7,14] cannot be easily applied. An alternative approach is to consider the contributions of the nodes of one element to each other, i.e. to consider the contribution to one node in the element from the other three nodes and repeating the same procedure, in succession, for the other three nodes. In this case Equation (3.3.2) can be written for an element ( $p = i, j, m, n$ , in nodal numbers) rather than for one node  $p$ . The summation of the contributions of all elements

sharing one node will then be satisfied when the equations of all elements are assembled.

In this case the purpose is to formulate the term  $\partial X_0^e / \partial \{\bar{\phi}^e\}$  rather than  $(\partial X_0^e / \partial \bar{\phi}_p)$  as

$$\frac{\partial X_0^e}{\partial \{\bar{\phi}^e\}} = [K^e] \{\bar{\phi}^e\} \quad (3.3.3)$$

From Equation (3.2.2) one can write for the element e

$$X_0^e = \int_{V^e} \frac{1}{2} \left[ \left( \frac{\partial \phi}{\partial x} \right)^2 + \left( \frac{\partial \phi}{\partial y} \right)^2 + \left( \frac{\partial \phi}{\partial z} \right)^2 \right] dV \quad (3.3.4)$$

where  $V^e$  is the volume of the element e.

Differentiating Equation (3.3.4) with respect to  $\bar{\phi}_i$  one obtains

$$\begin{aligned} \frac{\partial X_0^e}{\partial \bar{\phi}_i} &= \frac{\partial}{\partial \bar{\phi}_i} \int_{V^e} \frac{1}{2} \left[ \left( \frac{\partial \phi}{\partial x} \right)^2 + \left( \frac{\partial \phi}{\partial y} \right)^2 + \left( \frac{\partial \phi}{\partial z} \right)^2 \right] dV \\ &= \int_{V^e} \left[ \phi_x (\phi_x)_{\bar{\phi}_i} + \phi_y (\phi_y)_{\bar{\phi}_i} + \phi_z (\phi_z)_{\bar{\phi}_i} \right] dV \quad (3.3.5) \end{aligned}$$

where

$$\phi_x = \frac{\partial \phi}{\partial x}, \quad \phi_y = \frac{\partial \phi}{\partial y} \quad \text{and} \quad \phi_z = \frac{\partial \phi}{\partial z}$$

and

$$(\phi_x)_{\bar{\phi}_i} = \frac{\partial \phi_x}{\partial \bar{\phi}_i}, \quad (\phi_y)_{\bar{\phi}_i} = \frac{\partial \phi_y}{\partial \bar{\phi}_i} \quad \text{and} \quad (\phi_z)_{\bar{\phi}_i} = \frac{\partial \phi_z}{\partial \bar{\phi}_i}$$

Next one considers how to derive the terms on the right hand side of Equation (3.3.5). From Equation (3.1.18), differentiating with respect to  $x$  one obtains

$$\phi_x = (B) \{\bar{\phi}^e\}$$

in expanded form  $\phi_x$  is given by

$$\phi_x = (b_i \ b_j \ b_m \ b_n) \begin{Bmatrix} \bar{\phi}_i \\ \bar{\phi}_j \\ \bar{\phi}_m \\ \bar{\phi}_n \end{Bmatrix} \quad (3.3.6-a)$$

Similarly

$$\phi_y = (C) \{\bar{\phi}^e\} \\ = (c_i \ c_j \ c_m \ c_n) \begin{Bmatrix} \bar{\phi}_i \\ \bar{\phi}_j \\ \bar{\phi}_m \\ \bar{\phi}_n \end{Bmatrix} \quad (3.3.6-b)$$

and finally

$$\phi_z = (D) \{\bar{\phi}^e\} \\ = (d_i \ d_j \ d_m \ d_n) \begin{Bmatrix} \bar{\phi}_i \\ \bar{\phi}_j \\ \bar{\phi}_m \\ \bar{\phi}_n \end{Bmatrix} \quad (3.3.6-c)$$

Differentiating  $\phi_x$ ,  $\phi_y$  and  $\phi_z$  in Equation (3.3.6) with respect to  $\bar{\phi}_i$  one obtains

$$\left. \begin{aligned}
 (\phi_x)_{\bar{\phi}_i} &= b_i & (a) \\
 (\phi_y)_{\bar{\phi}_i} &= c_i & (b) \\
 (\phi_z)_{\bar{\phi}_i} &= d_i & (c)
 \end{aligned} \right\} \quad (3.3.7)$$

Now substituting Equation (3.3.6) and (3.3.7) in Equation (3.3.5) one finds that

$$\frac{\partial X_o^e}{\partial \bar{\phi}_i} = \int_{V^e} (b_i (B) + c_i (C) + d_i (D)) \{\bar{\phi}^e\} dV \quad (3.3.8)$$

Integrating one obtains

$$\frac{\partial X_o^e}{\partial \bar{\phi}_i} = V^e (b_i (B) + c_i (C) + d_i (D)) \{\bar{\phi}^e\} \quad (3.3.9)$$

where the volume of the element  $V^e$  is given by

$$V^e = \frac{1}{6} \begin{vmatrix} 1 & x_i & y_i & z_i \\ 1 & x_j & y_j & z_j \\ 1 & x_m & y_m & z_m \\ 1 & x_n & y_n & z_n \end{vmatrix} \quad (3.3.10)$$

Similar expressions as (3.3.9) can be obtained for  $(\partial X_o^e / \partial \bar{\phi}_j)$ ,  $(\partial X_o^e / \partial \bar{\phi}_m)$  and  $(\partial X_o^e / \partial \bar{\phi}_n)$ , that can be assembled with (3.3.9) in the matrix form shown below

$$\begin{Bmatrix} \frac{\partial X_o^e}{\partial \bar{\phi}_i} \\ \frac{\partial X_o^e}{\partial \bar{\phi}_j} \\ \frac{\partial X_o^e}{\partial \bar{\phi}_m} \\ \frac{\partial X_o^e}{\partial \bar{\phi}_n} \end{Bmatrix} = v^e \begin{bmatrix} b_i & c_i & d_i \\ b_j & c_j & d_j \\ b_m & c_m & d_m \\ b_n & c_n & d_n \end{bmatrix} \begin{bmatrix} b_i & b_j & b_m & b_n \\ c_i & c_j & c_m & c_n \\ d_i & d_j & d_m & d_n \end{bmatrix} \begin{Bmatrix} \bar{\phi}_i \\ \bar{\phi}_j \\ \bar{\phi}_m \\ \bar{\phi}_n \end{Bmatrix} \quad (3.3.11)$$

Carrying out the multiplication of the two matrices on the right hand side of Equation (3.3.11) together with the scalar volume  $v^e$ , one finally obtains the property matrix of the element  $[K^e]$ .

$$\begin{Bmatrix} \frac{\partial X_o^e}{\partial \bar{\phi}_i} \\ \frac{\partial X_o^e}{\partial \bar{\phi}_j} \\ \frac{\partial X_o^e}{\partial \bar{\phi}_m} \\ \frac{\partial X_o^e}{\partial \bar{\phi}_n} \end{Bmatrix} = \begin{bmatrix} K_{ii} & K_{ij} & K_{im} & K_{in} \\ K_{ji} & K_{jj} & K_{jm} & K_{jn} \\ K_{mi} & K_{mj} & K_{mm} & K_{mn} \\ K_{ni} & K_{nj} & K_{nm} & K_{nn} \end{bmatrix} \begin{Bmatrix} \bar{\phi}_i \\ \bar{\phi}_j \\ \bar{\phi}_m \\ \bar{\phi}_n \end{Bmatrix} \quad (3.3.12)$$

which is the required form of Equation (3.3.3).

Since the matrix  $[K^e]$  results from the multiplication of a matrix

by its transpose, as indicated by Equation (3.3.11), it is thus clear that the element property matrix is symmetric and has positive values on the diagonal. The matrix  $[K^e]$  is to be assembled in the system property matrix  $[K]$  which is also symmetric. The assemblage of  $[K]$  is carried out through an intermediate step in which  $[K^e]$  is assembled in the property matrix of a composite unit. The composite unit is composed of several tetrahedra and has eight nodal points at its corners and therefore has an  $(8 \times 8)$  property matrix that will be termed  $[Sk]$ .

The assemblage of the property matrices of the elements in the matrix  $[K]$  can be carried out for all the elements in the region, including those which have Dirichlet specified boundary conditions. After the matrix  $[K]$  is assembled the Dirichlet condition will be imposed by modifying the diagonal elements corresponding to the nodes where  $\phi$  is specified. In a similar fashion, when the system constraint vector  $\{F\}$  is assembled, the Dirichlet condition will be imposed by modifying the elements of  $\{F\}$ , which correspond to the nodes where  $\phi$  is specified. The procedure will be shown in subsequent sections.

#### 3.4 The Boundary Conditions (Constraint Vector)

In section (3.3), the minimization of the Dirichlet integral  $(\sum_{e=1}^k \partial X_0^e / \partial \bar{v}_p)$ , as given by Equation (3.2.9), was considered. In this section the surface integral in the basic Equation (3.2.9), which represents the contribution of the boundaries where the Neumann condition is specified, will be discussed. This integral will be shown to form part of the system constraint vector  $\{F\}$ , where the other part is the

values of  $\bar{\phi}$  specified for the Dirichlet boundary condition.

### 3.4.1 The Neumann Boundary Condition

From Equation (3.2.6) and Equation (3.2.9) one can write

$$\frac{\partial X_N}{\partial \bar{v}_p} = \left. \begin{aligned} & \int_{S_N} q \frac{\partial v}{\partial \bar{v}_p} dS \quad (a) \\ & \sum_{e \in S_N} \int_{S_N^e} q \frac{\partial v}{\partial \bar{v}_p} dS \quad (b) \end{aligned} \right\} (3.4.1.1)$$

where  $S_N^e$  is the surface area of the element  $e$  where the Neumann condition is specified.

In Equation (3.4.1.1-b) the summation reduced to the summation over the elements having the node  $p$  as a common vertex.

The linear variation of  $\phi$  within the element requires a linear variation of  $v$  within the same element. In fact, one can write  $\phi$  for  $v$  as the required solution. The integration in Equation (3.4.1.1-b) can be carried out knowing the variation of  $q$  over the surface of the element  $S_N^e$ . Alternatively, one may consider  $q$  as the average of the values of  $q$  at the nodes of the flow face of the element  $e$ . Thus, Equation (3.4.1.1) yields for the element  $e$

$$\frac{\partial X_N^e}{\partial \bar{\phi}_p} = q_{av} \int_{S_N^e} \frac{\partial \phi}{\partial \bar{\phi}_p} dS \quad (3.4.1.2)$$

As shown in Figure (2), if the element  $e$  has flow across the surface  $(i,j,m)$  the node  $n$  will be an interior point. At this point the purpose is to obtain the terms

$$\frac{\partial X_N^e}{\partial \phi_i}, \frac{\partial X_N^e}{\partial \phi_j} \text{ and } \frac{\partial X_N^e}{\partial \phi_m}, \text{ assembled in a vector form } \frac{\partial X_N^e}{\partial \{\phi_N^e\}}$$

The partial derivative  $\frac{\partial \phi}{\partial \phi_i}$  can be obtained from Equation (3.2.18-b),

$$\frac{\partial \phi}{\partial \phi_i} = a_i + b_i x + c_i y + d_i z \quad (3.4.1.3)$$

Substituting Equation (3.4.1.3) in Equation (3.4.1.2) one can write

$$\frac{\partial X_N^e}{\partial \phi_i} = q_{av} \int_{S_N^e} (a_i + b_i x + c_i y + d_i z) dS \quad (3.4.1.4)$$

where  $q_{av} = \frac{1}{3} (q_i + q_j + q_m)$

Similar expressions can be obtained for  $\frac{\partial X_N^e}{\partial \phi_j}$  and  $\frac{\partial X_N^e}{\partial \phi_m}$ , which can be assembled with (3.4.1.4) in the matrix form

$$\frac{\partial X_N^e}{\partial \{\phi_N^e\}} = q_{av} \int_{S_N^e} \begin{bmatrix} a_i & b_i & c_i & d_i \\ a_j & b_j & c_j & d_j \\ a_m & b_m & c_m & d_m \end{bmatrix} \begin{Bmatrix} 1 \\ x \\ y \\ z \end{Bmatrix} dS \quad (3.4.1.5)$$

Equation (3.4.1.5) reduces to



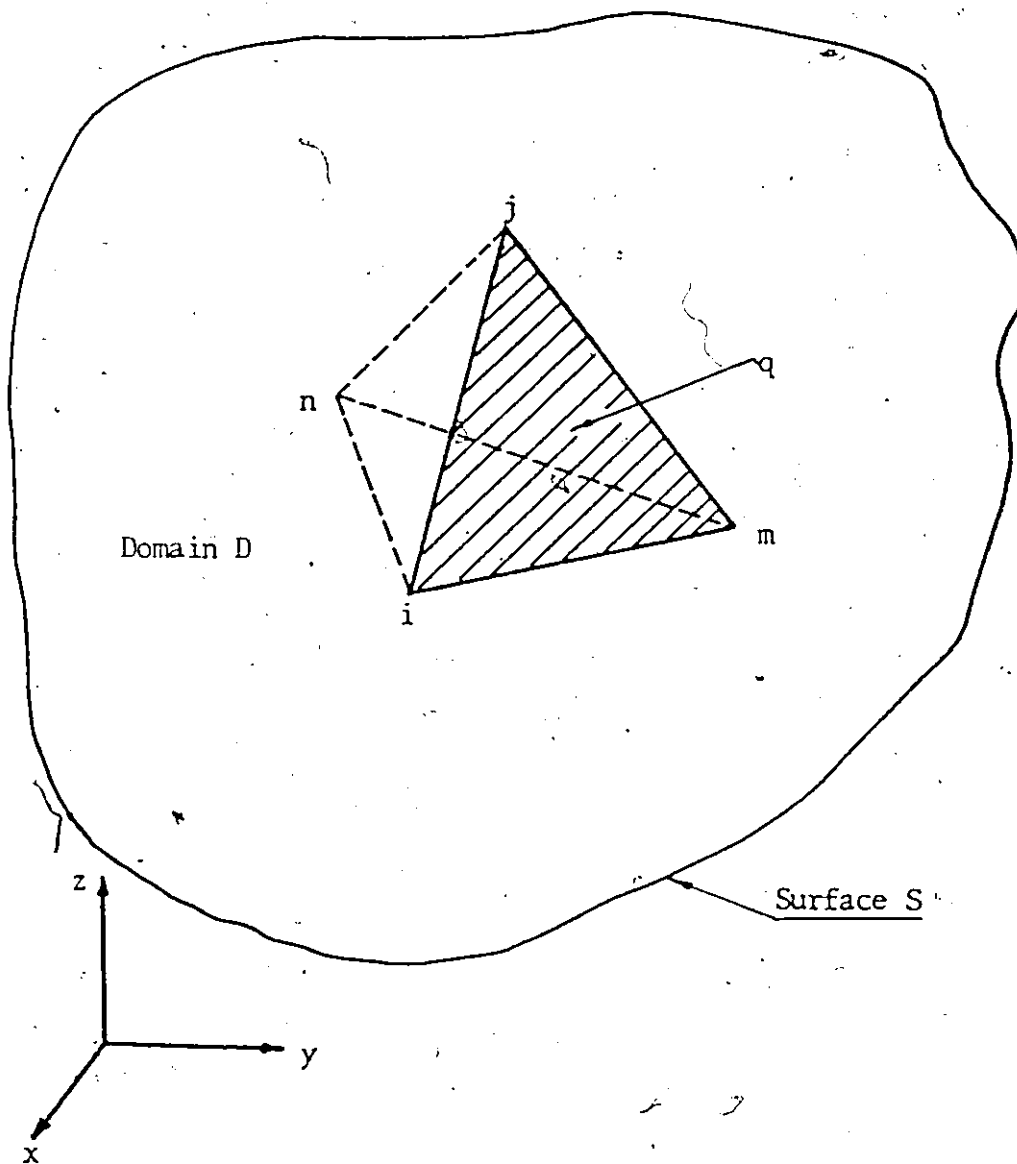


Figure 2. Element with an external face  $(i, j, m)$  where  $q$  is specified.

$$\frac{\partial \chi_N^e}{\partial \{\phi_N^e\}} = q_{av} \begin{bmatrix} a_i & b_i & c_i & d_i \\ a_j & b_j & c_j & d_j \\ a_m & b_m & c_m & d_m \end{bmatrix} \begin{Bmatrix} \int_{S_N^e} dS \\ \int_{S_N^e} x dS \\ \int_{S_N^e} y dS \\ \int_{S_N^e} z dS \end{Bmatrix} \quad (3.4.1.6)$$

It is noted that the integrals in the column vector in Equation (3.4.1.6) are the area of the face (i,j,m) and its moments about the x,y,z axes respectively. Denoting the area of the triangle (i,j,m) by  $\Delta_N^e$ , one can write Equation (3.4.1.6) as

$$\frac{\partial \chi_N^e}{\partial \{\phi_N^e\}} = \Delta_N^e q_{av} \begin{bmatrix} a_i & b_i & c_i & d_i \\ a_j & b_j & c_j & d_j \\ a_m & b_m & c_m & d_m \end{bmatrix} \begin{Bmatrix} 1 \\ \frac{x_i + x_j + x_m}{3} \\ \frac{y_i + y_j + y_m}{3} \\ \frac{z_i + z_j + z_m}{3} \end{Bmatrix} \quad (3.4.1.7)$$

Upon carrying out the multiplication in Equation (3.4.1.7) one obtains the constraint vector for the element e, namely

$$\frac{\partial \chi_N^e}{\partial \{\phi_N^e\}} = \begin{Bmatrix} f_i \\ f_j \\ f_m \end{Bmatrix} \quad (3.4.1.8)$$

The assumption that the node n of the element e is an interior point is arbitrary, in fact, any node: i, j, m or n can be an interior point.

Generally the constraints vector  $\{F_N^e\}$  has four elements one of which is zero, which corresponds to the interior point.

$$\{F_N^e\} = \begin{Bmatrix} f_i \\ f_j \\ f_m \\ 0 \end{Bmatrix} \quad (3.4.1.9)$$

If  $m$  is an interior point instead, then

$$\{F_N^e\} = \begin{Bmatrix} f_i \\ f_j \\ 0 \\ f_n \end{Bmatrix}$$

From Equation (3.4.1.7) it is clear that on a solid boundary ( $q = 0$ ) the constraint vector has zero elements. The constraint vectors of all elements are to be assembled in the system constraint vector  $\{F\}$ , by adding the elements that have the same number, thus imposing the Neumann boundary condition on the formulated problem.

If the problem is purely of the Neumann type, which is the case in the applications presented in this study, the system property matrix  $[K]$  will be singular [3]. To remove the singularity, at least one value of  $\bar{\phi}$  on the boundary (say  $\bar{\phi}_s = 0$ ) has to be specified. Imposing this condition on the problem is equivalent to the choice of an arbitrary constant for which the solution is determined. This step is necessary as indicated by the uniqueness theorems discussed in section 2.5.3. The dictation of this condition on the system of algebraic equations was done retaining

the symmetric banded nature of the system property matrix. As described in reference [15], the procedure is to multiply the diagonal element that corresponds to the node at which  $\bar{\phi}$  is specified by a large number (say  $10^6$ ). The corresponding element in the constraint vector {F} is also to be multiplied by the same large number.

#### 3.4.2 The Dirichlet Boundary Condition

Having  $\bar{n}_1$  specified values of  $\bar{\phi}$  on  $S_D$ , then one has a set of  $\bar{n}_1$  equations of the type

$$\bar{\phi}_h = g_h \quad (3.4.2.1)$$

This condition is to be imposed on the assembled matrix [K] and the constraint vector {F} in the same way followed in section 3.4.1. for specifying a value of  $\bar{\phi}$  on the boundary. However, it should be noted that when the boundary condition is of the Dirichlet type at a point, it is not necessary to specify the velocity at that point. As was mentioned in section 3.3., the system property matrix is assembled first and then the Dirichlet condition is imposed by modifying diagonal elements in [K] corresponding to the nodal points where  $\bar{\phi}$  is specified. The corresponding elements in {F} are modified accordingly.

#### 3.5 Discretization and Assemblage Procedure

The discretization and assemblage process is one of the complexities of three-dimensional field problems in the finite element procedure. Although the basic finite element used in the analysis is a simple tetrahedron, the discretization of the region directly into tetrahedra is

difficult. An important intermediate step in which the region is divided into composite modular units, is necessary. The composite unit is composed of several tetrahedral elements, and it should be chosen such that a recursive relation between the node numbers in the region is perceivable.

It is necessary at this point to distinguish between a nodal point "identifier" and a nodal point "number". The nodal point identifier is used to identify the node within a tetrahedral element within a composite unit, in other words it is a "local" identification for the node. The nodal point number, or node number, refers to the number of the node in the whole region, in other words it is a "global" identification for the node.

The composite unit used in this analysis is an eight-cornered unit with one nodal point at each corner. The discretization of the region is done by choosing the coordinates of the corners of the composite units in the region. A property matrix  $[S_k]$  of the composite unit is formulated by assembling the property matrices of the tetrahedra belonging to the unit. The choice of the number of tetrahedra and their orientation in the composite unit is essential in the discretization and assemblage procedure. A suitable choice of the modular unit can provide a versatile method of discretization and control on the element size. The basic requirement to be satisfied for proper discretization is to ensure the continuity of the region (no cavities or interferences between elements is allowed).

In this presentation, two types of the composite unit were used

and compared for the first application. The first type is a unit composed of five tetrahedral elements, while the second is a unit composed of six tetrahedral elements. The six-tetrahedra composite unit scheme gave more accurate results, and therefore was used in conjunction with the three applications considered in this study.

### 3.5.1 Five Tetrahedra Composite Unit

The five-tetrahedra, eight-cornered unit is shown in Figure (3). The unit has plane faces, and therefore can be used in the solution of problems having simple geometry [13]. The restriction that the faces are quadrilaterals (opposite sides in one face must be planar), gives rise to difficulties in the discretization of the region. The choice of the location of the nodal points in the region is subject to that restriction, otherwise the continuity of the region is not systematically satisfied. To overcome this difficulty, if the faces of the unit are not planar, the orientation of the composite units has to be permuted to insure continuity. However, the permutation of the units gives rise to another difficulty in the prediction of node identifiers, and complicates the computer programming of the problem.

### 3.5.2 Six Tetrahedra Composite Unit

The six tetrahedra, eight-cornered unit is shown in Figure (4). The unit provides a systematic way of discretization of the region. The continuity of the region is automatically satisfied because such units can fit together without permutation. The selection of the nodes is more versatile, and the size of tetrahedral elements is comparatively smaller

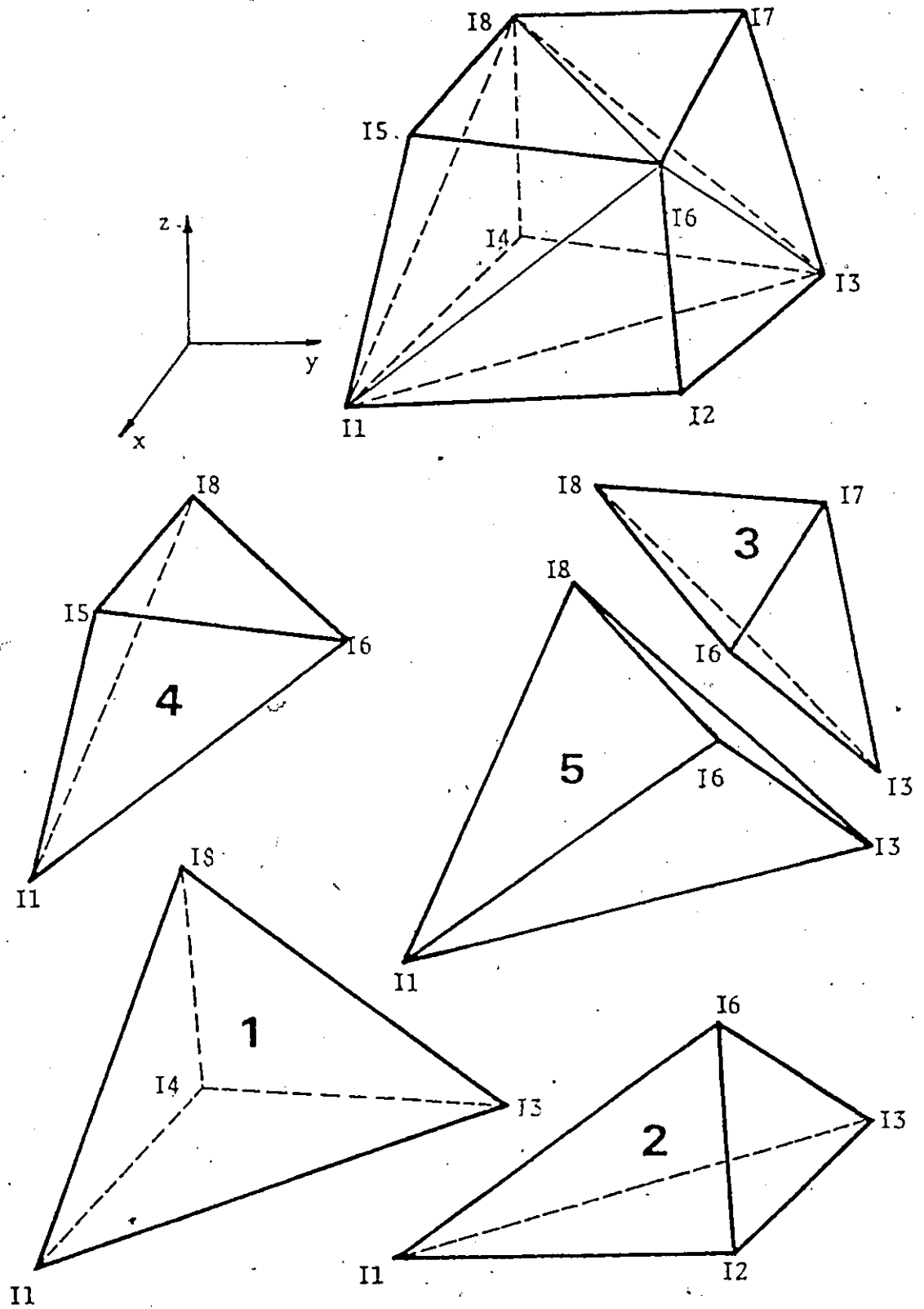


Figure 3. Five-Tetrahedra Composite Unit.

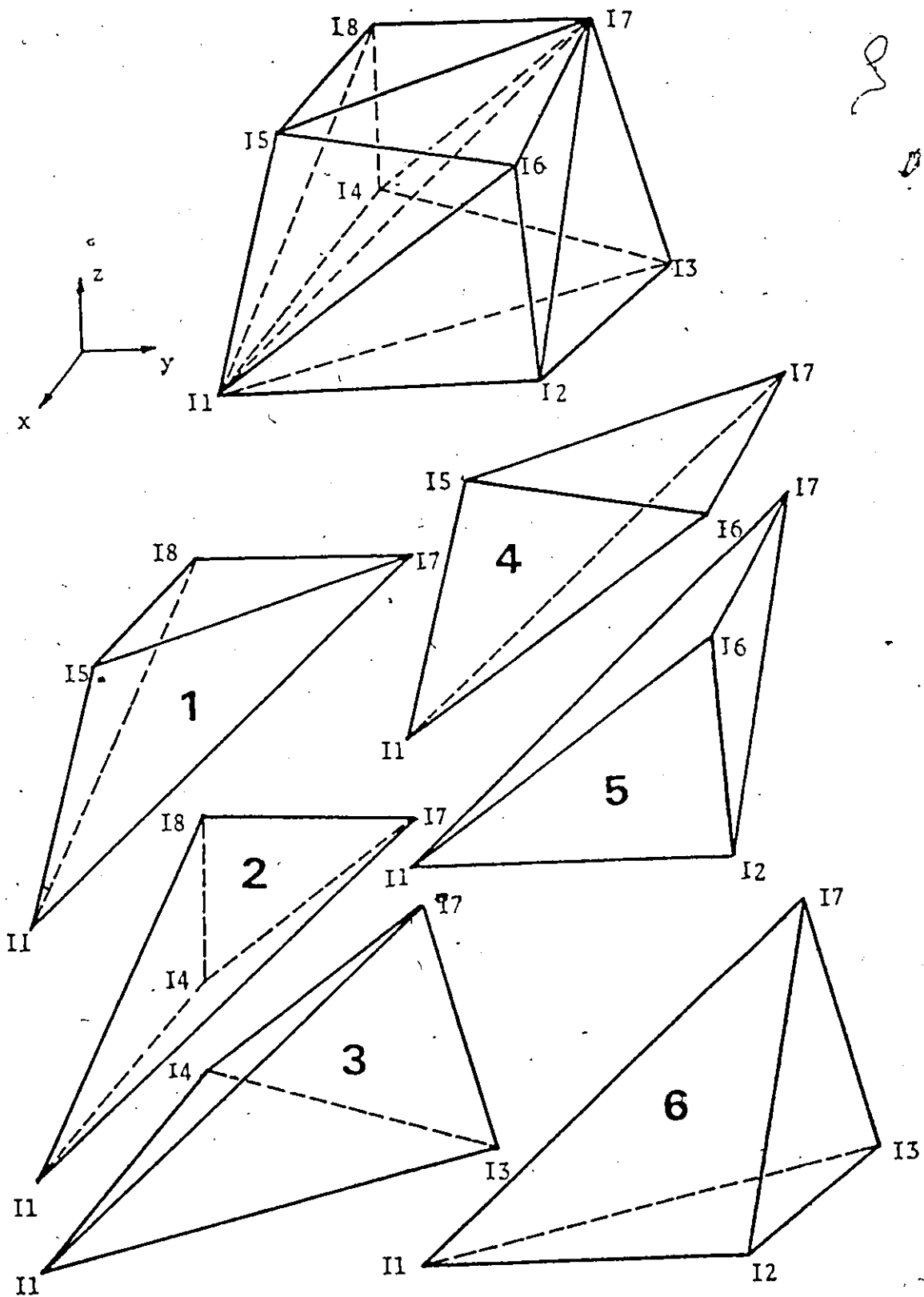


Figure 4. Six-Tetrahedra Composite Unit



than that in the five tetrahedra scheme for the same number of nodal points. This scheme was used for the three applications presented in this study.

### 3.5.3 Discretization of the region, Node Identifiers and Node Numbers.

The region is sliced into a finite number of slabs. On each section the same number of nodal points is maintained to obtain a recursive relation between the node numbers in the system. Figure (5) shows a schematic illustration of the discretization of the region into composite units. Nodes are given numbers to identify each of them in the region. For example, the nodal point numbers of the first composite unit are 1, 2, 38, 37, 7, 8, 44, 43, which correspond to 11, 12, ..., 18 in Figures (3) and (4). The corresponding node identifiers are 1, 2, ..., 8. It should also be noted that the nodal point identifiers in the tetrahedral element were  $i$ ,  $j$ ,  $m$  and  $n$ .

The mesh shown in Figure (5) is to be adjusted to fit the boundaries of the particular problem under consideration. Numbering the nodal points in the shortest direction reduces the band width of the system property matrix, thus saving storage in the computer memory.

When using the six-tetrahedral unit scheme, no restriction is imposed on the distribution of the nodes on each face in the discretized region. In fact, the faces do not have to be planar.

In this study the region was sliced into a maximum of 12 slabs (13 sections), with 36 nodes per face. The total number of nodal points is thus 468 nodes, corresponding to 1800 tetrahedra when using the six tetrahedral scheme.

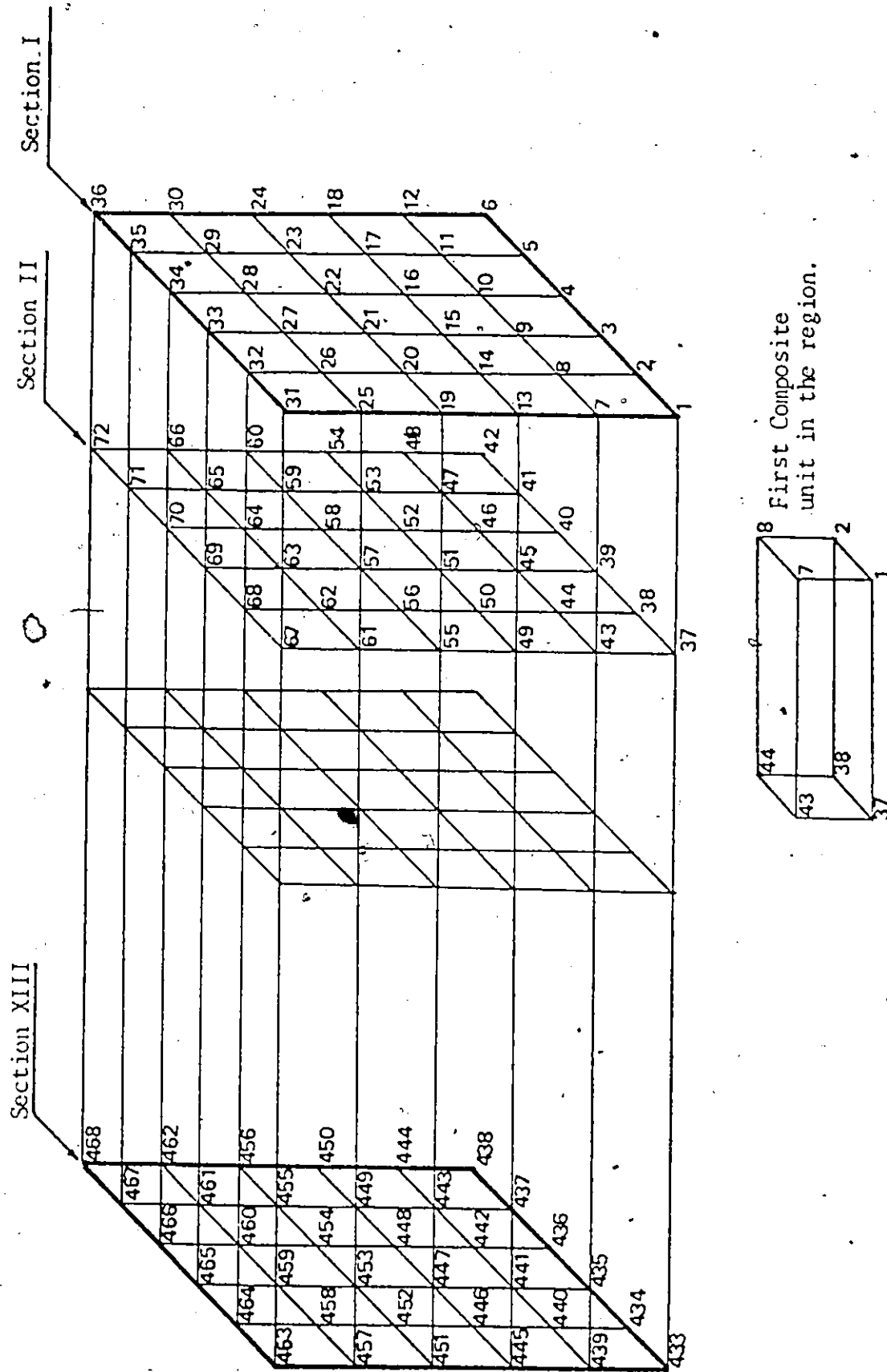


Figure 5. Discretization Mesh

Discretization can be done using a simple computer program if the boundaries can be described either numerically or by a simple function. For complicated geometries, manual discretization can be used as in the third application.

The recursive relation between nodal point numbers, as shown in Figures (3), (4) and (5), is summarized as follows

$$I_2 = I_1 + 1$$

$$I_5 = I_1 + \bar{n}_r$$

$$I_6 = I_5 + 1$$

$$I_4 = I_1 + \bar{n}_f$$

$$I_3 = I_4 + 1$$

$$I_8 = I_4 + \bar{n}_r$$

$$I_7 = I_8 + 1$$

where  $(I_1, I_2, \dots, I_8)$  are the node numbers in the composite unit,  $\bar{n}_r$  is the number of nodes per row in one section and  $\bar{n}_f$  is the number of nodes on one face (section).

It is to be noted that, for the first row of nodes in the region,  $I_1$  has the values 1, 2, 3, 4 and 5. It cannot have the value 6, in other words it would not have the node numbers of the last column. Also  $I_1$  cannot have the numbers of the last row in the face.

#### 3.5.4 Assembly of the Finite Element Equations

The assemblage of the finite element equations in a matrix form is carried out in two steps. The first is to assemble the composite unit property matrix  $[S_k]$ , using local node identifiers within the unit,

adding the terms that fall in the same location. The second step is to assemble the property matrix of the global system from the matrices of the composite units, using nodal point numbers. The property matrix of the composite unit is shown on the following pages for the five tetrahedral scheme as well as for the six tetrahedral scheme. The assembly procedure of the system property matrix  $[K]$  is shown on page 44 for the first composite unit in the region. The constraint vector is assembled in a similar fashion.

It is noted that the half-band-width in the system property matrix is of the same order as the maximum difference between node numbers in one composite unit. Thus, it is clear that numbering the nodes in the direction of the shortest dimension of the region would reduce the band width of the matrix  $[K]$ , and accordingly save computer storage.

### 3.5.5 Solution of the System of Equations

A key factor in any finite element program is the subroutine for the solution of the system of simultaneous linear algebraic equations. The choice of the technique depends on the size of the problem envisaged and upon the type of computer available.

In the simplest formulation the equations are completely formed. This approach requires storage equal to  $\bar{n}^2$ , where  $\bar{n}$  is the number of equations (the number of nodal points as well). Such formulation can be used only where the size of the problem is small and the computer is large. The solution of the system of equations in this case can be obtained by direct methods such as matrix inversion. This method was used in the present analysis for solution attempts with small number of

$K_{11}^1 + K_{11}^2 +$ $K_{11}^4 + K_{11}^5$	$K_{12}^2$	$K_{13}^1 + K_{13}^2 +$ $K_{13}^5$	$K_{14}^1$	$K_{15}^4$	$K_{16}^2 + K_{16}^4 +$ $K_{16}^5$		$K_{18}^1 + K_{18}^4 +$ $K_{18}^5$
$K_{21}^2$	$K_{22}^2$	$K_{23}^2$			$K_{26}^2$		
$K_{31}^1 + K_{31}^2 +$ $K_{31}^5$	$K_{32}^2$	$K_{33}^1 + K_{33}^2 +$ $K_{33}^3 + K_{33}^5$	$K_{34}^1$		$K_{36}^2 + K_{36}^3 +$ $K_{36}^5$	$K_{37}^3$	$K_{38}^1 + K_{38}^3 +$ $K_{38}^5$
$K_{41}^4$		$K_{43}^2$	$K_{44}^4$				$K_{48}^4$
$K_{51}^4$				$K_{55}^4$	$K_{56}^4$		$K_{58}^4$
$K_{61}^2 + K_{61}^3 +$ $K_{61}^4 + K_{61}^5$	$K_{62}^2$	$K_{63}^2 + K_{63}^5$		$K_{65}^4$	$K_{66}^2 + K_{66}^3 +$ $K_{66}^4 + K_{66}^5$	$K_{67}^3$	$K_{68}^3 + K_{68}^4 +$ $K_{68}^5$
		$K_{73}^3$			$K_{76}^3$	$K_{77}^3$	$K_{78}^3$
$K_{81}^1 + K_{81}^4 +$ $K_{81}^5$		$K_{83}^1 + K_{83}^2 +$ $K_{83}^5$	$K_{84}^1$	$K_{85}^4$	$K_{86}^3 + K_{86}^4 +$ $K_{86}^5$	$K_{87}^3$	$K_{88}^1 + K_{88}^3 +$ $K_{88}^4 + K_{88}^5$

PROPERTY MATRIX OF THE FIVE-TETRAHEDRA COMPOSITE UNIT.  $Sk(8 \times 8)$

$K_{11}^1+K_{11}^2+K_{11}^3+K_{11}^4+K_{11}^5+K_{11}^6$	$K_{12}^5+K_{12}^6$	$K_{13}^7+K_{13}^8$	$K_{14}^1+K_{14}^2$	$K_{15}^3+K_{15}^4$	$K_{16}^7+K_{16}^8$	$K_{17}^1+K_{17}^2+K_{17}^3+K_{17}^4+K_{17}^5+K_{17}^6$	$K_{18}^1+K_{18}^2$
$K_{21}^5+K_{21}^6$	$K_{22}^5+K_{22}^6$	$K_{23}^6$			$K_{26}^5$	$K_{27}^5+K_{27}^6$	
$K_{31}^2+K_{31}^3$	$K_{32}^6$	$K_{33}^2+K_{33}^3$	$K_{34}^2$			$K_{37}^2+K_{37}^3$	
$K_{41}^1+K_{41}^2$		$K_{43}^2$	$K_{44}^1+K_{44}^2$			$K_{47}^1+K_{47}^2$	$K_{48}^1$
$K_{51}^3+K_{51}^4$				$K_{55}^3+K_{55}^4$	$K_{56}^3$	$K_{57}^3+K_{57}^4$	$K_{58}^3$
$K_{61}^3+K_{61}^5$	$K_{62}^5$			$K_{65}^3$	$K_{66}^3+K_{66}^5$	$K_{67}^3+K_{67}^5$	
$K_{71}^1+K_{71}^2+K_{71}^3+K_{71}^4+K_{71}^5+K_{71}^6$	$K_{72}^5+K_{72}^6$	$K_{73}^2+K_{73}^3$	$K_{74}^1+K_{74}^2$	$K_{75}^3+K_{75}^4$	$K_{76}^7+K_{76}^8$	$K_{77}^1+K_{77}^2+K_{77}^3+K_{77}^4+K_{77}^5+K_{77}^6$	$K_{78}^1+K_{78}^2$
$K_{81}^1+K_{81}^2$			$K_{84}^1$	$K_{85}^4$		$K_{87}^1+K_{87}^2$	$K_{88}^1+K_{88}^2$

PROPERTY MATRIX OF THE SIX-TETRAHEDRA COMPOSITE UNIT  $S_k(8 \times 8)$

$K_{\bar{1},\bar{1}}$	$K_{\bar{1},\bar{2}}$	$K_{\bar{1},\bar{38}}$	$K_{\bar{1},\bar{37}}$	$K_{\bar{1},\bar{7}}$	$K_{\bar{1},\bar{8}}$	$K_{\bar{1},\bar{44}}$	$K_{\bar{1},\bar{43}}$
	$K_{\bar{2},\bar{2}}$	$K_{\bar{2},\bar{38}}$	$K_{\bar{2},\bar{37}}$	$K_{\bar{2},\bar{7}}$	$K_{\bar{2},\bar{8}}$	$K_{\bar{2},\bar{44}}$	$K_{\bar{2},\bar{43}}$
		$K_{\bar{38},\bar{38}}$	$K_{\bar{38},\bar{37}}$	$K_{\bar{38},\bar{7}}$	$K_{\bar{38},\bar{8}}$	$K_{\bar{38},\bar{44}}$	$K_{\bar{38},\bar{43}}$
			$K_{\bar{33},\bar{37}}$	$K_{\bar{37},\bar{7}}$	$K_{\bar{37},\bar{8}}$	$K_{\bar{37},\bar{44}}$	$K_{\bar{37},\bar{43}}$
				$K_{\bar{7},\bar{7}}$	$K_{\bar{7},\bar{8}}$	$K_{\bar{7},\bar{44}}$	$K_{\bar{7},\bar{43}}$
					$K_{\bar{8},\bar{8}}$	$K_{\bar{8},\bar{44}}$	$K_{\bar{8},\bar{43}}$
						$K_{\bar{44},\bar{44}}$	$K_{\bar{44},\bar{43}}$
							$K_{\bar{43},\bar{43}}$

LOCATIONS OF THE ELEMENTS OF COMPOSITE UNIT PROPERTY MATRIX  $S_k$  INTO THE SYSTEM MATRIX  $K$  FOR THE FIRST COMPOSITE UNIT IN THE REGION.

nodal points.

For larger systems of linear algebraic equations with special features, such as having a banded-symmetric matrix, a different type of storage is used to save computer memory.

In the present study the banded symmetric matrix [K] was stored in one column vector starting from the diagonal down to the end of the band. The band at the lower right-hand side corner was extended and zeros were inserted in the added space, as shown in Figure (6). This type of storage was required for the subroutine used for solving the system of equations. The solution subroutine is based on Cholesky factorization method.

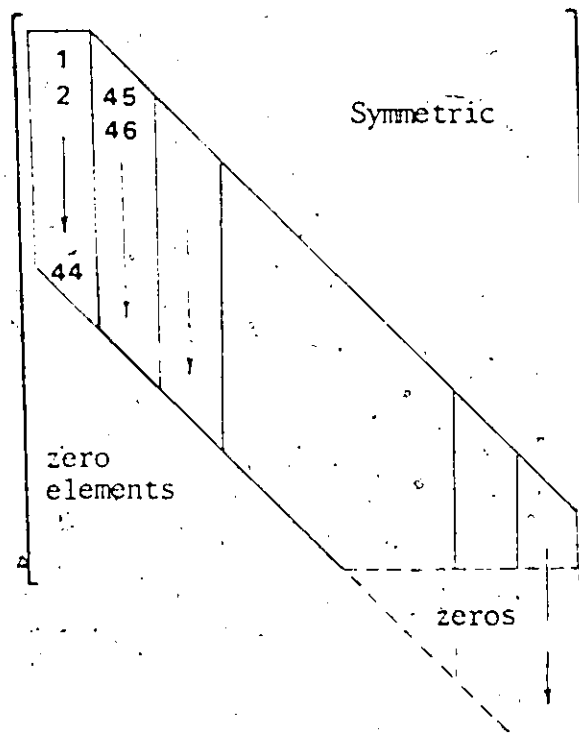


Figure 6. Layout of Equation Storage in Solution Subroutine

### 3.6 - The Velocity Field

The velocity field is related to the potential by Equation (2.5.

1.2) which can be written in component form as

$$\left. \begin{aligned} u &= \phi_x & (a) \\ v &= \phi_y & (b) \\ w &= \phi_z & (c) \end{aligned} \right\} \quad (3.6.1)$$

where  $u$ ,  $v$  and  $w$  are the velocity components in the  $x$ ,  $y$  and  $z$



directions, respectively. The derivatives of the potential within a tetrahedral element are given by Equation (3.3.6). When the values of the potential at the nodal points are determined, they can be substituted back into Equation (3.3.6) to obtain the velocity components within the tetrahedral element. However, the following considerations are to be noted:

1. The assumed linear shape function for the potential  $\phi$  yields a fairly accurate solution for  $\phi$ , yet it implies that the velocity within each element has an average constant value. A higher order shape function will give more accurate values for the velocity as the derivatives of  $\phi$  are no longer constant within the element.
2. The size of the element is a basic factor for accurate velocity calculation. In case of a linear shape function of the potential, the elements have to be made small enough so that a constant velocity within the element could be an acceptable assumption.
3. Similar situations arise in structural mechanics. Zienkiewicz [16] suggested the averaging of the stress of two triangular elements, and considered it as the average stress at some point within the quadrilateral formed by the two adjacent triangles. Another averaging method is to average the stress, at all the elements surrounding one nodal point and consider it as the stress at that node. Norrie and DeVries [4] used the latter averaging method to apply the Kutla condition

to an aerofoil. However, the averaging procedure is not recommended at boundary points or in the region of high stress gradients. Both of the above mentioned averaging methods do not take care of the relative size of the elements encountered in the averaging procedure.

In the present analysis the velocity was checked within some composite units using the averaging procedure, yet the results were found unsatisfactory because the element sizes were not small enough to consider the velocity constant within the tetrahedral element.

## CHAPTER 4

### RESULTS AND CONCLUSIONS

The finite element method, as described in previous chapters, is applied to solve three problems. The results of the three applications are presented in subsequent sections. A Flow Chart of the computer program used for the solution is given in Appendix II.

#### 4.1 Dimensionless Representation of Results

It is useful to represent the results of the problem in terms of dimensionless quantities. Some characteristic (reference) parameters are to be introduced in terms of which the results can be expressed. The variables in a problem can be scaled as multiples of these parameters, regardless of any system of units. One can choose a characteristic length  $L'$  to which all the dimensions of the problem are to be referred. Accordingly, one can define a characteristic velocity  $V'$  as

$$V' \equiv L'/T' \quad (4.1.1)$$

where  $T'$  is a unit time.

Also a characteristic potential  $\phi'$ , can be defined as

$$\phi' \equiv L'V' \quad (4.1.2)$$

Denoting any dimensionless quantity by an asterisk one can express any length in terms of  $L'$ . For example the  $x, y$  and  $z$  coordinates can be written as multiples of  $L'$  as follows:

$$x^* = \frac{x}{L'} \quad (a)$$

$$y^* = \frac{Y}{L}, \quad (b)$$

$$z^* = \frac{z}{L}, \quad (c) \quad (4.1.3)$$

Similarly, the velocity of  $V$  can be expressed in terms of  $V'$  as

$$V^* = \frac{V}{V'}, \quad (4.1.4)$$

Also the potential  $\phi$  can be referred to  $\phi'$  as

$$\phi^* = \frac{\phi}{\phi'}, \quad (4.1.5)$$

Thus, the results can be scaled from the dimensionless representation in any system of units and for any problem having the same proportions.

#### 4.2 Application 1. Flow Around 90° Corner

A three-dimensional analogue of the two-dimensional flow around 90° corner is investigated. This problem was selected to test and compare the results obtained by the finite element method with the exact solution.

The two-dimensional problem has the solution [17]

$$\phi^* = \xi^{*2} - \eta^{*2} = \text{constant},$$

$$\psi^* = 2\xi^*\eta^* = \text{constant}$$

where  $\phi^*$  and  $\psi^*$  are independent of  $z^*$

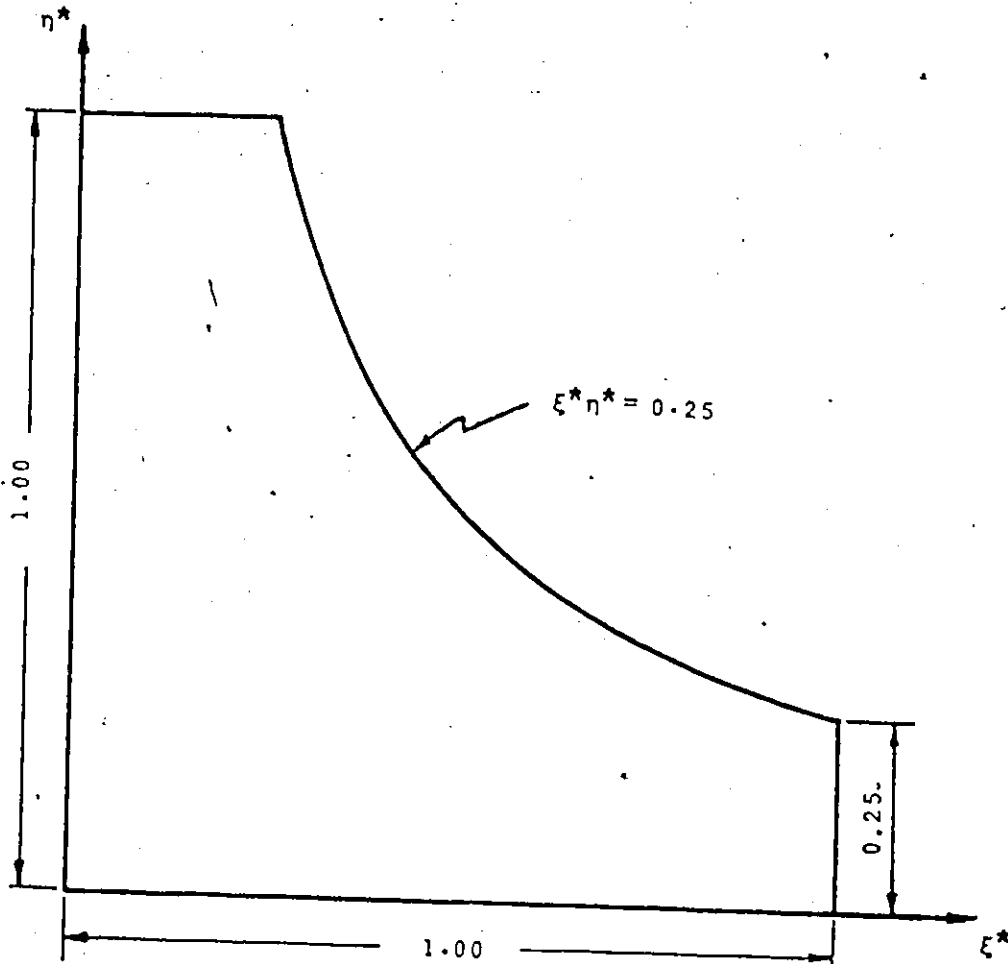


Figure 7. Flow around 90° Corner

The boundaries were selected, as shown in Figure (7) and Figure (8), at

$$\begin{aligned} \xi^* &= 0.0, & \xi^* &= 1.0 \\ \eta^* &= 0.0, & \eta^* &= 1.0 \\ \xi^* \eta^* &= 0.25 \\ z^* &= 0.0, & z^* &= 0.156 \end{aligned}$$

The normal velocity component at the flow boundaries is uniform and has a magnitude of 2.0. The three-dimensional configuration of the flow region is shown as an isometric drawing in Figure (8) with axes re-located for the finite element procedure. The Roman numbers, in Figure (8) indicate the sections into which the region is sliced. The

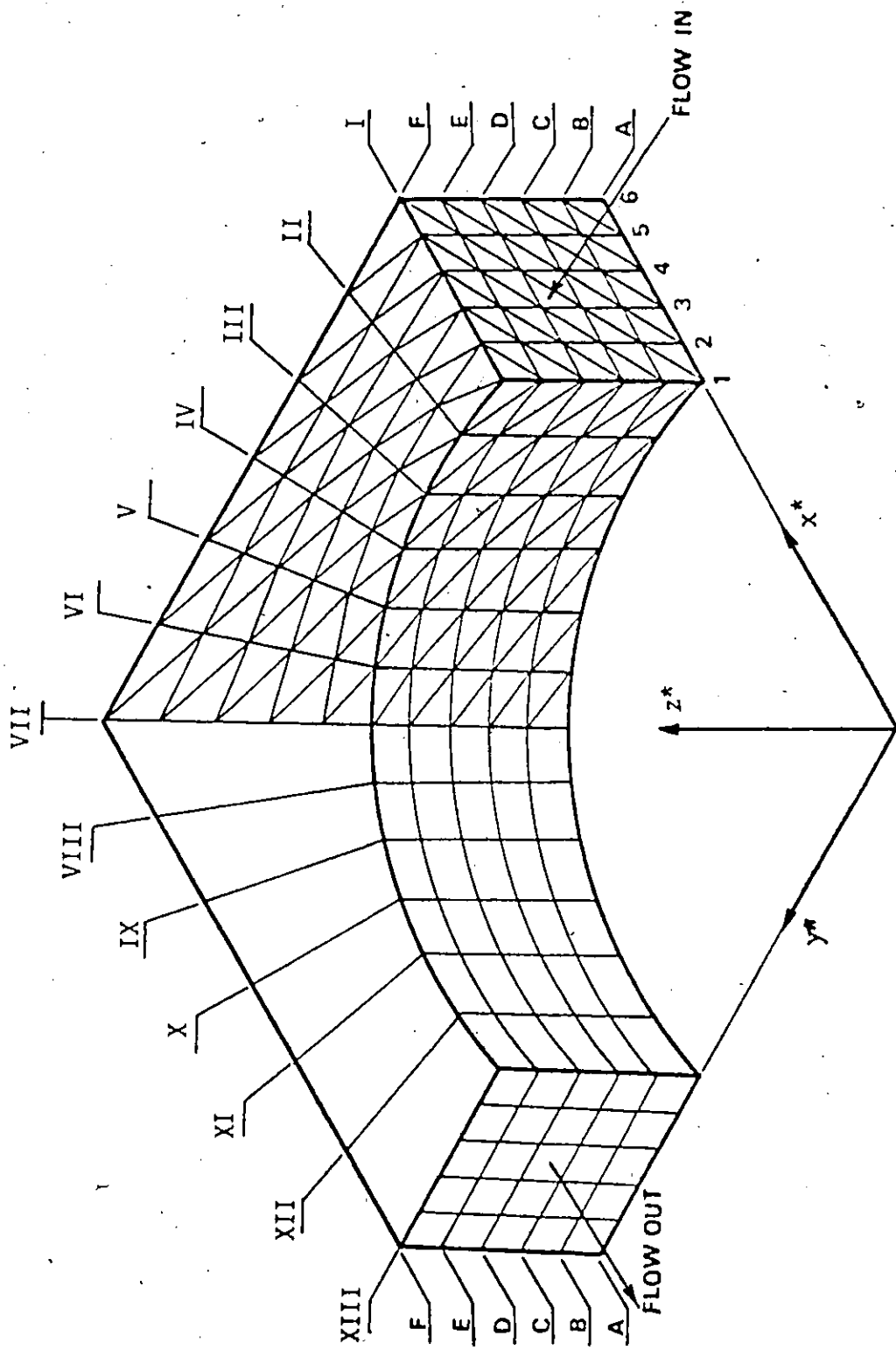


Figure 8. Isometric Configuration  
(Not to scale)

nodal points in one row of each section are labelled 1,2,.....,6. The distance between any two neighbouring horizontal planes is 0.0313. A top view of the discretized region is given in Figure (9), which shows the location of the nodal points on identical horizontal sections.

The results obtained are presented for each horizontal plane, in comparison with the exact solution. Figures (10) through (15) show the results obtained when using the five-tetrahedra composite unit scheme. Figures (16) through (21) show the results of the six tetrahedra composite unit scheme. The maximum absolute error  $\delta$  is written beside each curve. In each of these figures, the nodal points in one section are located on the ~~abscissa~~ with an equal spacing in between, and the values of  $\phi^*$  are represented on the ordinate. The actual distance between two neighbouring nodes in one section can be mapped from Figure (9).

The problem of the  $90^\circ$  bend was solved varying two parameters; the height of the flow region and the number of finite elements. The solution was found to converge towards the exact solution as the element size was decreased. The six-tetrahedra scheme showed better accuracy for the same number of nodes, than the five-tetrahedra scheme (the six-tetrahedra scheme yielded results with less absolute error than the five-tetrahedra scheme).

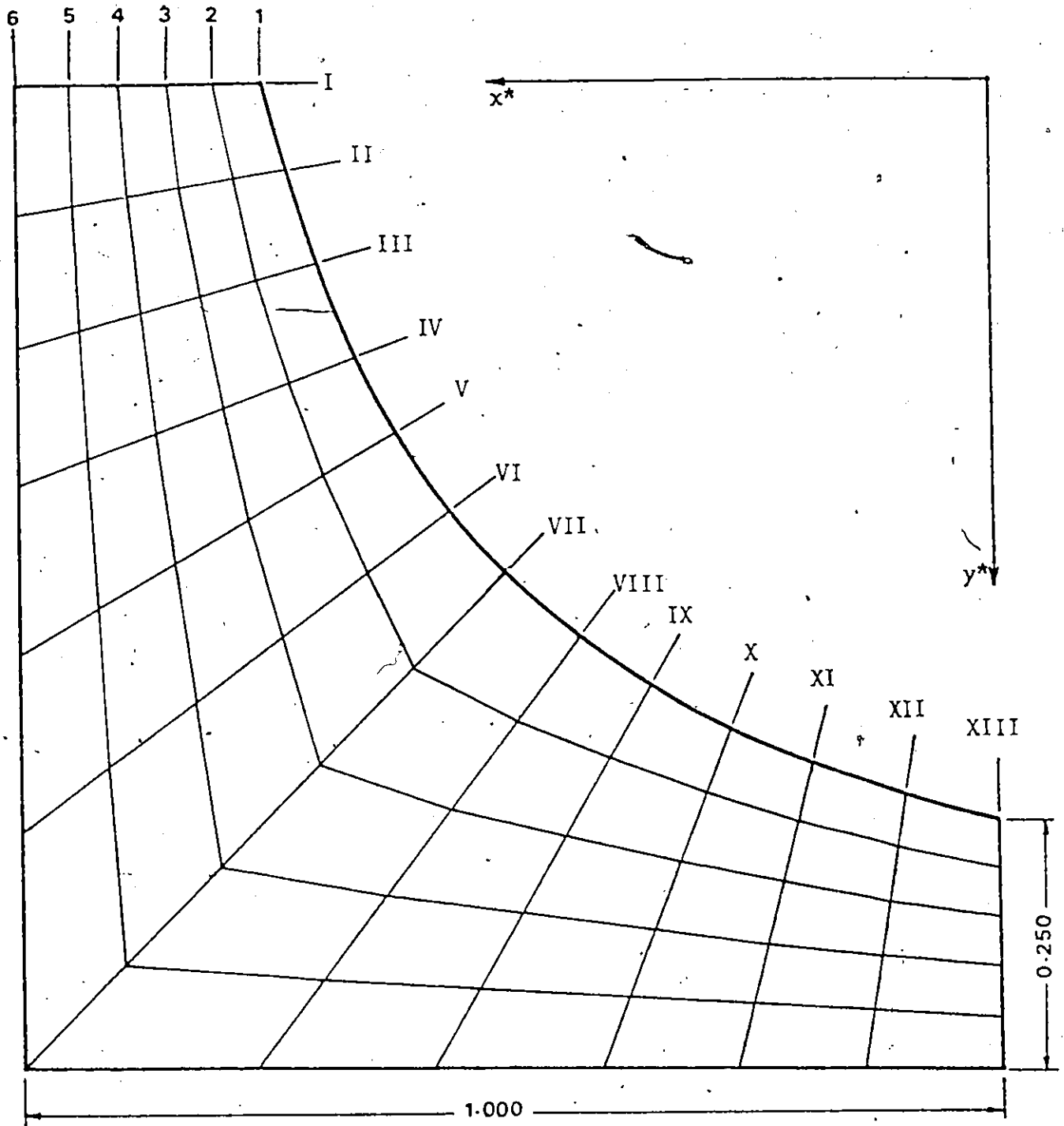


Figure 9. Location of Nodal Points on a Horizontal Plane.



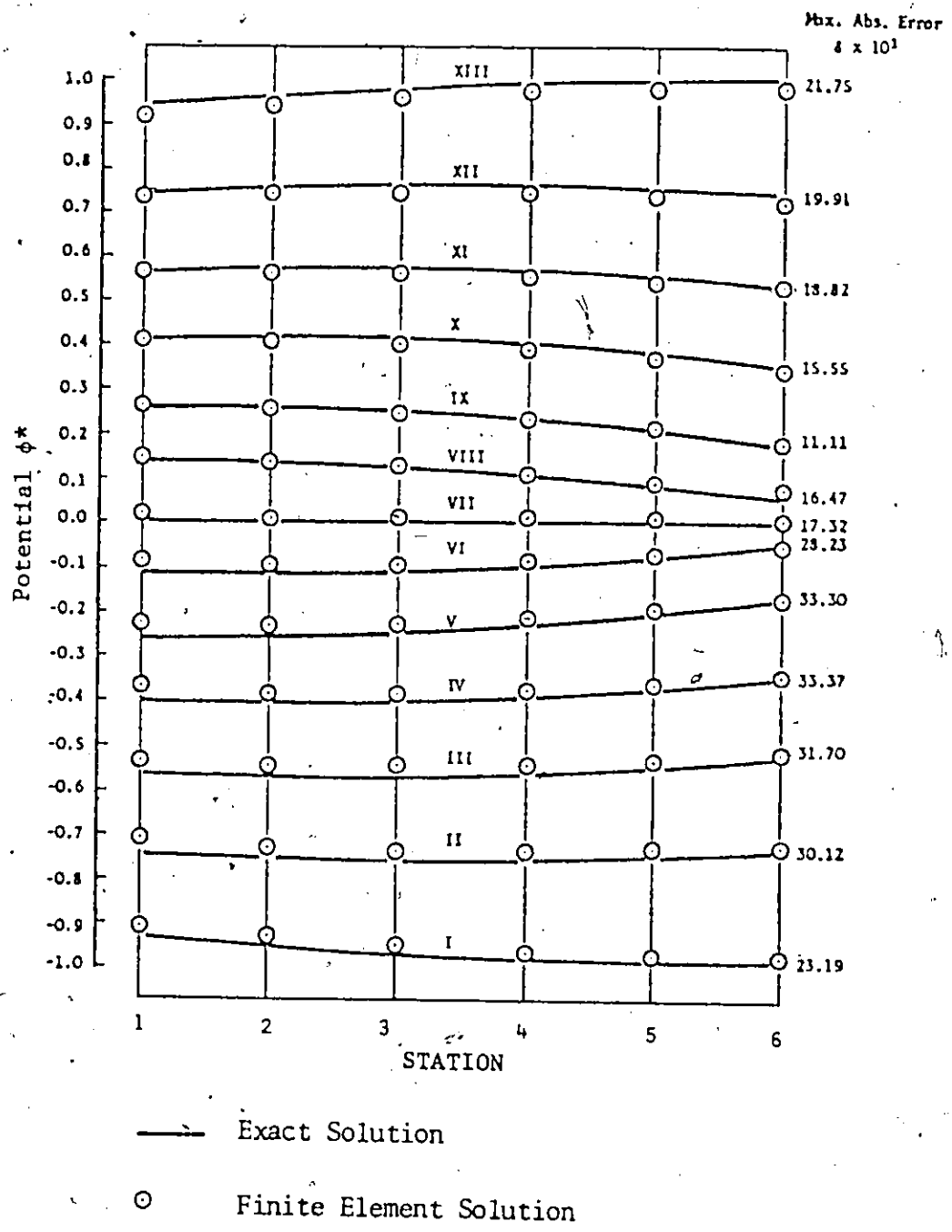


Figure 10. Potential Distribution on Plane A-A  
 (Five Tetrahedral Scheme)

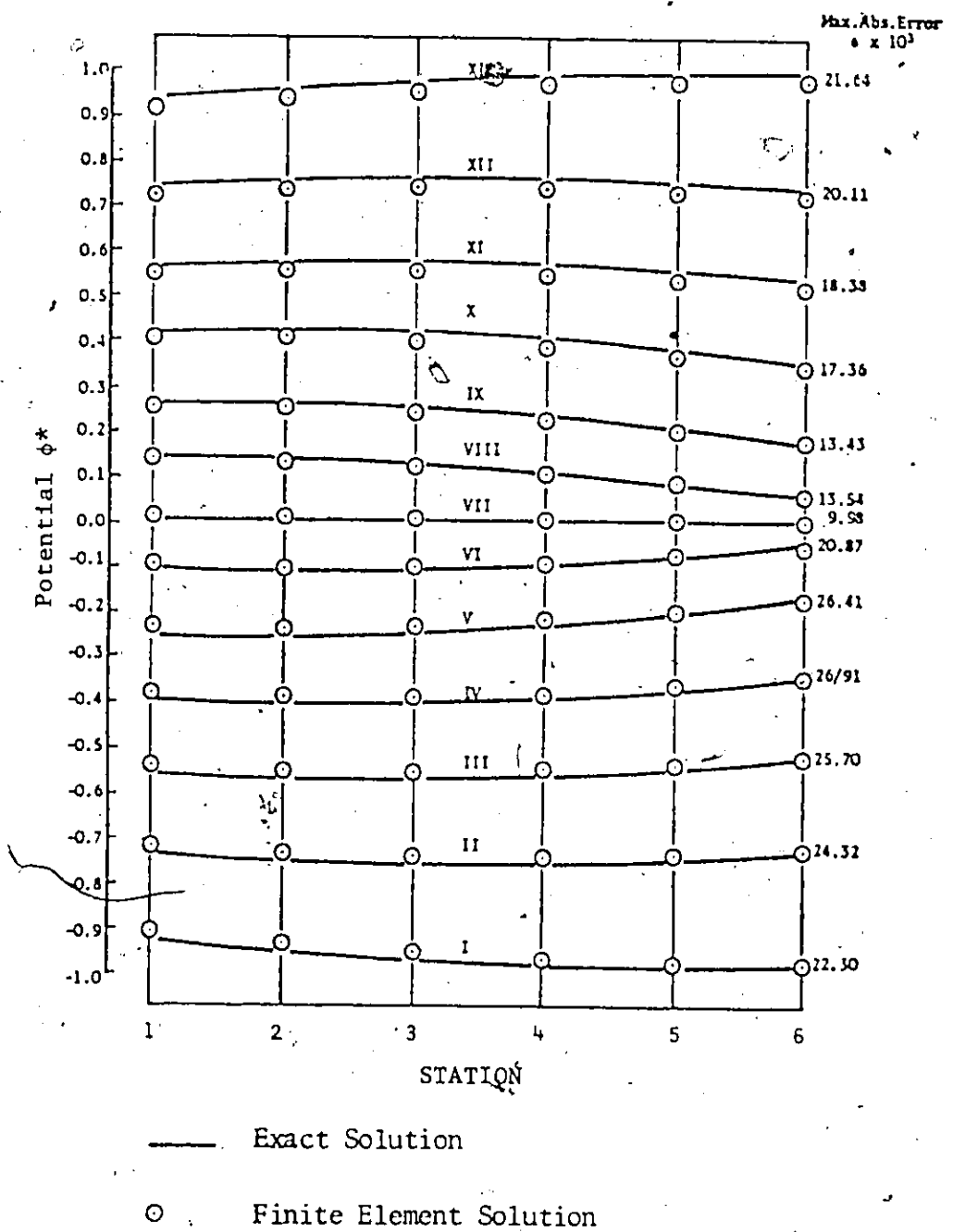
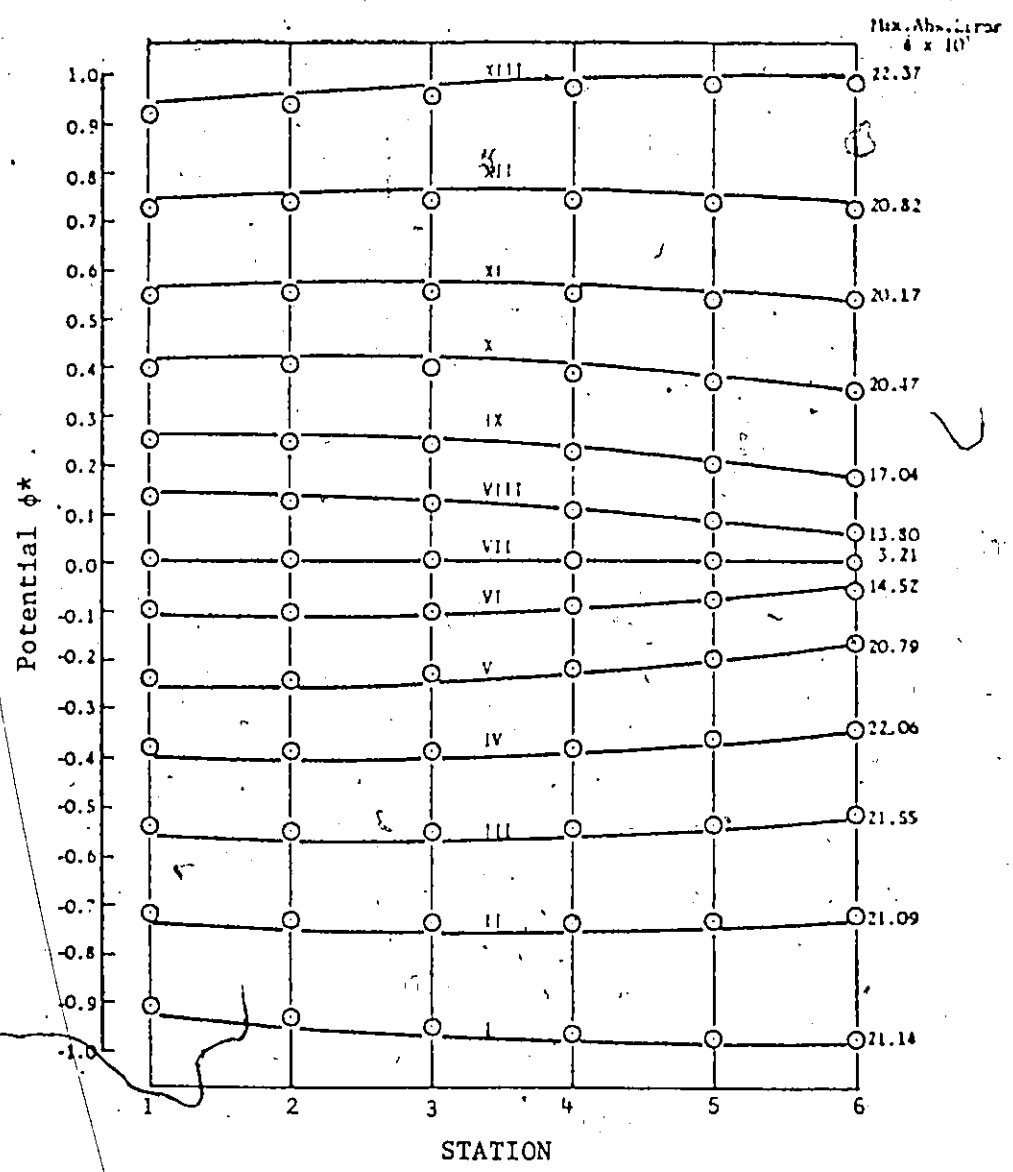
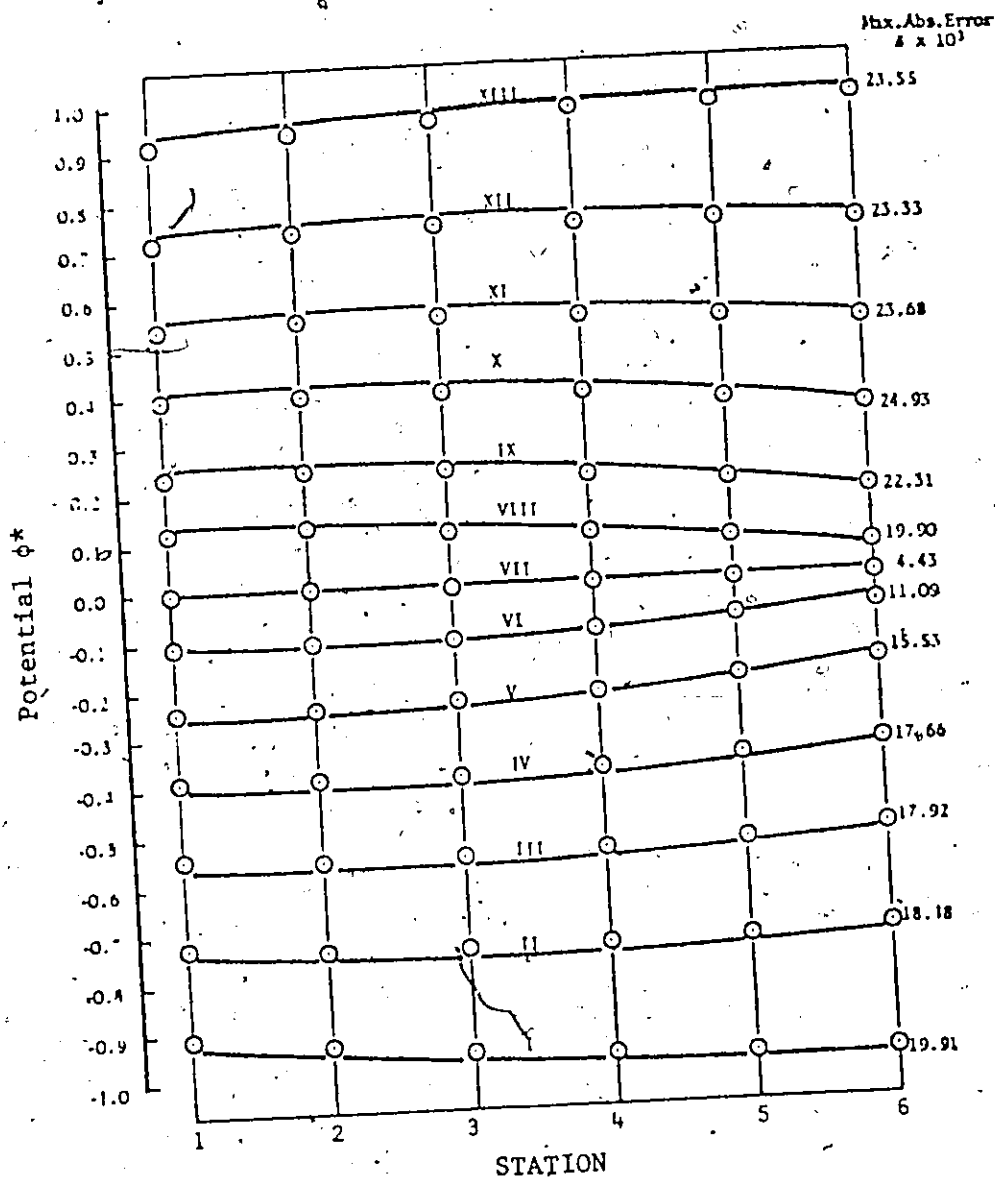


Figure 11. Potential Distribution on Plane B-B (Five Tetrahedral Scheme)



— Exact Solution  
○ Finite Element Solution.

Figure 12. Potential Distribution on Plane C-C (Five Tetrahedral Scheme)



— Exact Solution

○ Finite Element Solution.

Figure 13. Potential Distribution on Plane D-D  
(Five Tetrahedral Scheme)

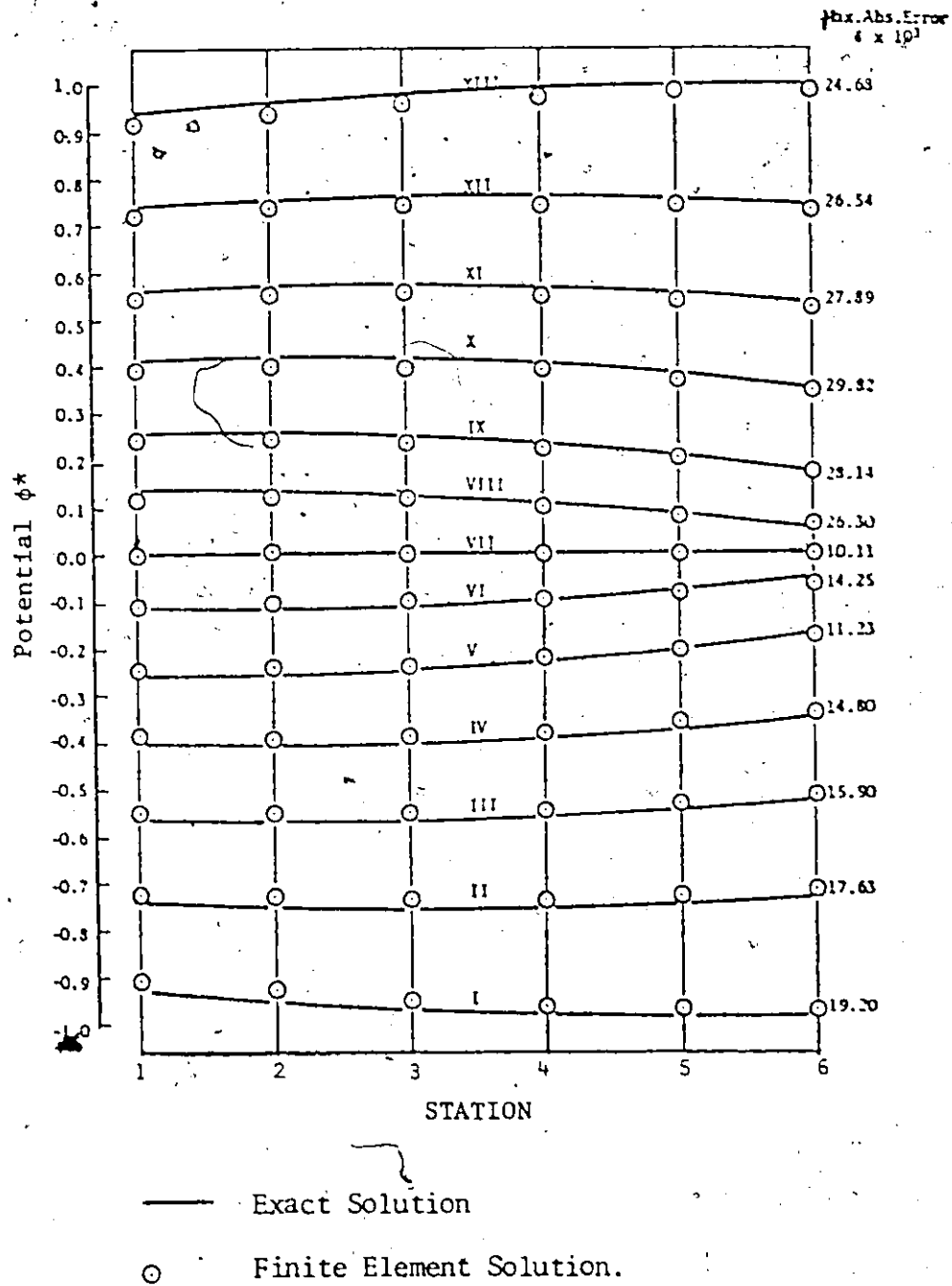
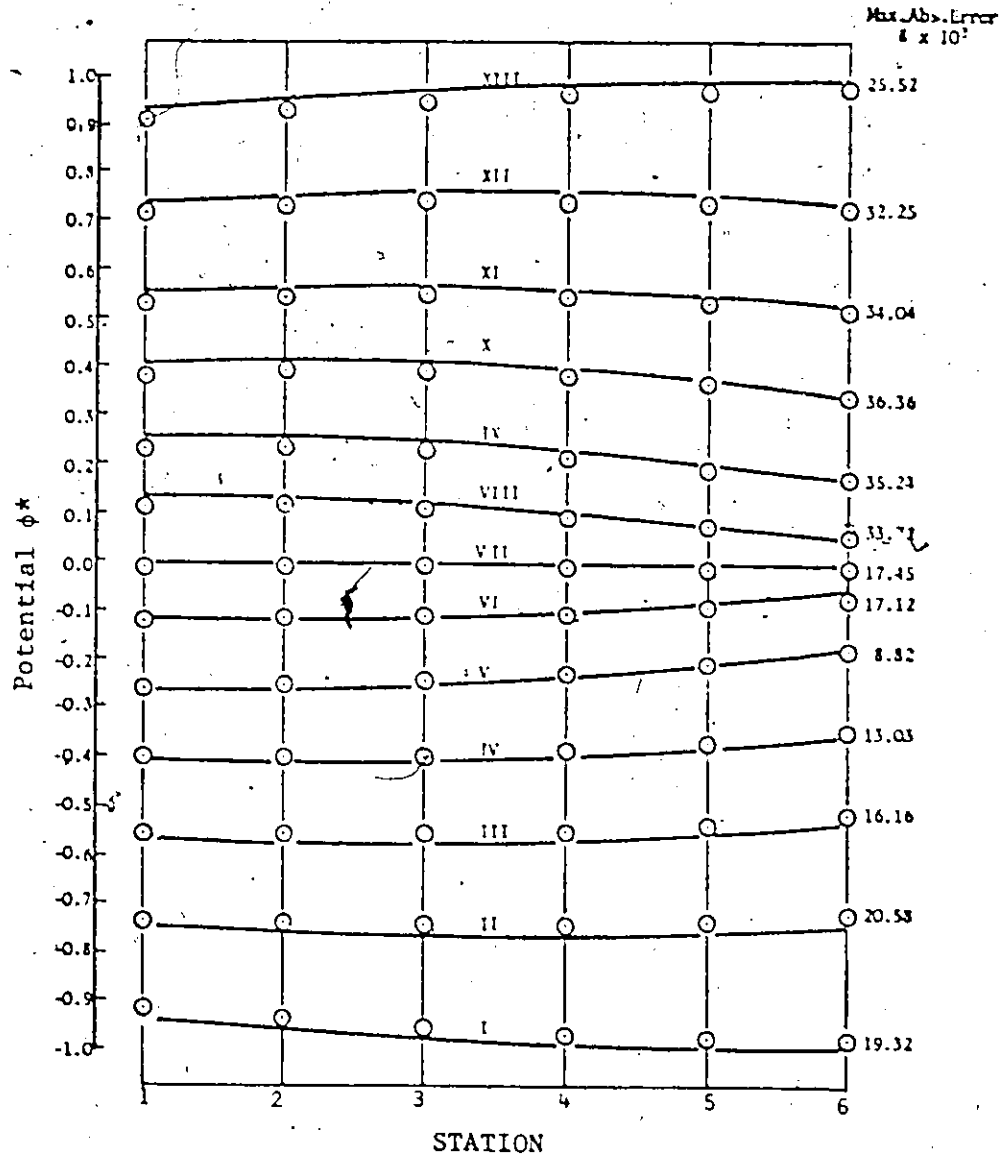
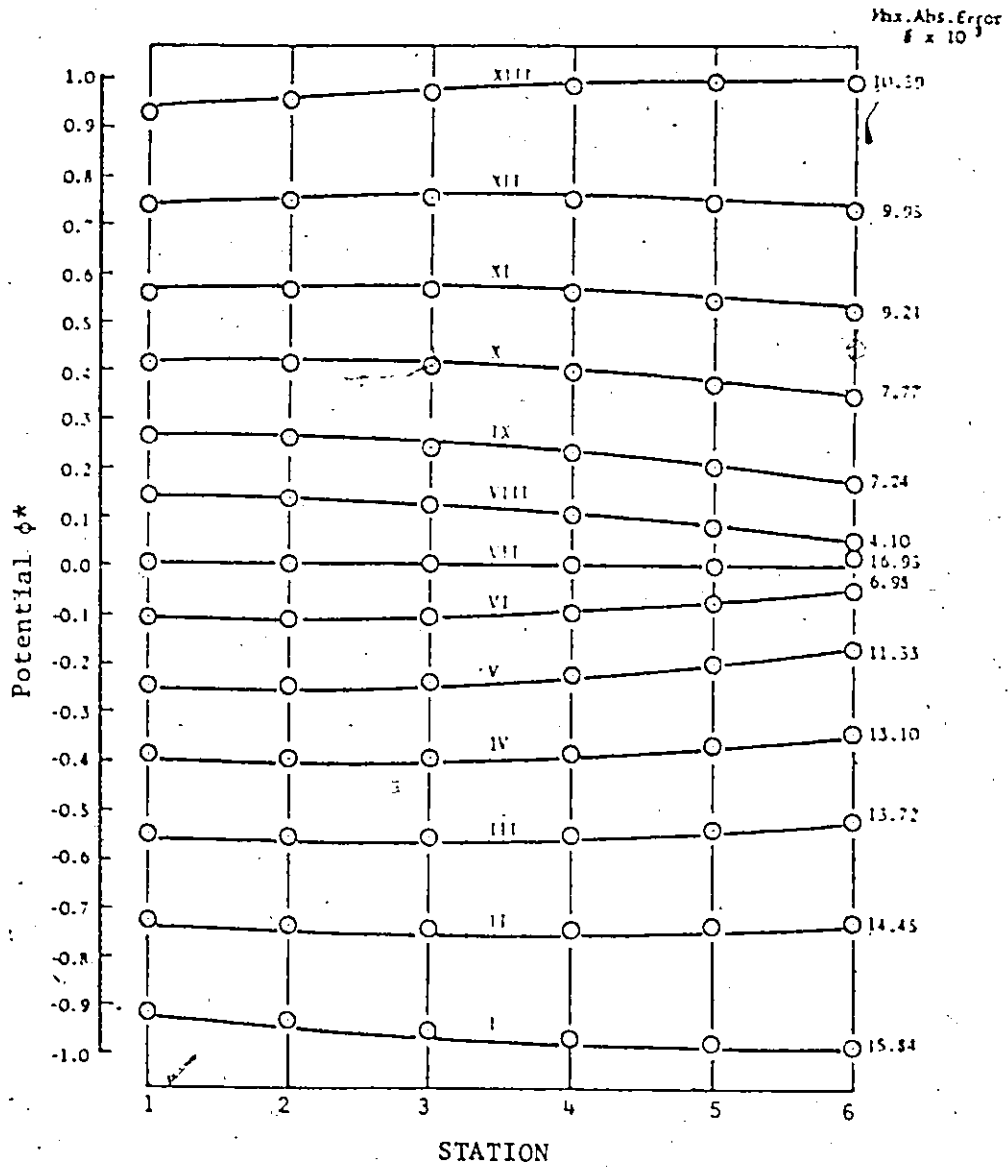


Figure 14. Potential Distribution on Plane E-E  
(Five Tetrahedral Scheme).



— Exact Solution  
 ○ Finite Element Solution

Figure 15. Potential Distribution on Plane F-F  
 (Five Tetrahedral Scheme)



— Exact Solution  
 ○ Finite Element Solution

Figure 16. Potential Distribution on Plane A-A  
 (Six Tetrahedral Scheme)

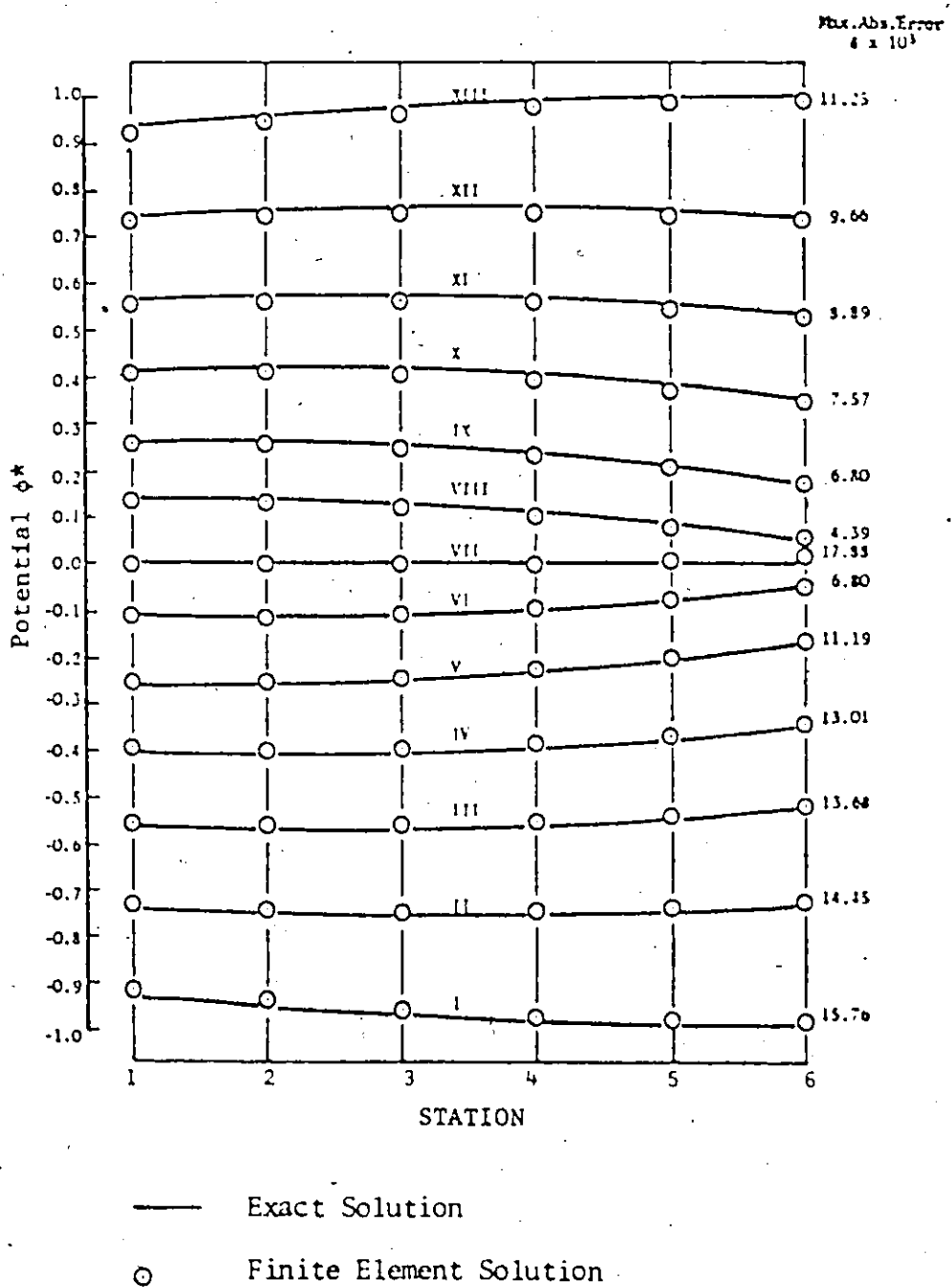


Figure 17. Potential Distribution on Plane B-B  
(Six Tetrahedral Scheme)



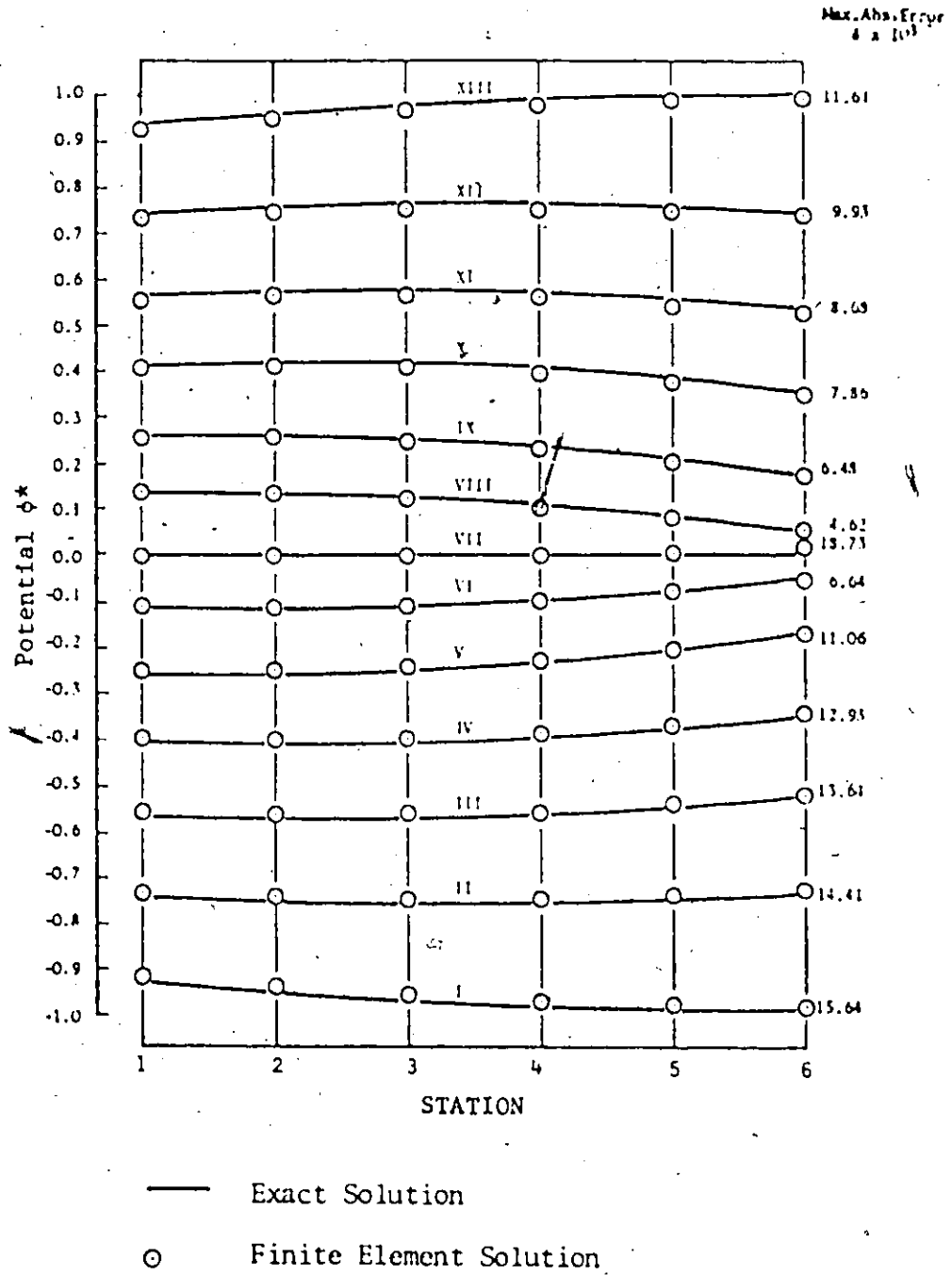


Figure 18. Potential Distribution on Plane C-C  
(Six Tetrahedral Scheme)

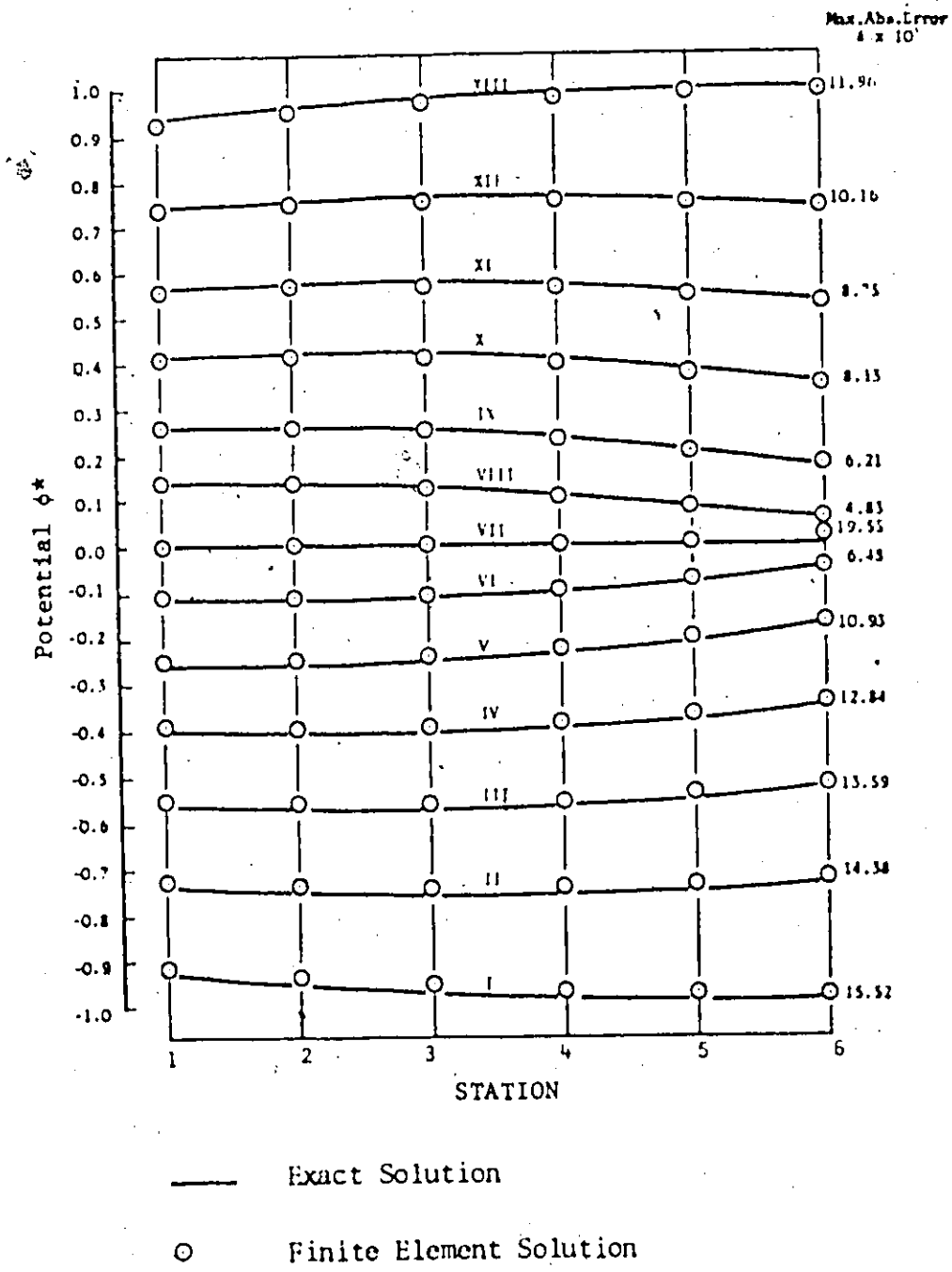


Figure 19. Potential Distribution on Plane D-D  
(Six Tetrahedral Scheme)

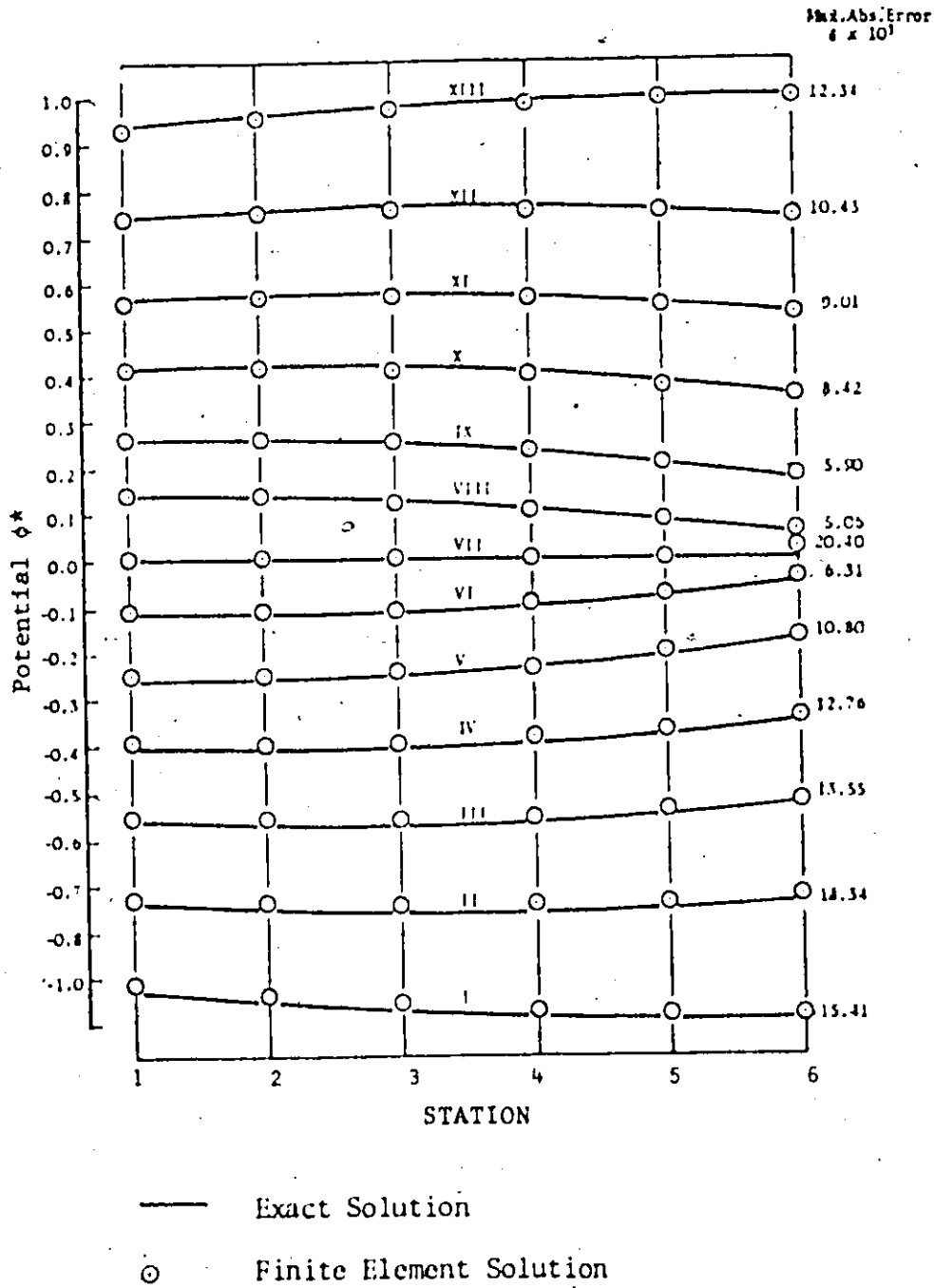


Figure 20. Potential Distribution on Plane E-E  
(Six Tetrahedral Scheme)

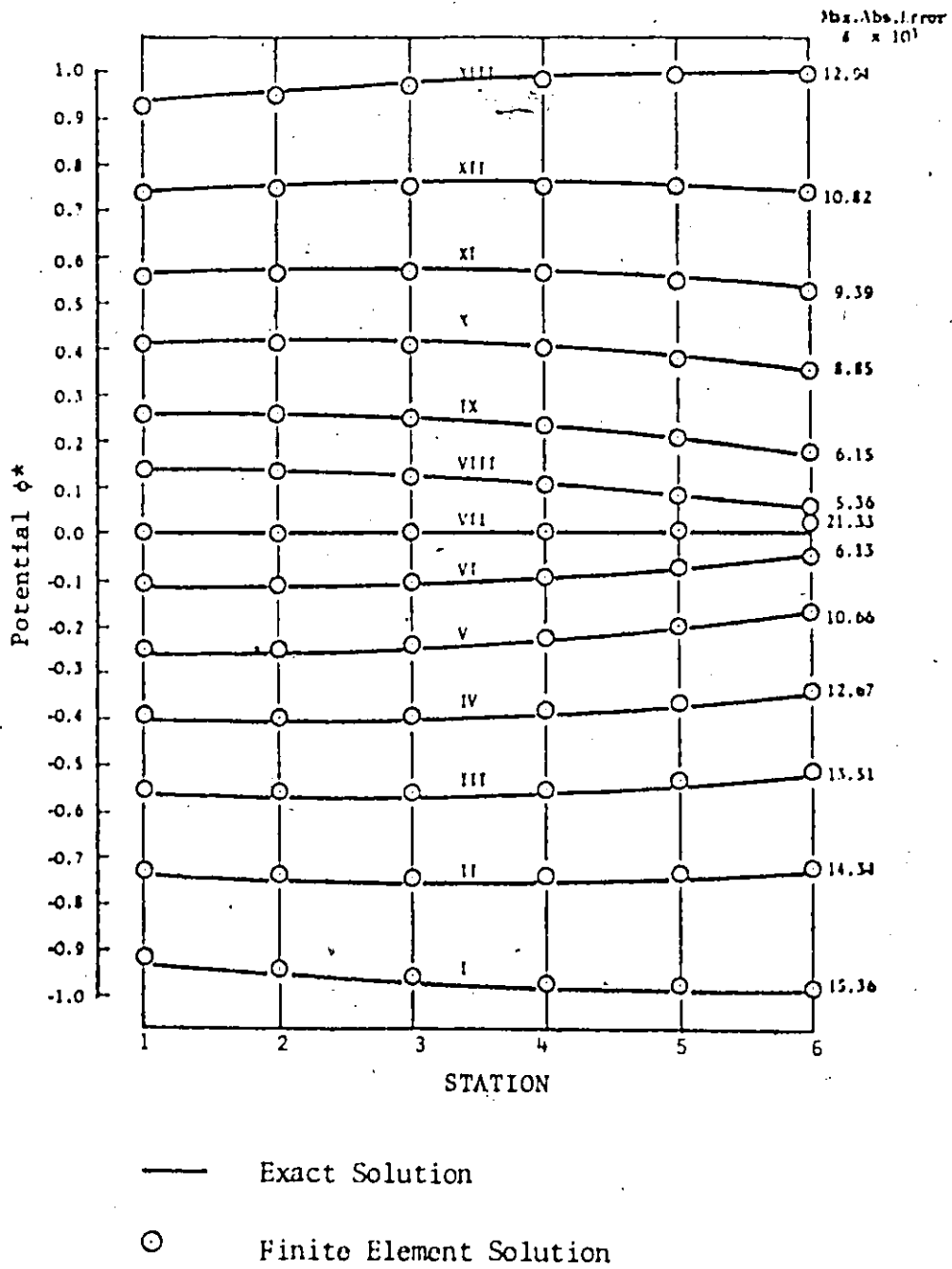


Figure 21. Potential Distribution on Plane F-F  
 (Six Tetrahedral Scheme)

#### 4.3 Application 2. Reducing Bend of Square Cross-Section Base Centred on a Circular Arc.

The three projections of the reducing bend, in this application, are shown in Figure (22). Figure (23) shows a top view of the discretization of the flow region in which each cross section is square. The sections are labelled with Roman numbers. The normal velocity component at the inlet and exit planes is assumed to have a flat profile. The normal component at the inlet is assumed to be 1.0, and at the exit 9.0. Figures (24) through (36) show the equi-potential contours on each section. In each of these figures, the left edge is the base of the cross section and the lower edge is the side of the section nearest to the centre of the circular arc. The equi-potential levels are indicated by sets of numbers increasing in size to show the trend of increase of the potential. The finite element method gave the potential at 36 points (6 x 6) on one cross-section. This has been expanded to 900 points (30 x 30) using a bi-cubic spline interpolation subroutine. The region was discretized using a simple computer program to obtain the nodal point coordinates. An arbitrary nodal point was selected and assumed to have zero potential to remove the singularity from the system property matrix.

Figure 22. Reducing Bend Projections

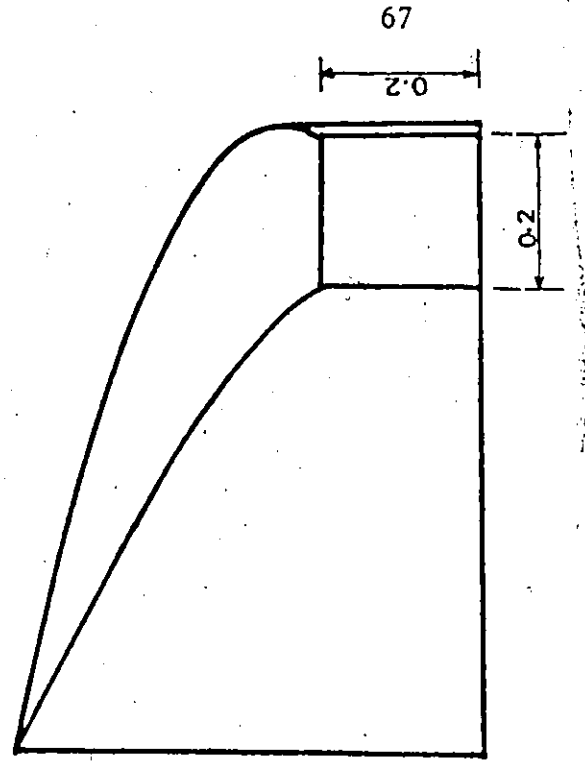
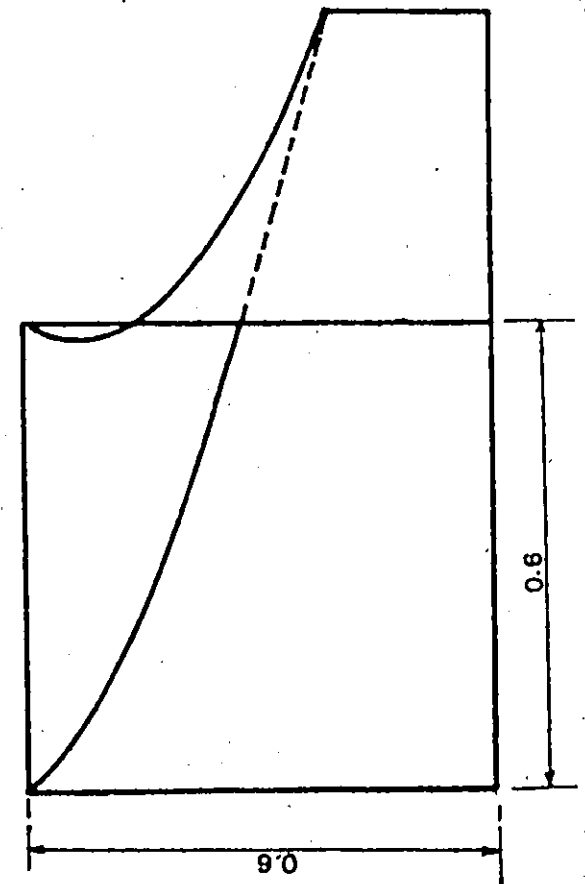
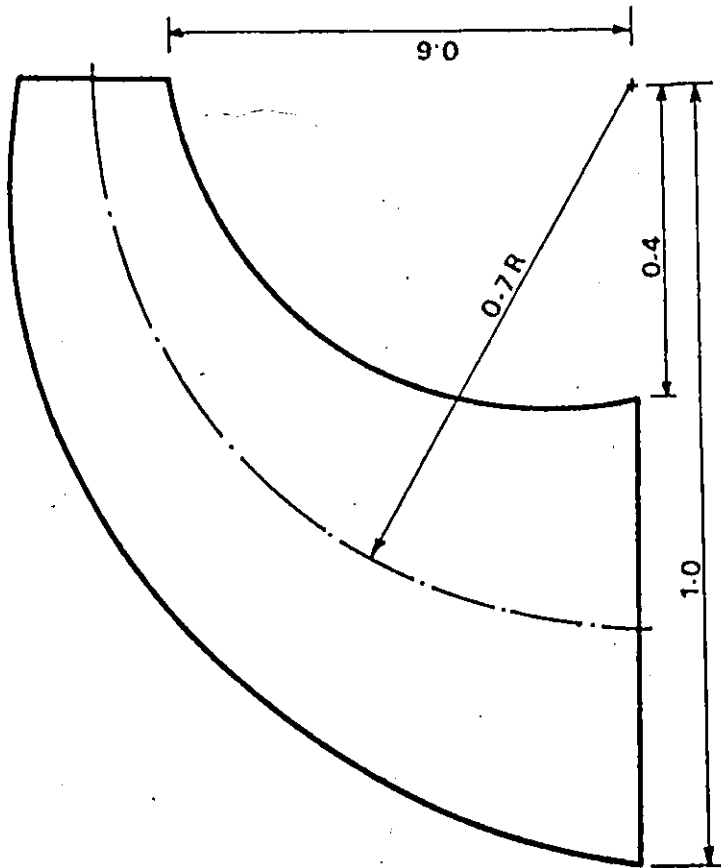
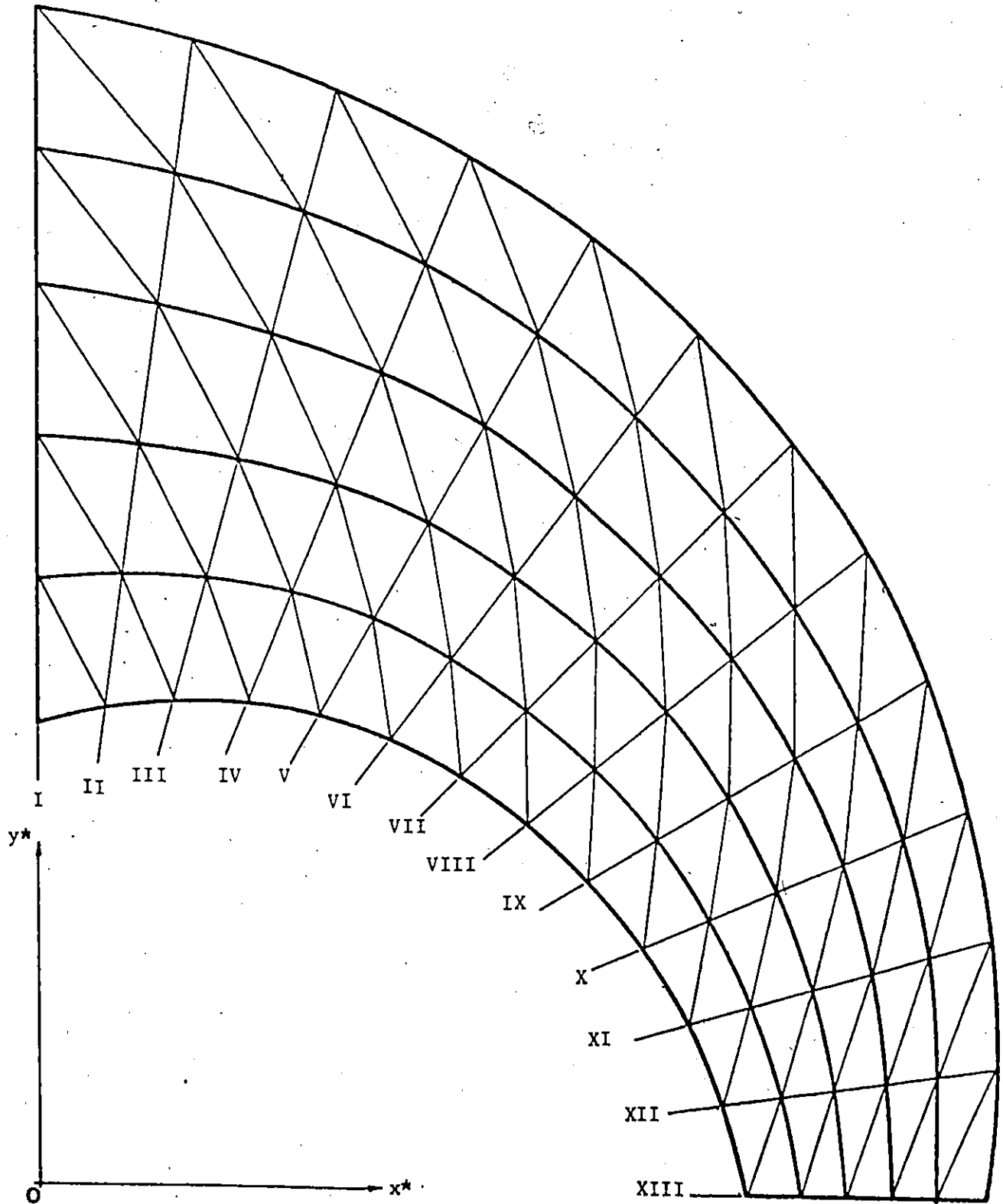
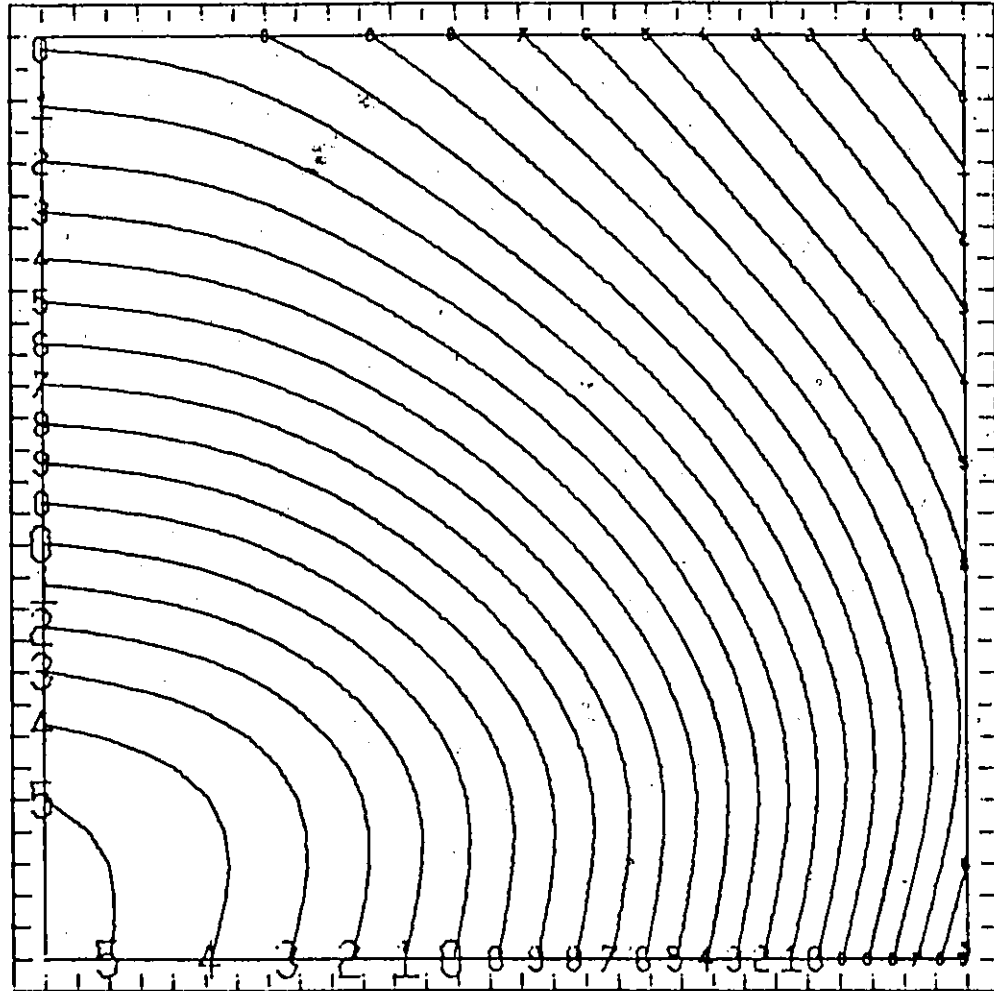


Figure 23. Top View of Discretized Region

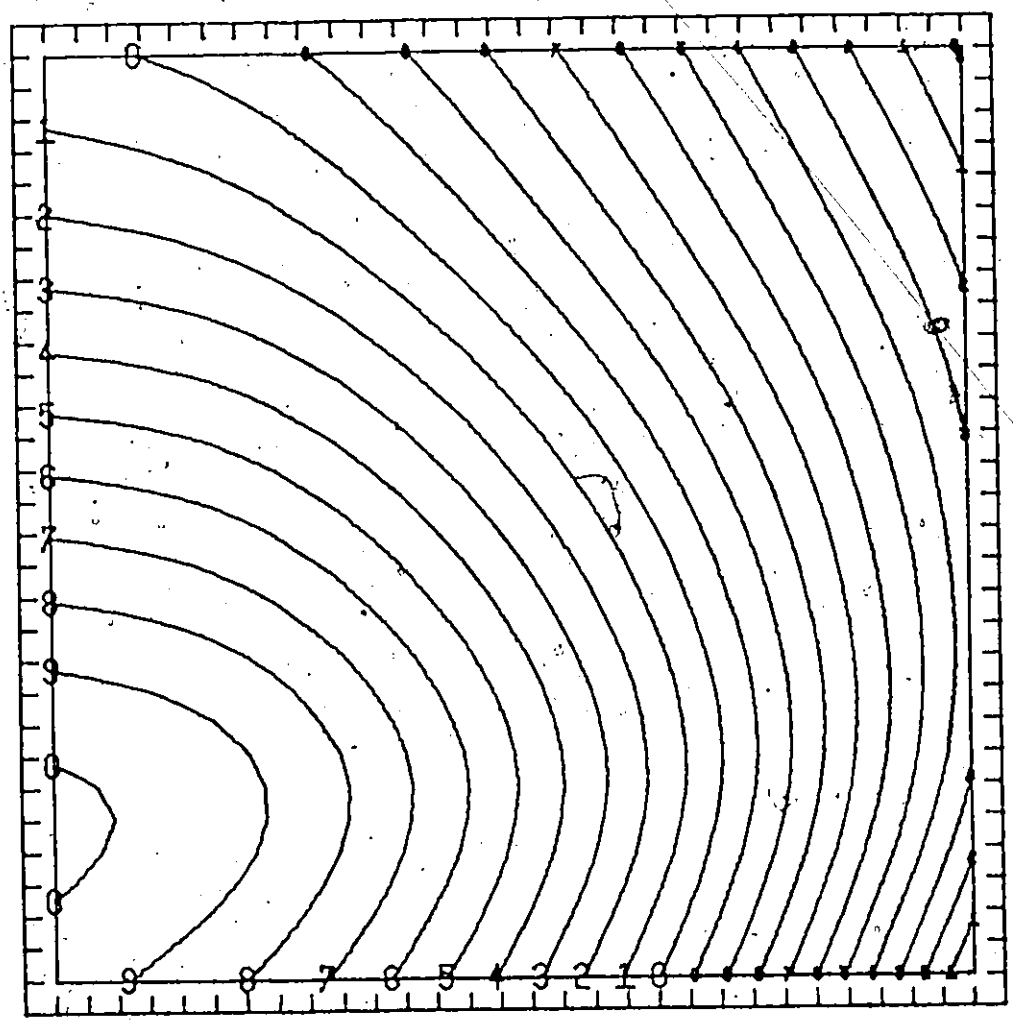




Min. - 0.900  
Max. - 0.630  
Step 0.01  
Section Size (0.600 x 0.600)

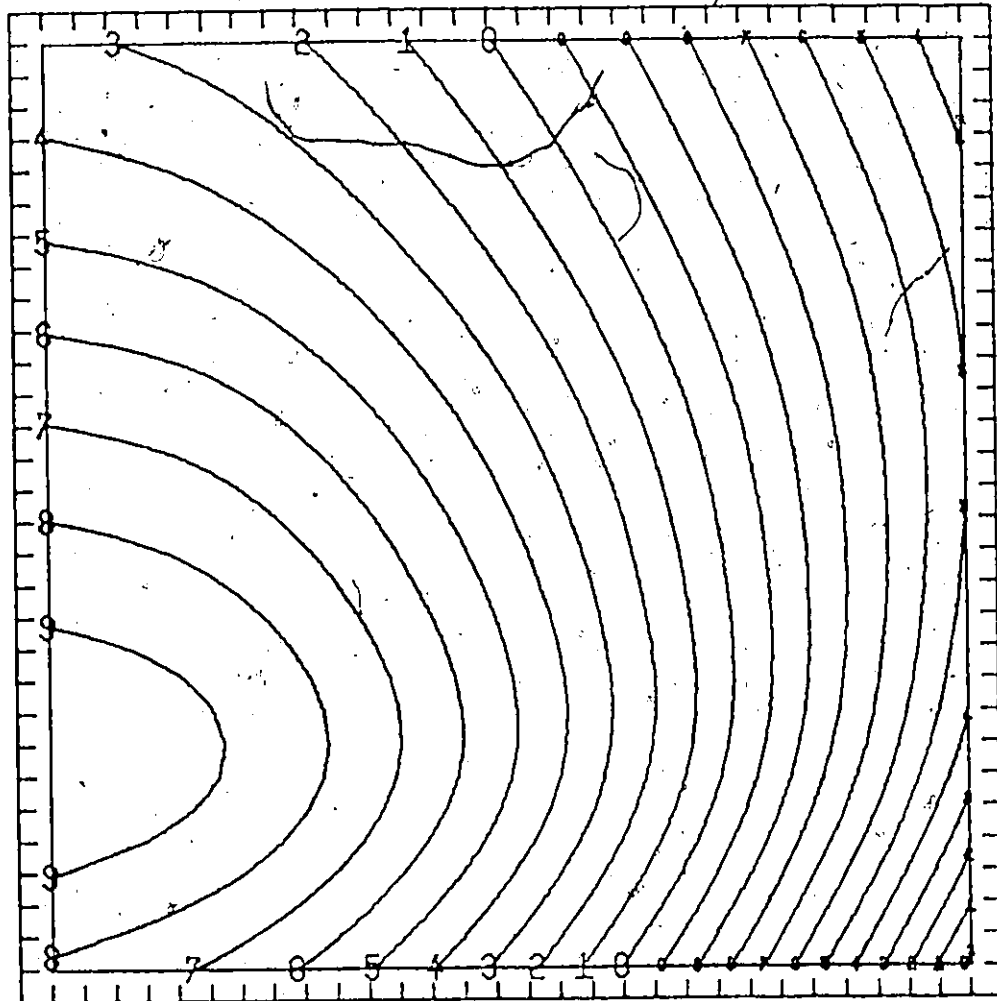
Figure 24. Equipotential Contours on Section I





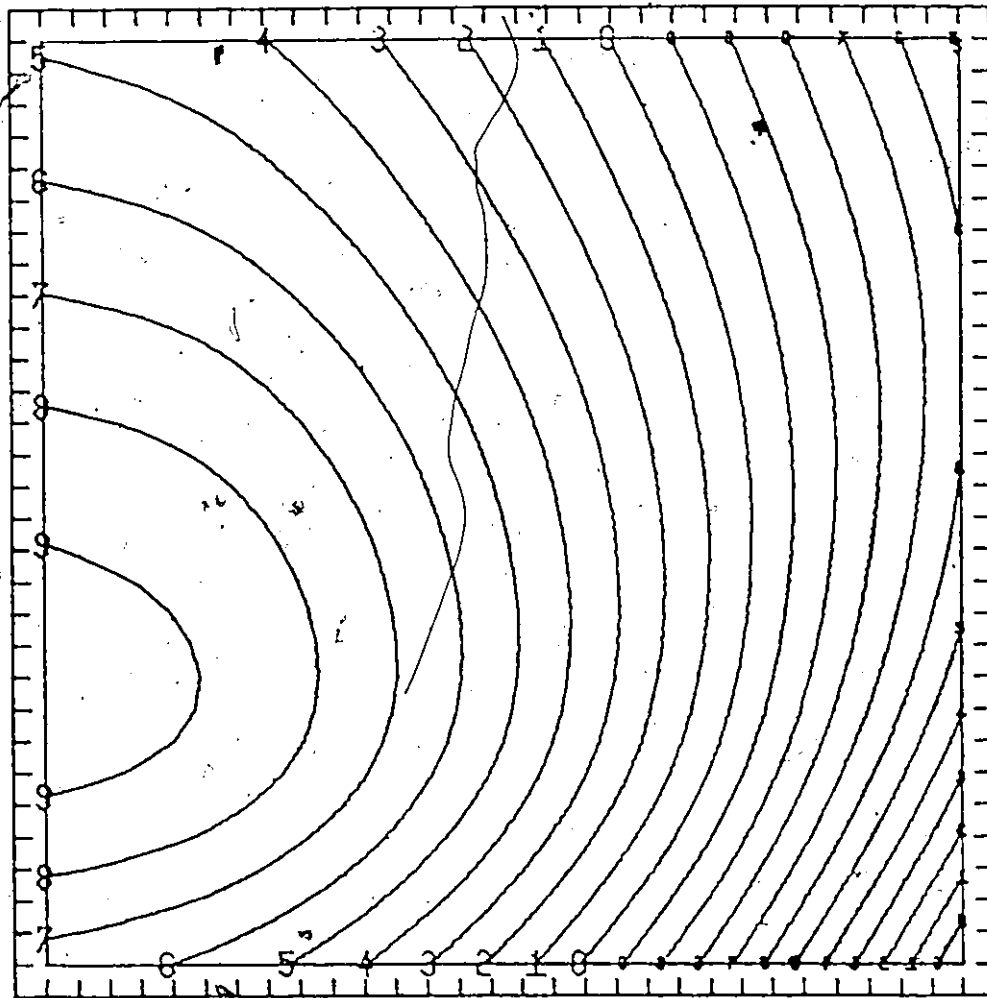
Min. - 0.770  
Max - 0.560  
Step 0.01  
Section Size (0.567 x 0.567)

Figure 25. Equipotential Contours on Section II



Min. - 0.670  
Max. - 0.470  
Step 0.01  
Section Size (0.533 x 0.533)

Figure 26. Equipotential Contours on Section III



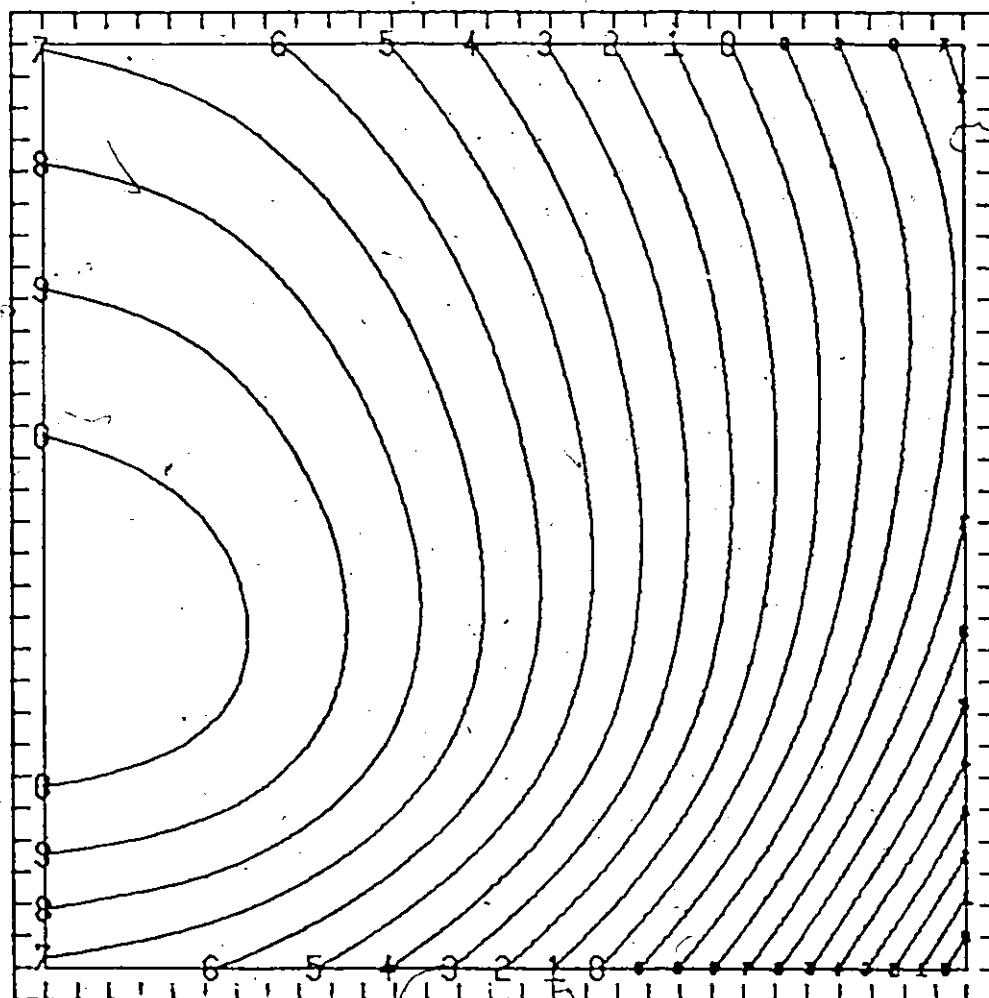
Min. - 0.550

Max. - 0.350

Step 0.01

Section Size (0.500 x 0.500)

Figure 27. Equipotential Contours on Section IV



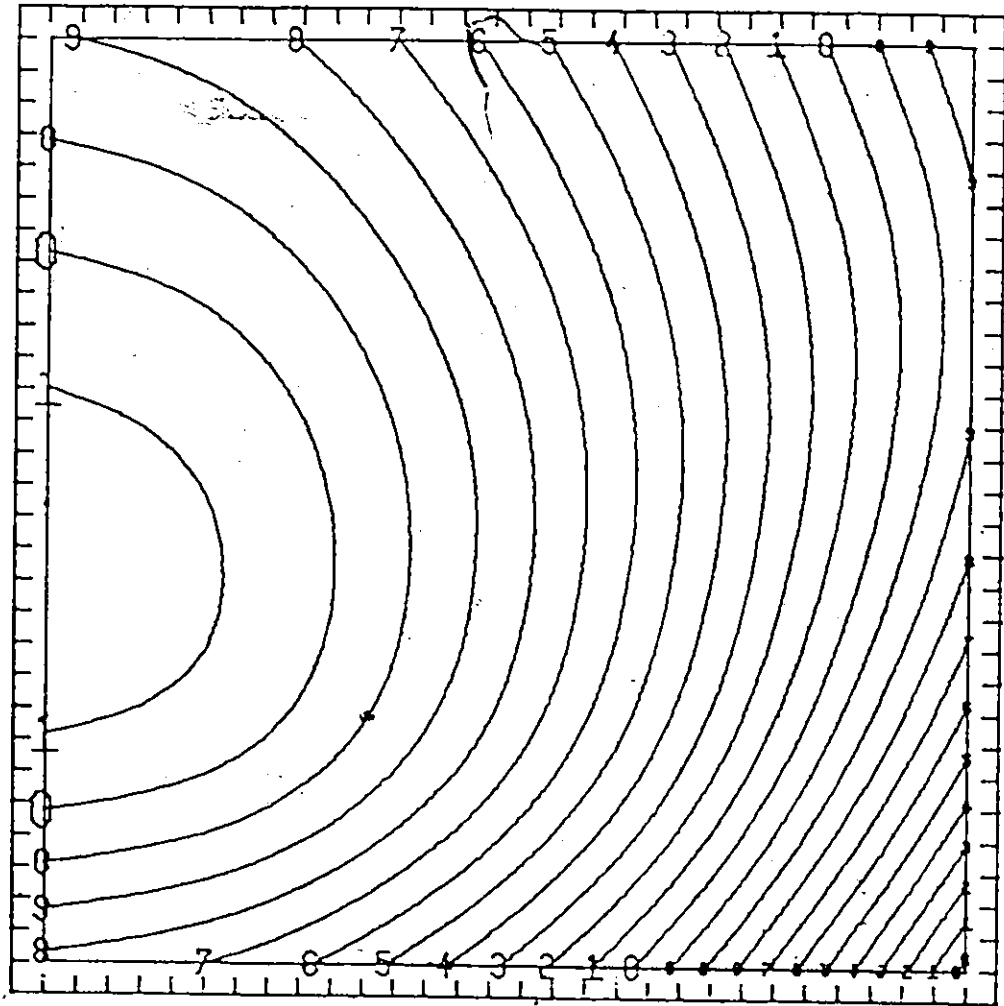
Min. = 0.420

Max. = 0.210

Step = 0.01

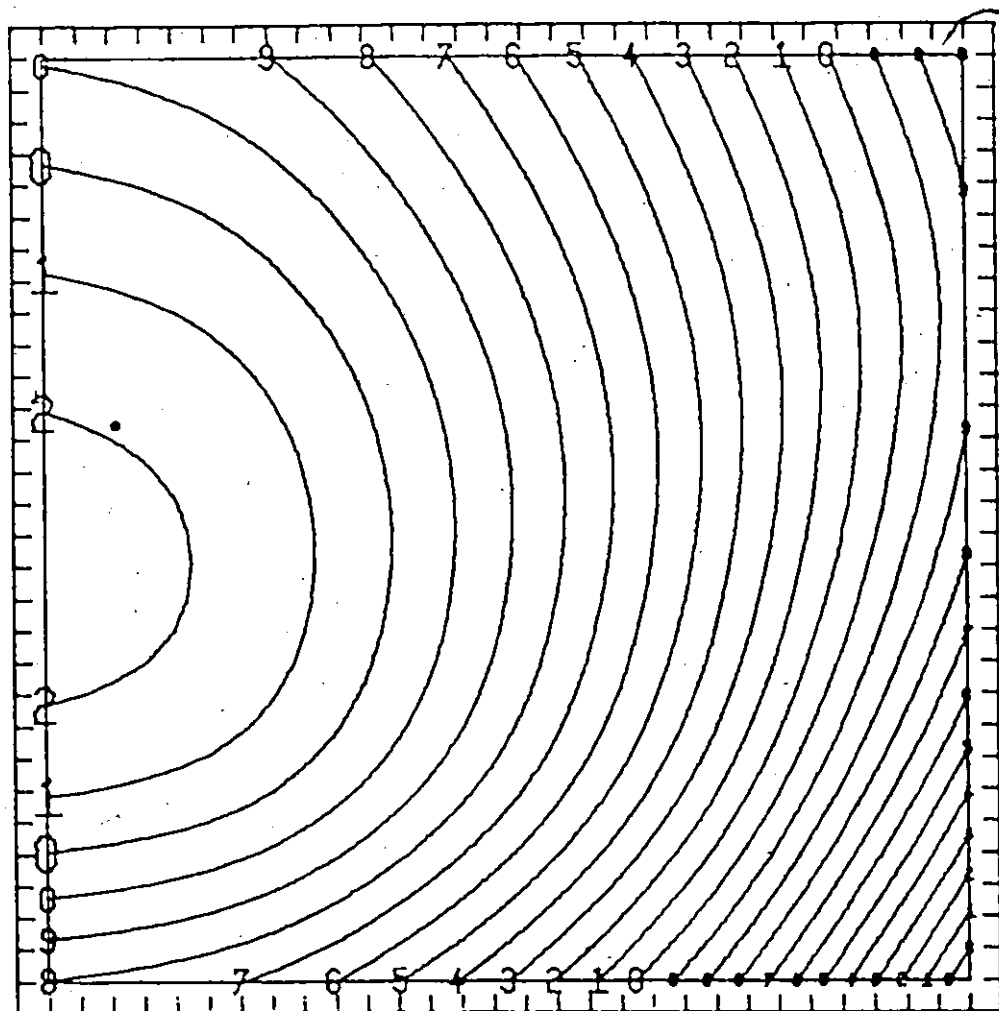
Section Size (0.467 x 0.467)

Figure 28. Equipotential Contours on Section V



Min. - 0.270  
Max. - 0.040  
Step 0.01  
Section Size (0.433 x 0.433)

Figure 29. Equipotential Contours on Section VI



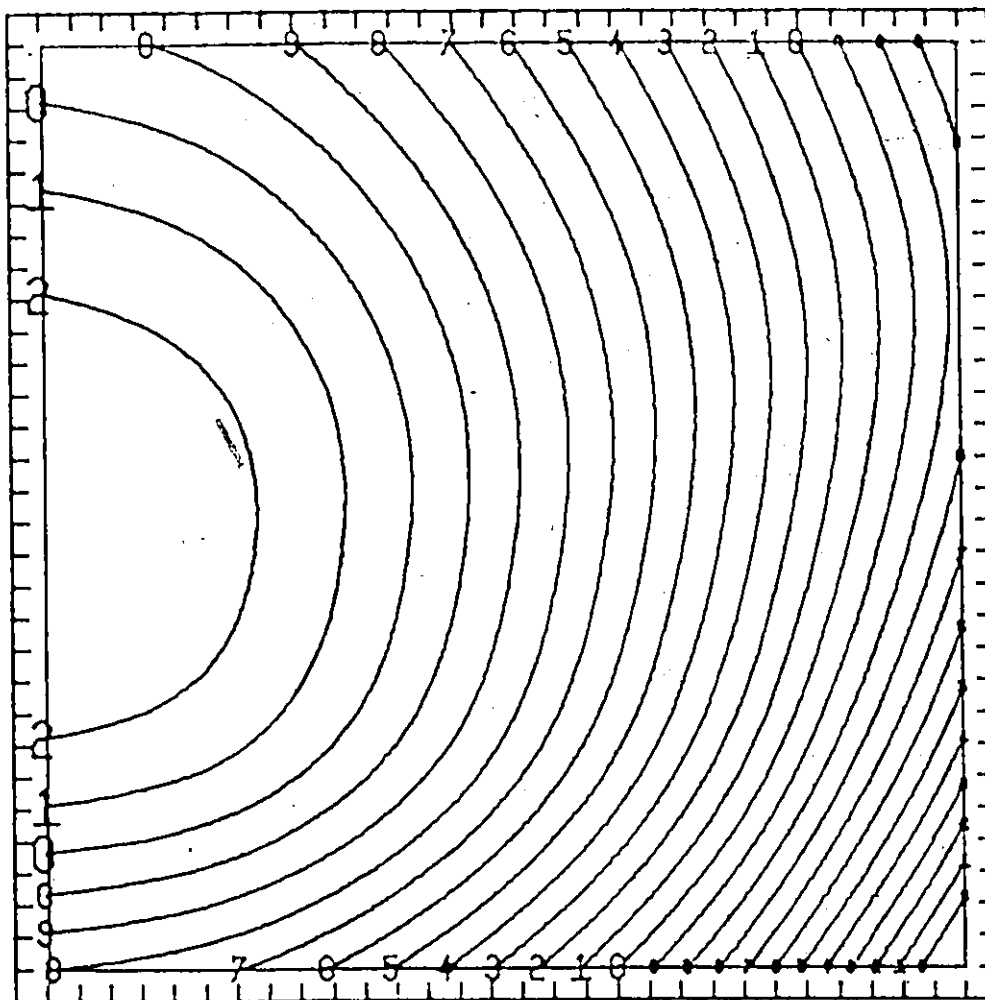
Min. - 0.080

Max + 0.160

Step. 0.01

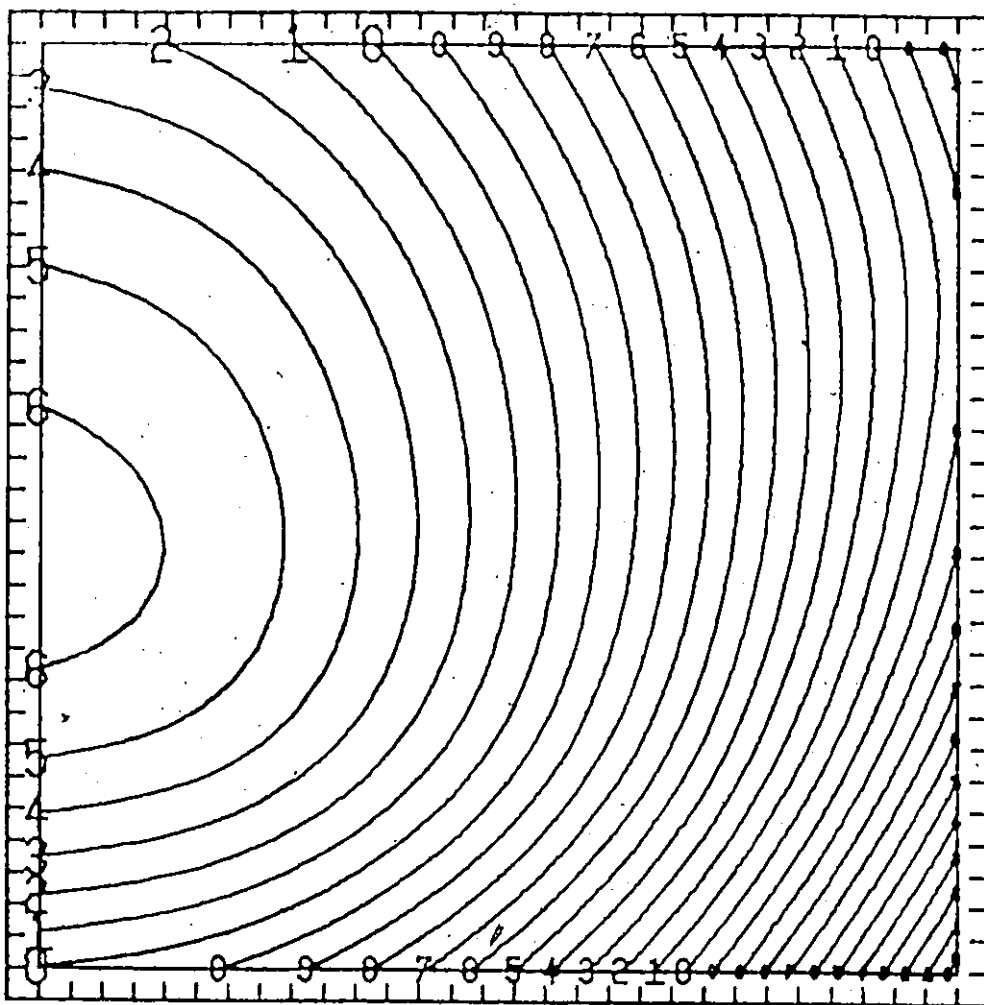
Section Size (0.400 x 0.400)

Figure 30. Equipotential Contours on Section VII



Min. 0.150  
Max 0.390  
Step 0.01  
Section Size (0.367 x 0.367)

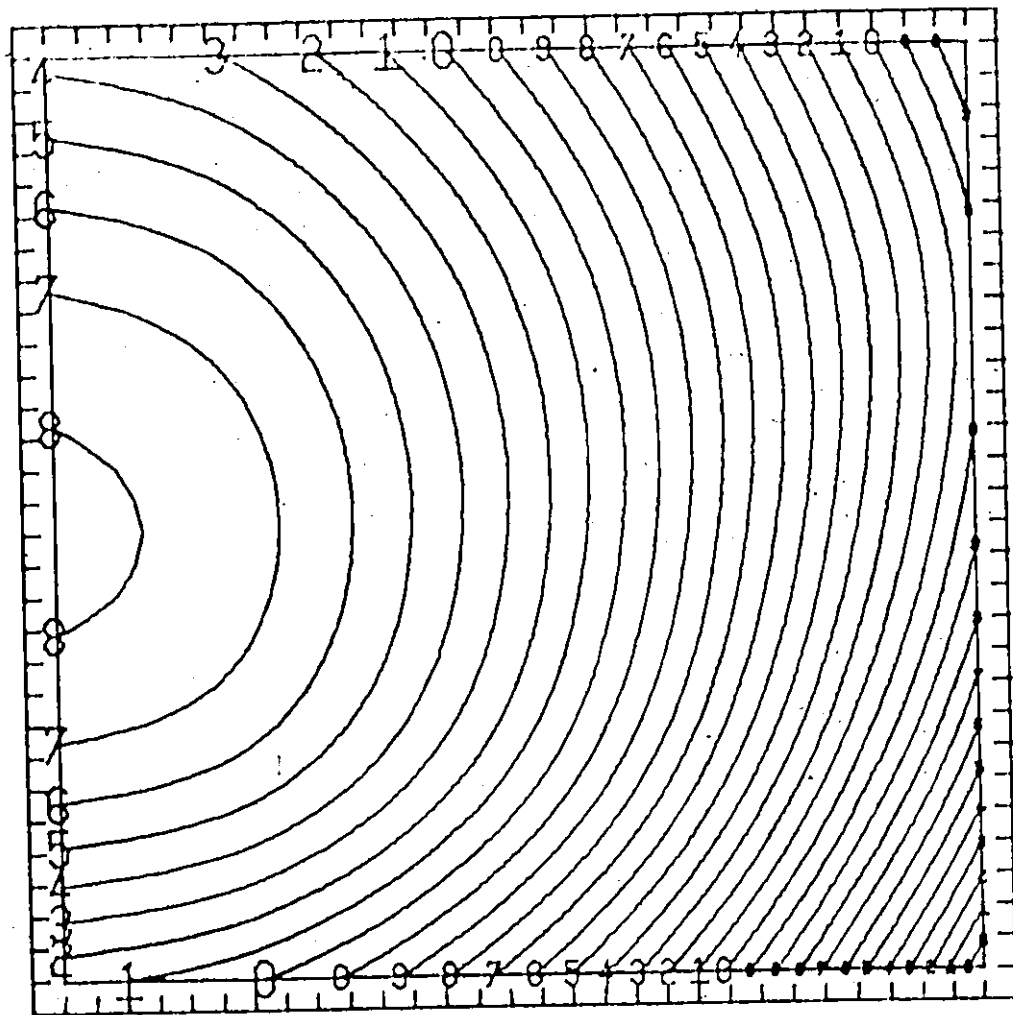
Figure 31. Equipotential Contours on Section VIII



Min. 0.400  
Max. 0.680  
Step 0.01  
Section Size (0.333 x 0.333)

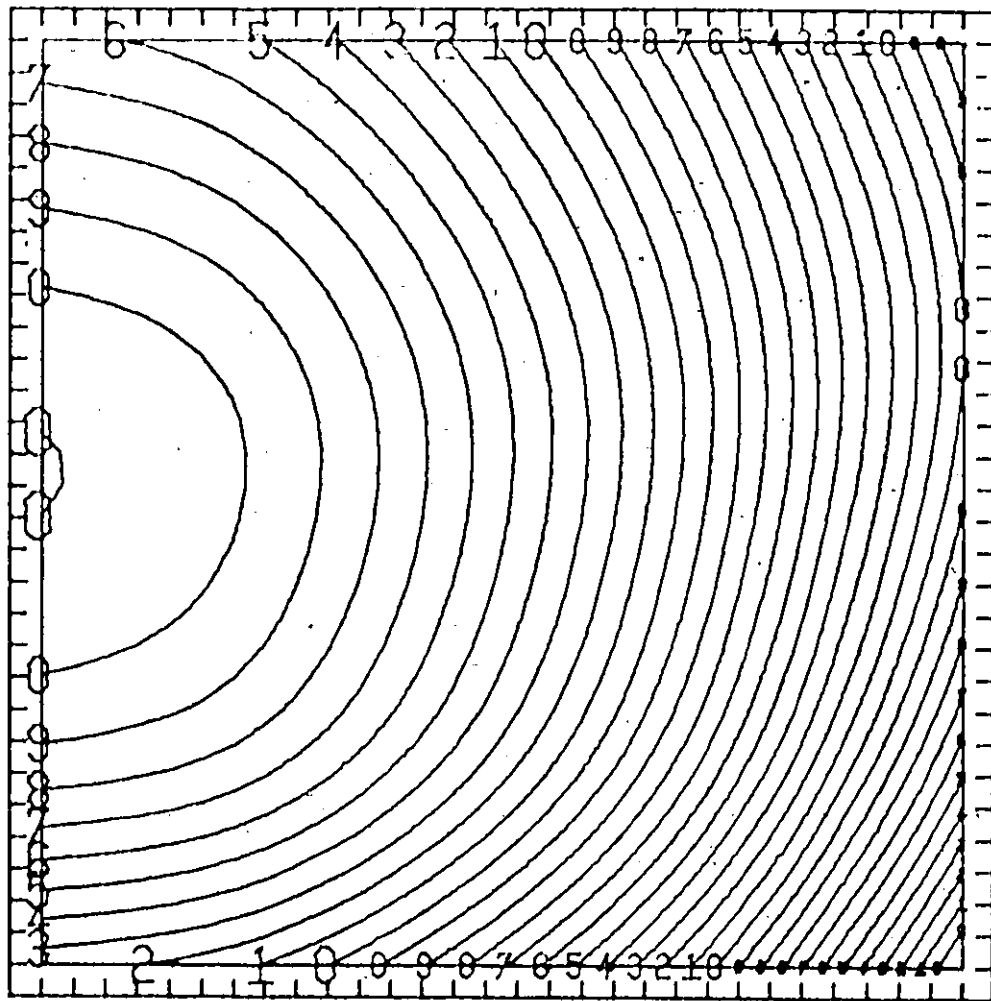
Figure 32. Equipotential Contours on Section IX





Min. 0.730  
Max. 1.030  
Step 0.01  
Section Size (0.300 x 0.300)

Figure 33. Equipotential Contours on Section X



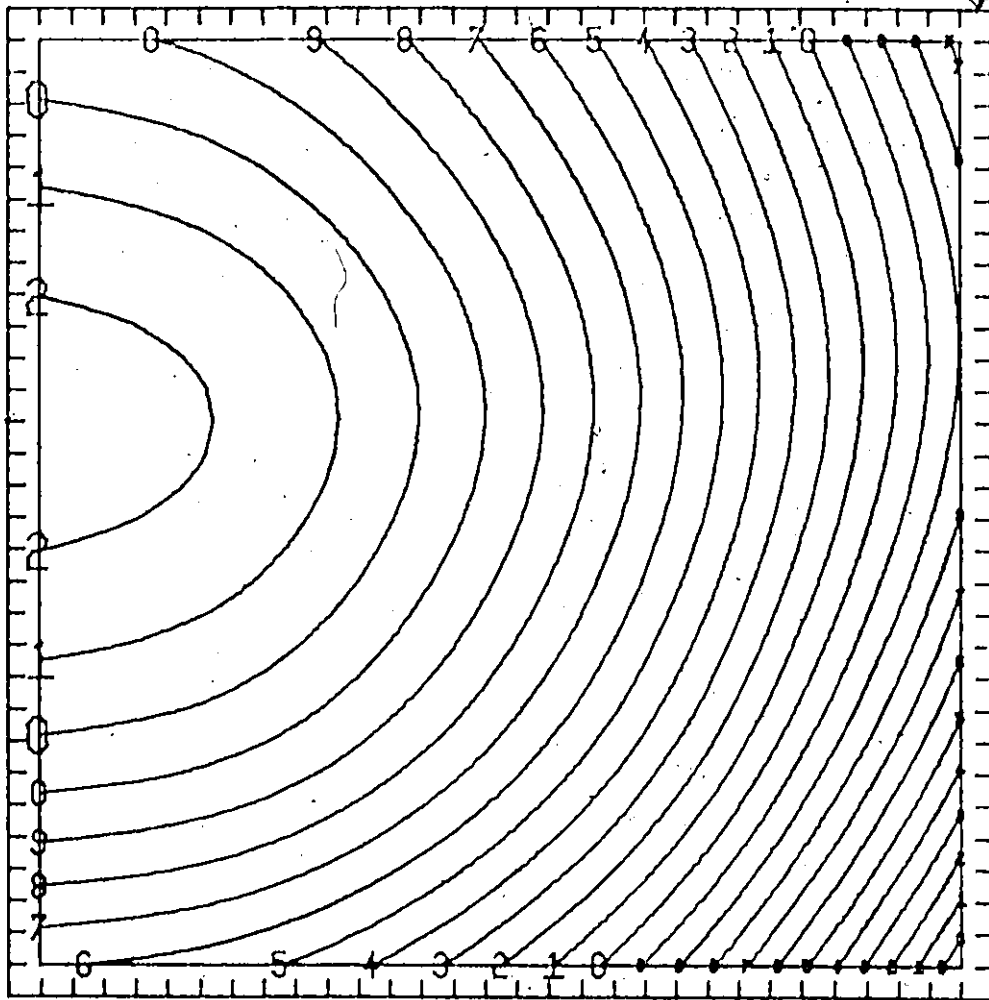
Min. 1.135

Max. 1.465

Step 0.01

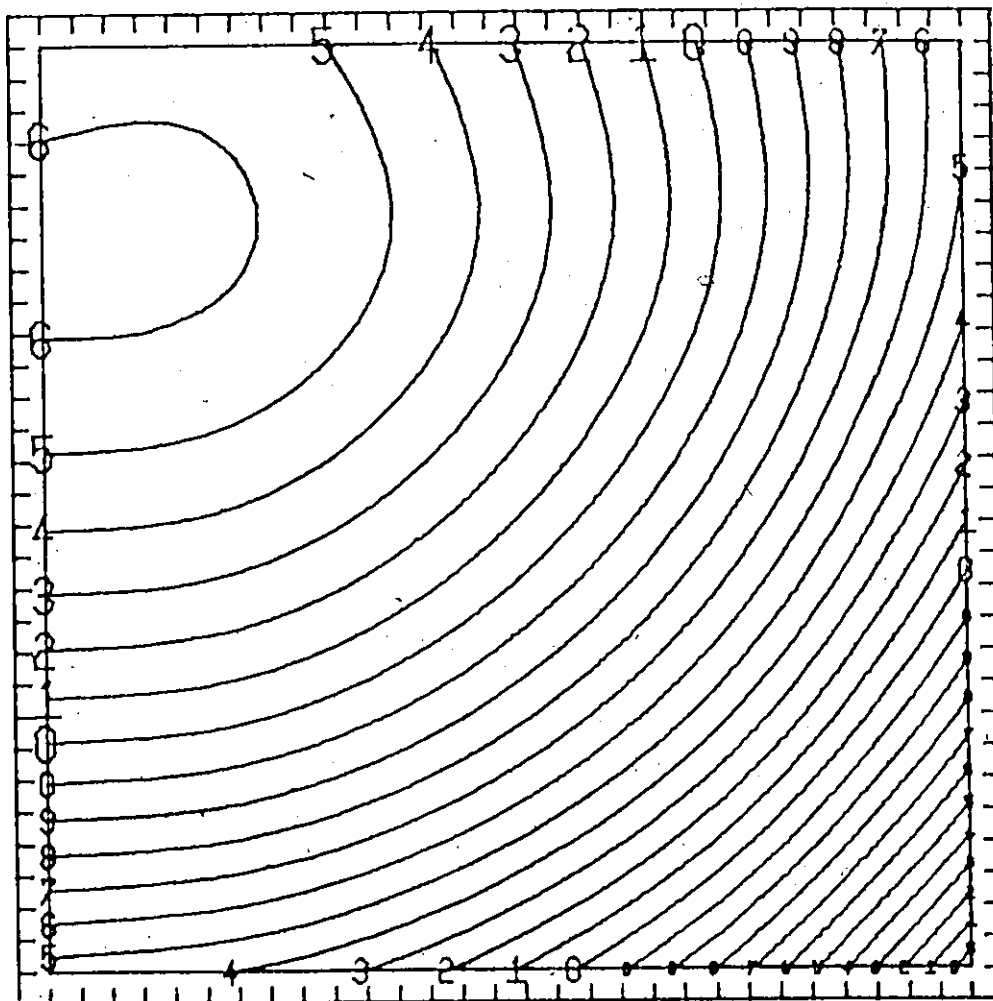
Section Size (0.267 x 0.267)

Figure 34. Equipotential Contours on Section XI



Min. 1.655  
Max. 2.015  
Step 0.015  
Section Size (0.233 x 0.233)

Figure 35. Equipotential Contours on Section XII



Min. 2.335

Max. 2.755

Step 0.015

Section Size (0.200 x 0.200)

Figure 36. Equipotential Contours on Section XIII

#### 4.4 Application 3. Reducing Bend with a Rectangular Inlet and an Annular Outlet

In this application the problem of a reducing bend of complicated geometry is considered. The bend is a compressor intake in a ground power unit. Due to certain space limitations and other design considerations the bend has non-streamlined shape. In an attempt to modify the present boundaries, to produce a more useful configuration, the potential solution is sought for uniform normal component of velocity at the inlet and the outlet planes. Figure (37) and Figure (38) show an isometric configuration of the upper half of the bend, while Figure (39) shows the bend in three projections. The bend is symmetric about the bottom plane. This symmetry condition allows the flow region to be considered simply-connected. The flow region is divided radially, as shown in Figure (37), with the angle  $\theta$  measured in counter-clockwise direction. The sections are labelled with Roman numbers as shown in Figure (37). The area ratio of the inlet to the outlet is 5:1. The normal velocity at the inlet is assumed to be 2.0, and at the outlet 10.0. Figure (40) shows the potential values at the nodal points on the inlet plane, and Figure (41) shows the corresponding values at the exit. Figures (42) through (54) show the potential values on the thirteen sections of the discretized region. The discretization of the region for this problem was carried out manually. The use of the six-tetrahedra scheme provided a versatile way for the selection of the nodal points on each section.

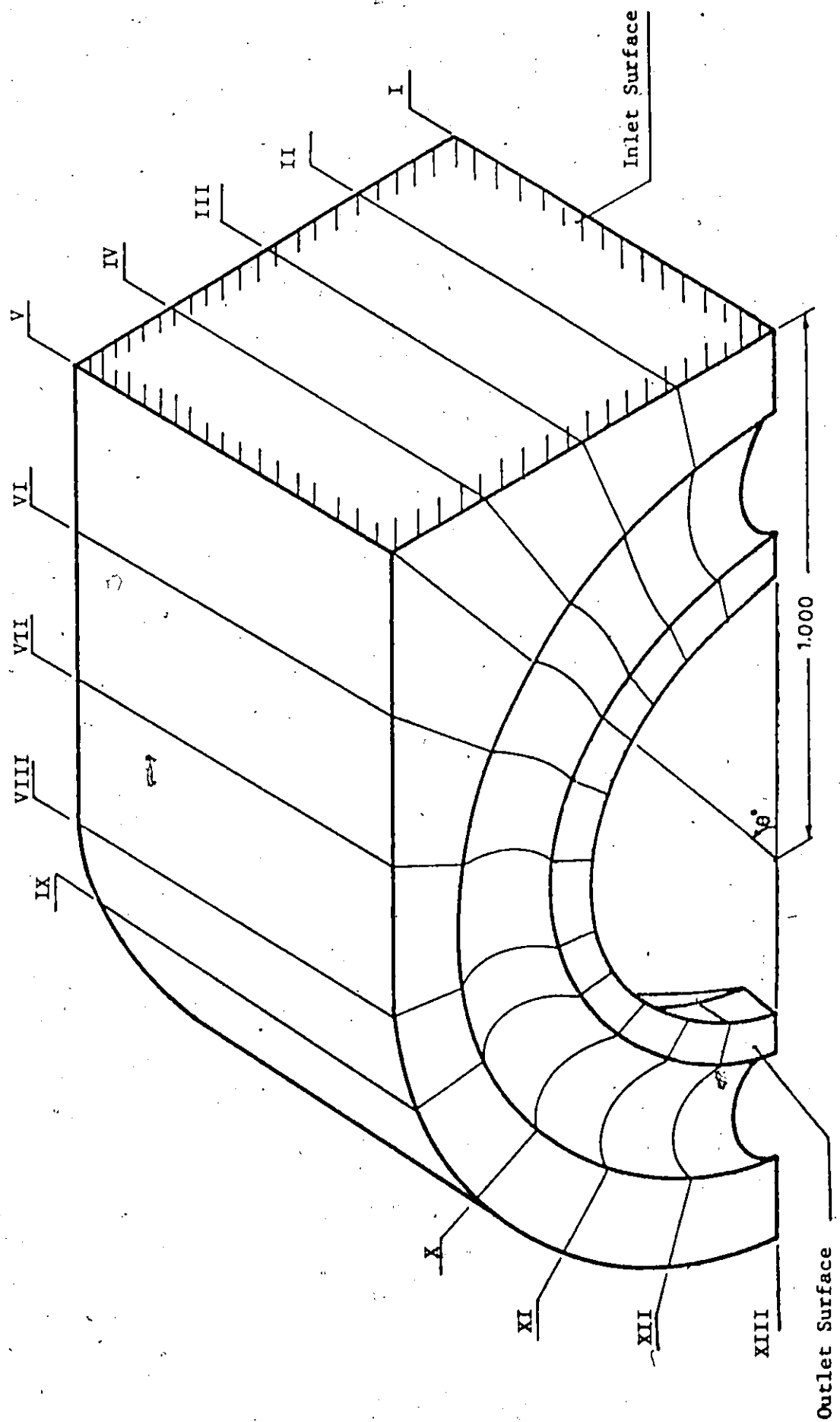


Figure 37. Isometric Configuration - Front View

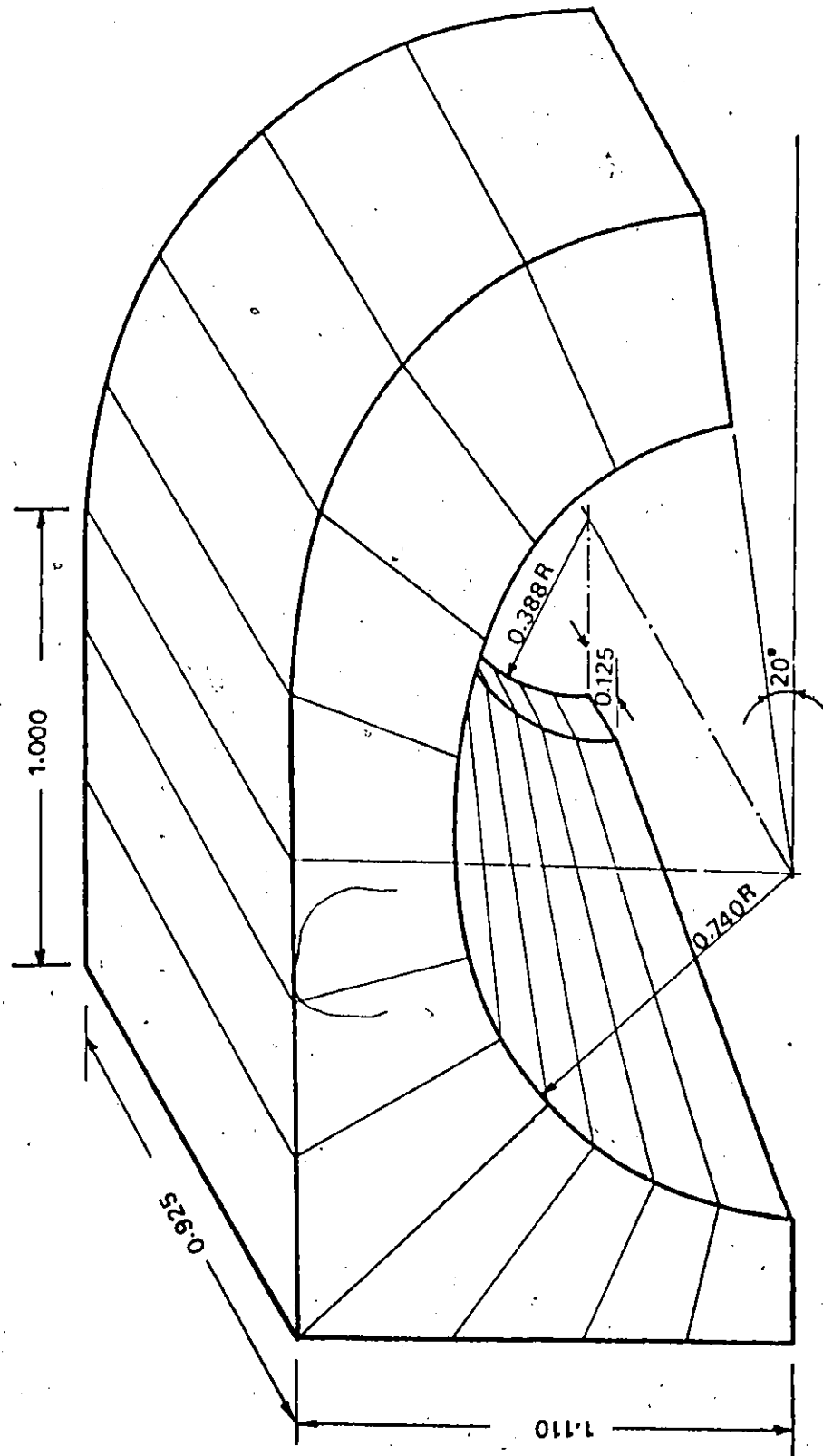


Figure 38. Isometric Configuration - Back View

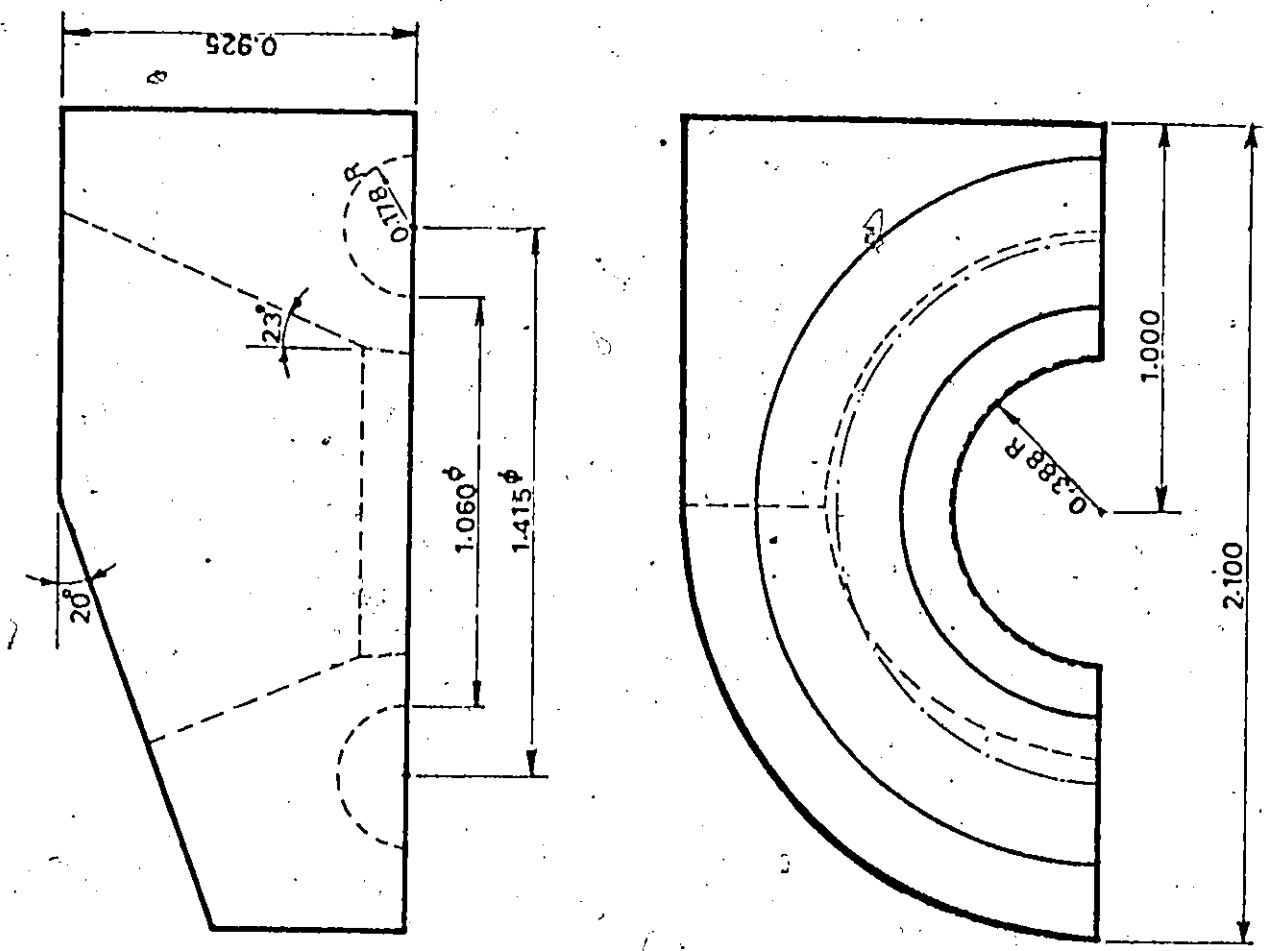


Figure 39. Reducing Bend Projections.



-1.582	-1.591	-1.615	-1.639	-1.655	-1.654
-1.562	-1.560	-1.624	-1.673	-1.713	-1.726
-1.613	-1.589	-1.653	-1.718	-1.799	-1.824
-1.676	-1.626	-1.687	-1.772	-1.880	-1.914
-1.693	-1.632	-1.701	-1.794	-1.909	-1.937

Figure 40. Potential Values on Inlet Surface

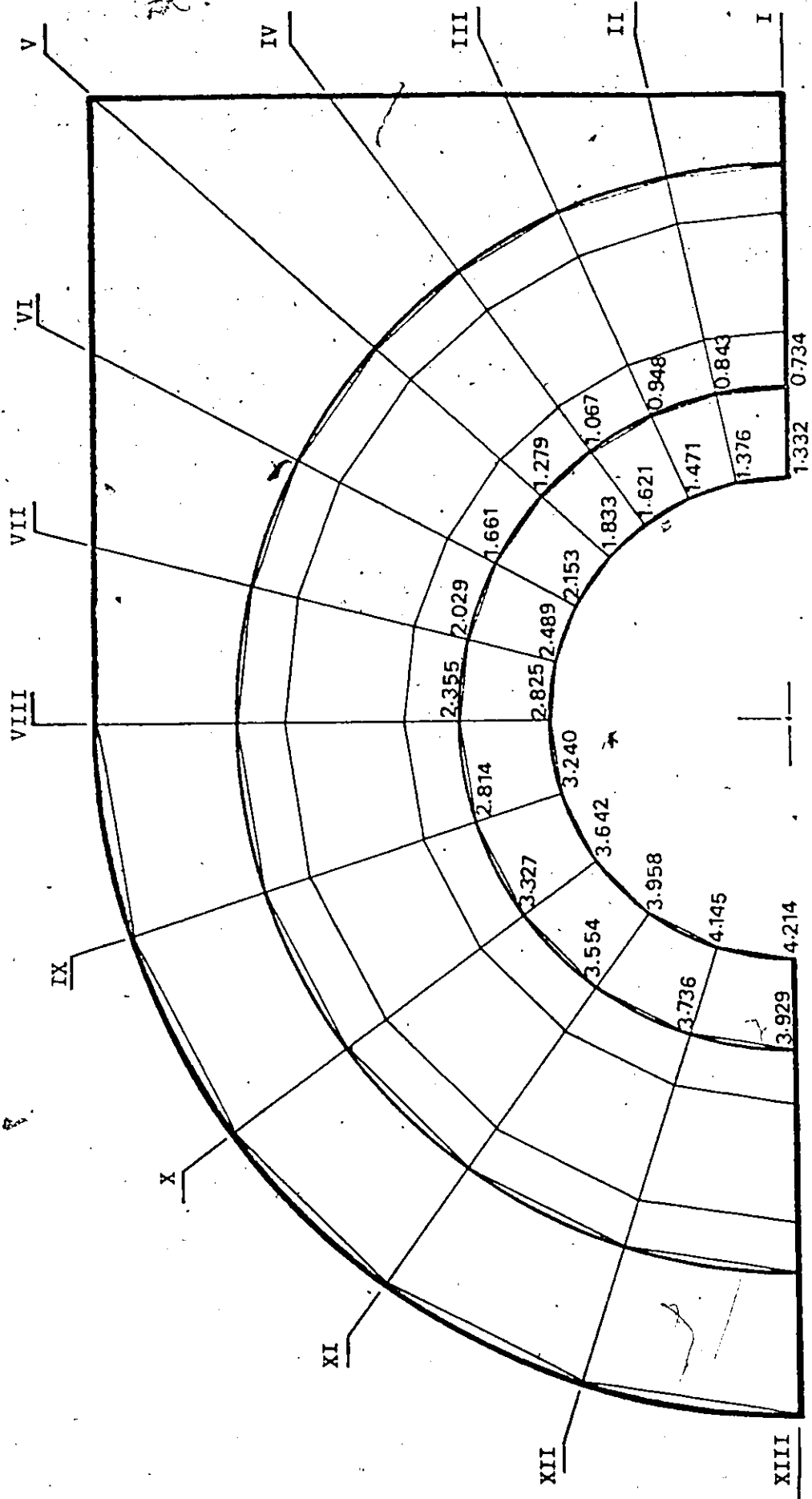


Figure 41. Potential Values On Exit Plane

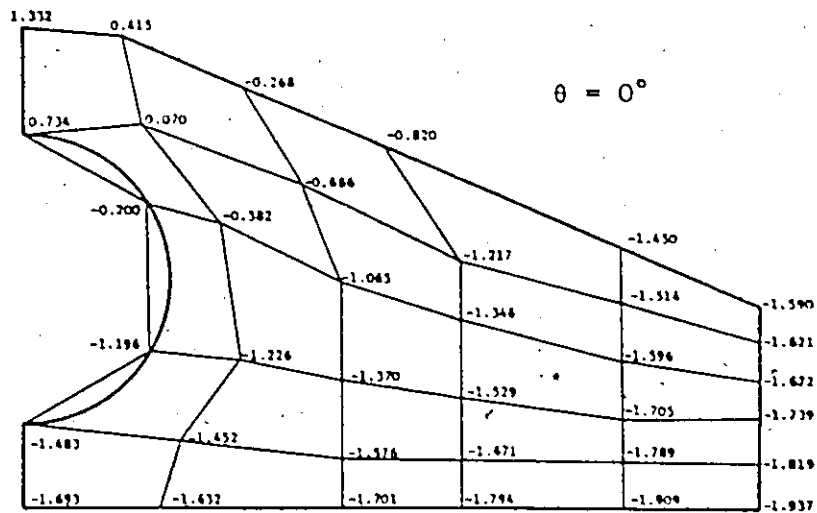


Figure 42. Potential Values on Section I.

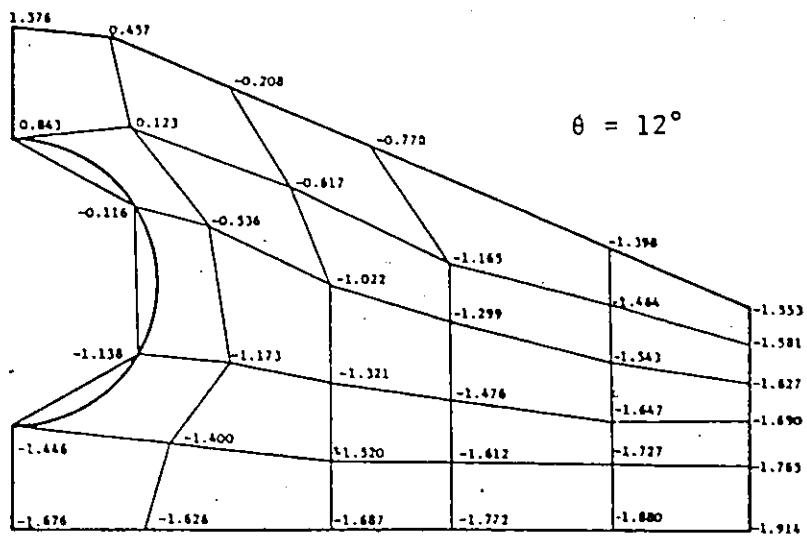


Figure 43. Potential Values on Section II

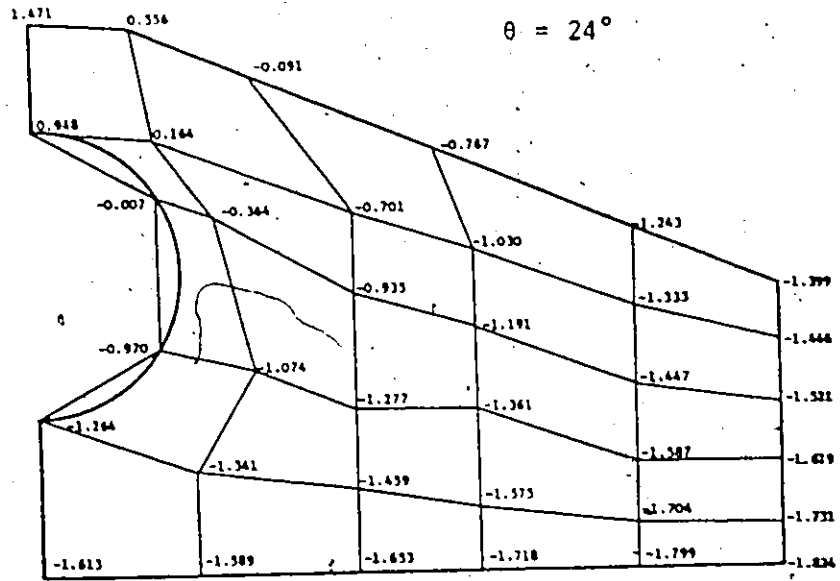


Figure 44. Potential Values on Section III

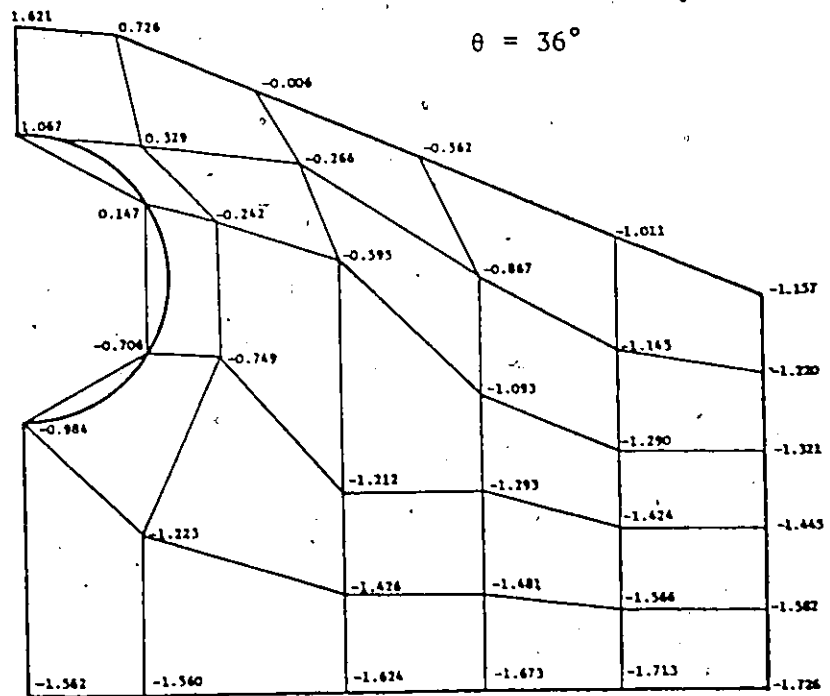


Figure 45. Potential Values on Section IV

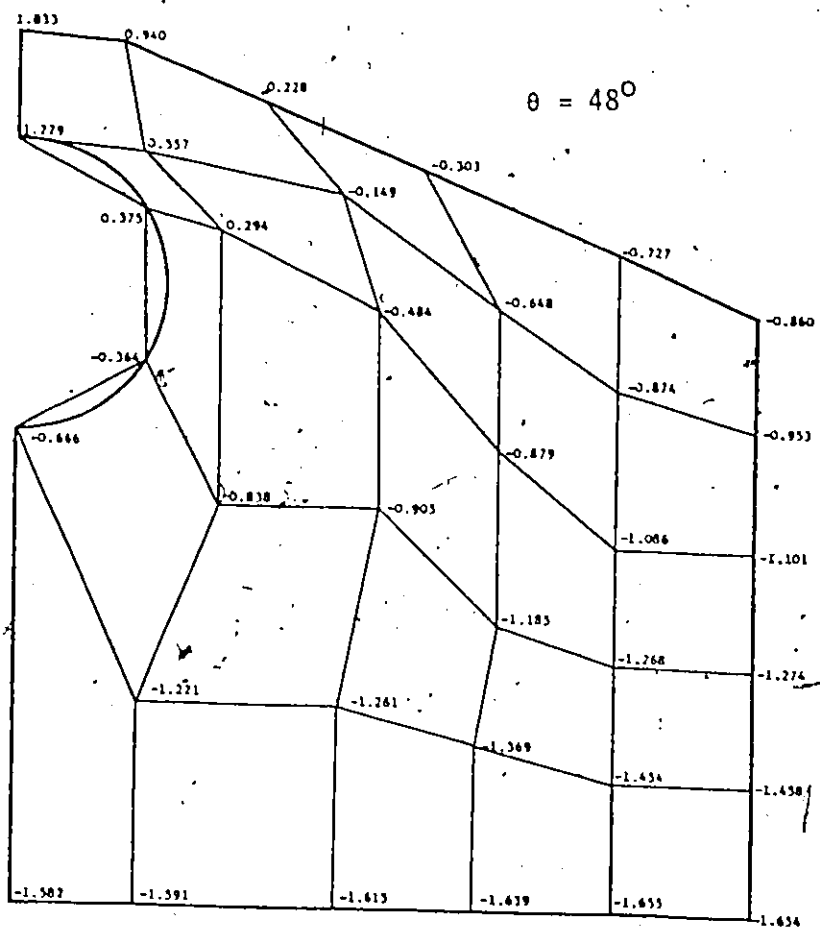


Figure 46. Potential Values on Section V

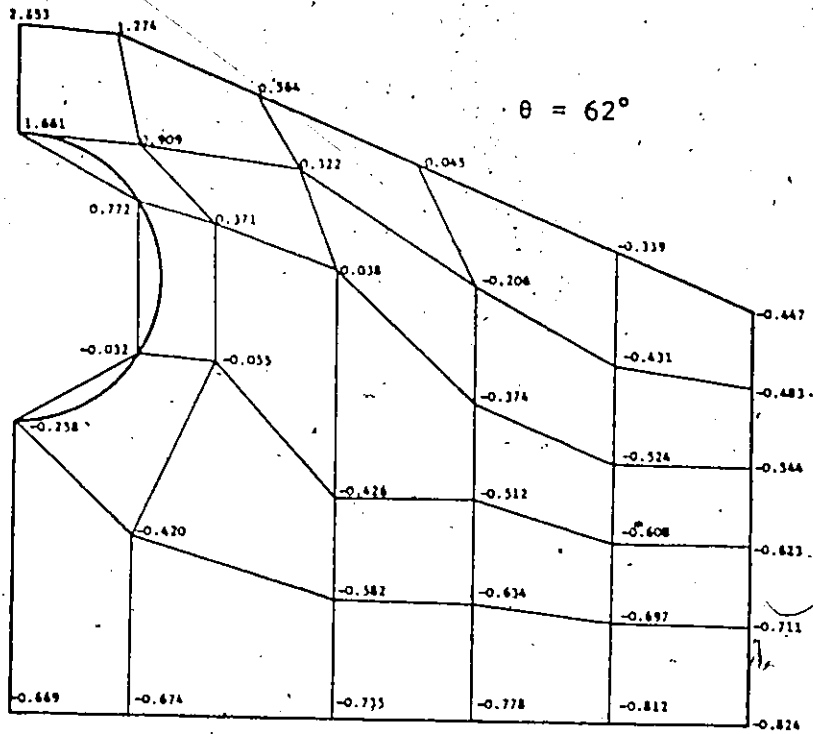


Figure 47. Potential Values on Section VI

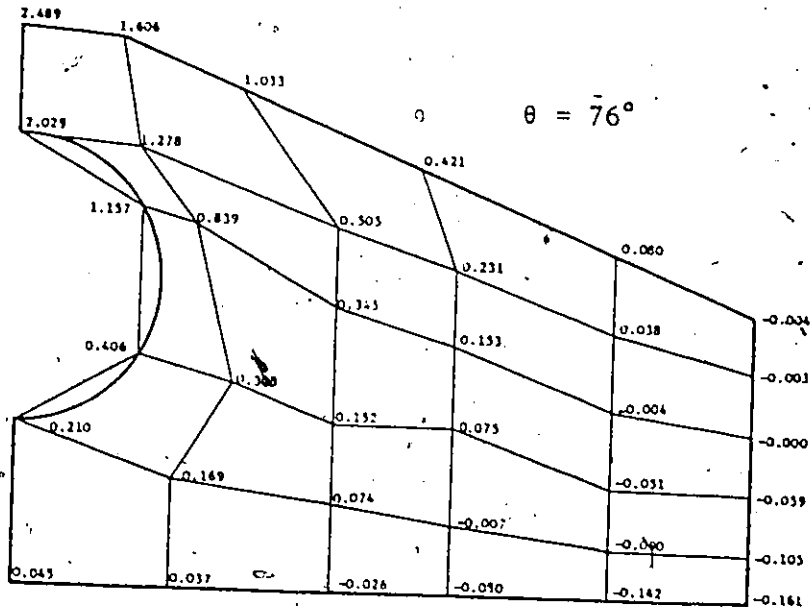


Figure 48. Potential values on Section VII

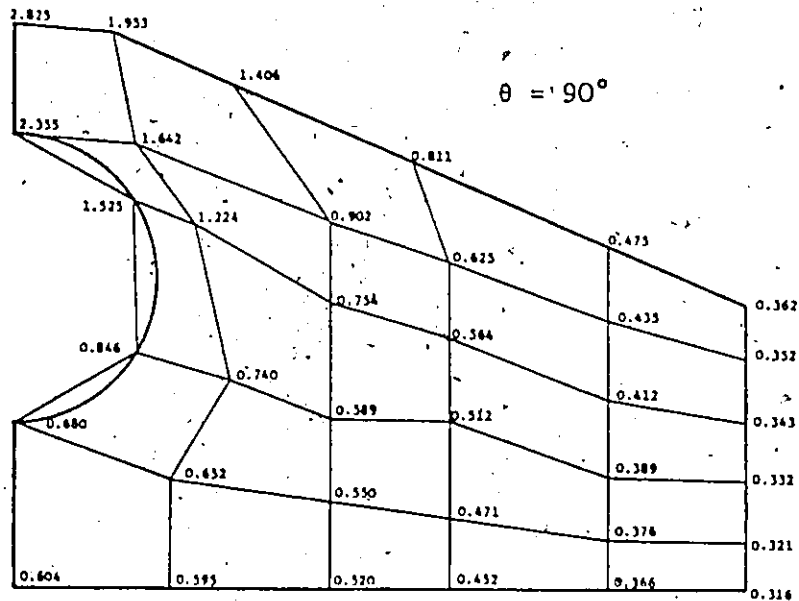


Figure 49. Potential Values on Section VIII

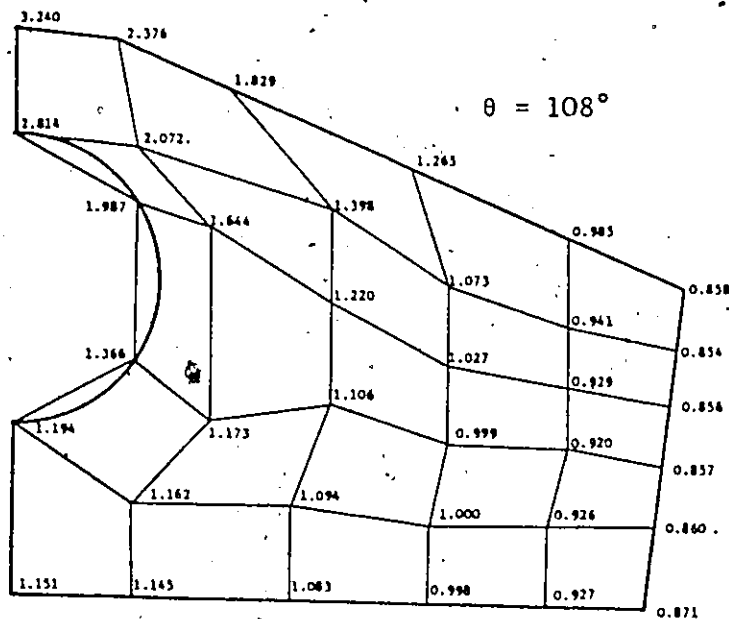


Figure 50. Potential Values on Section IX

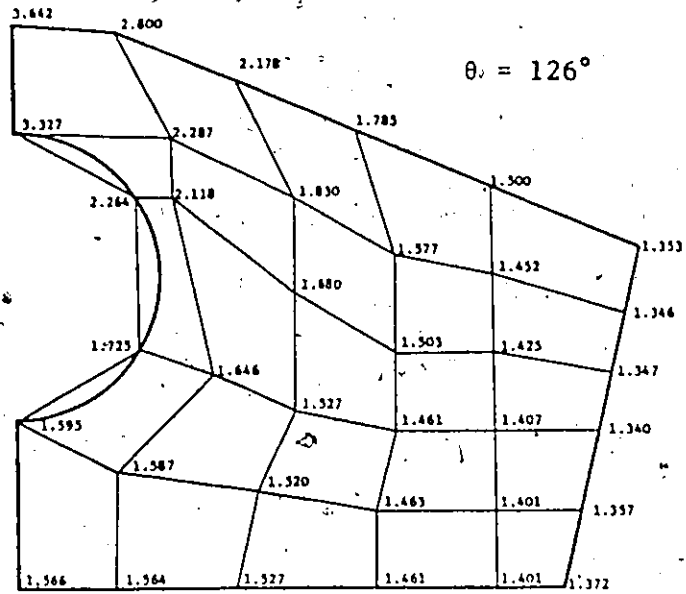


Figure 51. Potential Values on Section X.

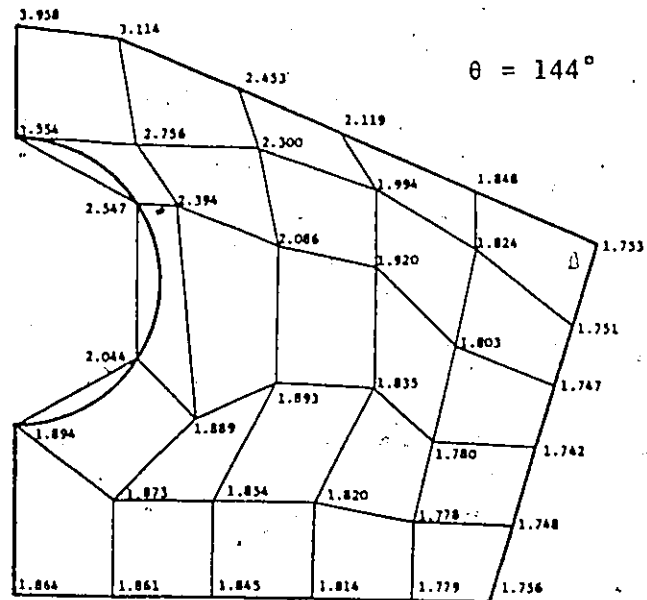


Figure 52. Potential Values on Section XI



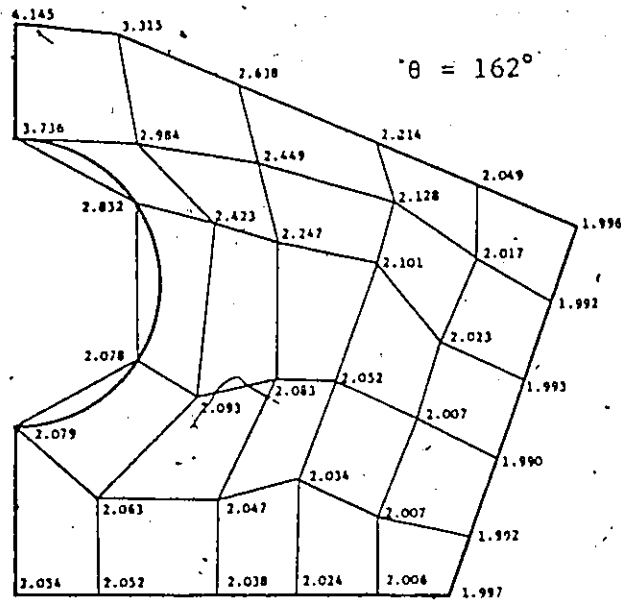


Fig.53. Potential Values on Section XII

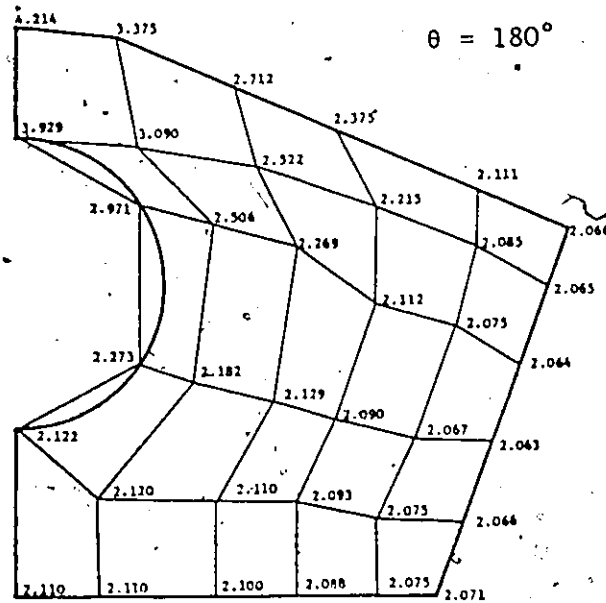


Figure 54. Potential Values on Section XIII

#### 4.5 Concluding Remarks

The study presented is an attempt to solve the three-dimensional Laplace field problem for complicated geometries, using the finite element method. The problem is difficult to handle with conventional methods. For example:

- a. In the finite difference method, it is difficult to implement the boundaries if they are irregular. Also the book keeping of the numerical analyses, already bulky for plane flow, becomes even more cumbersome for the three-dimensional case.
- b. The experimental alternative of electrolytic tank analogy is more expensive. Also imposing the boundary conditions (such as specified normal velocity component) is not practical. Furthermore the tank has to be built for the specific problem and may not be used for another problem.
- c. One can realize that there is no point in considering graphical methods for such a problem since a satisfactory depiction of the solution is difficult and progressive modification is inconceivable.

In the present study the simple tetrahedral finite element was used with a linear shape function. Two discretization schemes were followed and compared with the exact solution of a test problem:

- In the first scheme the region was divided into a number of composite eight cornered units, each of which is subdivided into five tetrahedra. The total number of tetrahedra in the region was 1500 joined at 468 nodal points. The discreti-

zation was subject to the restriction that the surfaces of the composite unit must be planar.

In the second scheme the composite eight cornered unit was divided into six tetrahedra. The total number of tetrahedra was 1800, joined at 468 nodal points. Thus, more elements were used for the same number of nodes, as given in the first scheme. The results obtained, using this scheme, were more accurate; the average error was approximately half the error encountered when using the first scheme. Moreover, the scheme provided a versatile discretization procedure, and therefore was used in the further applications considered in this thesis.

The finite element solution developed was applied to three problems:

1. Flow around 90° corner with a known two-dimensional exact solution. The results obtained from the finite element method were compared with the exact solution. The potential values calculated were in good agreement with the exact values (see Figures(16)through(21)).
2. A reducing bend of square cross section. The equi-potential contours on several sections in the flow region are plotted in Figure (24) through (36).
3. A reducing bend of complicated geometry. The bend has a rectangular inlet and an annular outlet. One would find difficulties in obtaining the solution of this problem using other

methods. The potential values were computed at various

sections in the flow region (see Figure 40) through (54)).

For each of the three applications, and as a corollary to the mean value theorem of a harmonic function, it is noticed that the potential does not have a maximum or a minimum in the interior of the flow domain.

A versatile, economical computer program was formulated for solving the problem, using less than 50 seconds (central processing) execution time for each one of the three problems. The program can be used to solve similar problems (same governing equation and boundary conditions) in related fields such as heat transfer, electrostatics and electromagnetic problems.

The accuracy attained was limited by the capacity of the computer storage available, which was in turn determined by the subroutine used for solving the system of linear algebraic equations. As a direct consequence of this limitation the velocity field could not be accurately determined.

Further extension of the study may consider more efficient computer storage techniques for the sparse, banded, symmetric matrix of the resulting system of equations. Thus, a more accurate solution for the potential as well as the velocity field can be obtained using more elements in the region. Another alternative would be to consider a second, or higher, order shape function for the tetrahedral element. Also, one may consider the use of curved surface elements. The extension of the method for solving the vorticity transport equations may also be investigated.

A detailed computer listing is documented in reference [19].

BIBLIOGRAPHY

1. Robertson, "Hydrodynamics in Theory and Application", Prentice-Hall, 1965.
2. O.C. Zienkiewicz and Y.K. Cheung, "Finite Elements in the solution of field problems", The Engineer (Sept.24, 1965).
3. Harold C. Martin, "The finite element analysis of fluid flows", AFFDL-TR. 68-150.
4. G. de Vries and D.H. Norrie, "The Application of The Finite Element Technique to Potential Flow Problems", Part 2, Mech. Rep. 8, Dept. of Mech. Eng., Univ. of Calgary, Alberta, Canada (July 1969).
5. G. de Vries and D.H. Norrie, "The Application of The Finite Element Technique to Potential Flow Problems", Part 3, Mech. Rep. 9, Dept. of Mech. Eng., Univ. of Calgary, Alberta, Canada (June 1973).
6. G. de Vries and D.H. Norrie, "The Application of The Finite Element Technique to Potential Flow Problems", J. Appl. Mech, 38, 798-802 (1971).
7. Norrie, de Vries, "The Finite Element Method", Academic Press, New York and London, 1973.
8. J.H. Argyris, G. Mareczek and D.W. Scharpf, "Two and three-dimensional flow using finite elements", Aero.J.Roy.Aoc., 73, 961-964 (1969).
9. L.J. Doctors, "An application of the finite element technique to boundary value problems of potential flow", I.J.Neum. Methods.E. Vol.2, 243-252 (1970).
10. Udo Meissner, "A mixed finite element model for use in potential flow problems", I.J.Neum. Methods in Eng. Vol.6, 467-473 (1973).
11. V. Cranstan and J.E. Devos, "Finite element solution of the three-dimensional flow problem and of Reynold's equation for incompressible and compressible fluids", Nuc. Eng. Design. 22, 225-232 (1972).
12. O.C. Zienkiewicz and C.J. Parekh, "Transient field problems: Two-dimensional and three-dimensional analysis by isoparametric finite elements", I.J.Neum. Methods in Eng. Vol.2, 61-71(1970).

Bibliography (Cont)

13. O.C. Zienkiewicz, A.K. Bahrani and P.L. Arlett, "Numerical solution of three-dimensional field problems", The Engineer (Oct.27, 1967).
14. G. de Vries and D.H. Norrie, "The Application of The Finite Element Technique to Potential Flow Problems", Part 1, Mech. Rep. 7, Dept. of Mech. Eng., Univ. of Calgary, Alberta, Canada (1969).
15. Kalipada Palit and Roger T. Fenner, "Finite Element Analysis of Two-dimensional slow non-Newtonian flows", AIChE. Journal (Vo.18, No.6) November 1972, pp.1163-1170.
16. O.C. Zienkiewicz, "The Finite Element Method in Engineering Science", McGraw-Hill, London, 1971.
17. S. Eskinazi, "Vector Mechanics of Fluids and Magnetofluids", Academic Press, New York and London, 1967.
18. J.W. Dettman, "Mathematical Methods in Physics and Engineering", McGraw-Hill, New York, 1962.
19. S. El-Shammaa, M. A. Dokainish and J. H. T. Wade, "The Application of the Finite Element Method to Three-Dimensional Potential Flow", Mech. Rep. ME/75/FM/R13. Dept. of Mech. Eng., McMaster Univ., Ontario, Canada. Oct. 1975.

APPENDIX I\*

REFORMATION OF A BOUNDARY-VALUE PROBLEM IN TERMS OF  
THE CALCULUS OF VARIATIONS

Since the Finite Element Technique is a method of solution based on the calculus of variations, the following boundary-value problem, which is frequently encountered in the solution of field problems, is of particular interest. Obtain the solution surface

$$\phi = \phi(x, y, z)$$

which satisfies

$$\frac{\partial}{\partial x} \left( X \frac{\partial \phi}{\partial x} \right) + \frac{\partial}{\partial y} \left( Y \frac{\partial \phi}{\partial y} \right) + \frac{\partial}{\partial z} \left( Z \frac{\partial \phi}{\partial z} \right) + G = 0 \text{ in } D,$$

subject to either

(1)  $\phi$  is specified on  $S$ ,

or

(2)  $X \frac{\partial \phi}{\partial x} n_x + Y \frac{\partial \phi}{\partial y} n_y + Z \frac{\partial \phi}{\partial z} n_z + q + a\phi = 0$  on  $S$ ,

where  $X$ ,  $Y$ ,  $Z$ ,  $G$ ,  $q$  and  $a$  are functions of  $x$ ,  $y$  and  $z$ , and  $n_x$ ,  $n_y$  and  $n_z$  are the three components of the unit outward normal,  $\hat{n}$ , to  $S$ .  $S$  is the surface enclosing the three-dimensional region  $D$ . It is assumed that this bounding surface  $S$  is sufficiently regular so that the divergence theorem applies.

This boundary value problem can be transformed to the following

=====

\* This appendix is taken from Reference [4].

problem in the calculus of variations (see Reference [18]).

Among all functions  $v$  which are continuous and have piecewise continuous first derivatives in  $D$ , (i.e.,  $D$  can be subdivided into a finite number of subregions in each of which the first partial derivatives of  $v$  are continuous and have limits as the boundary is approached from the interior), minimize the functional

$$X(v) = \iiint_D [\frac{1}{2} \{Xv_x^2 + Yv_y^2 + Zv_z^2\} - Gv] dx dy dz + \iint_S [qv + \frac{1}{2} av^2] dS \quad (I-1)$$

where  $v_x = \frac{\partial v}{\partial x}$  etc., and  $dS$  is an element of surface area. The minimizing function will be a solution to the boundary-value problem stated above.

Only the necessary conditions for the solution of this variational problem will be derived. In order to obtain these necessary conditions, it is assumed that there exists a solution  $\phi$ , with continuous second order derivatives in  $D$ , which minimizes the functional (I-1).

Then

$$X(\phi + \epsilon h) - X(\phi) \geq 0 \quad (I-2)$$

where  $\epsilon$  is an arbitrary constant and  $h$  is an arbitrary function from the class of admissible functions, i.e. is continuous and has piecewise continuous first derivatives in  $D$ . Using relation (I-1), the inequality (I-2) reduces to



$$\epsilon^2 \left[ \iiint_D \frac{1}{2} (Xh_x^2 + Yh_y^2 + Zh_z^2) dx dy dz + \iint_S \frac{1}{2} ah^2 dS \right] +$$

$$\epsilon \left[ \iiint_D \{Xh_x \phi_x + Yh_y \phi_y + Zh_z \phi_z - Gh\} dx dy dz + \iint_S \{qh + ah\phi\} dS \right] \geq 0$$

..... (I-3)

The result (I-3) must be true for arbitrary  $\epsilon$ . Therefore

$$\iiint_D \{Xh_x \phi_x + Yh_y \phi_y + Zh_z \phi_z - Gh\} dx dy dz + \iint_S \{qh + ah\phi\} dS = 0$$

for arbitrary  $h$ . Otherwise given an  $h$ , an  $\epsilon$  could be chosen sufficiently small and of the proper sign, so that

$$\epsilon^2 \left[ \iiint_D \frac{1}{2} (Xh_x^2 + Yh_y^2 + Zh_z^2) dx dy dz + \iint_S \frac{1}{2} ah^2 dS \right] +$$

$$\epsilon \left[ \iiint_D \{Xh_x \phi_x + Yh_y \phi_y + Zh_z \phi_z - Gh\} dx dy dz + \iint_S \{qh + ah\phi\} dS \right] < 0$$

contradicting the inequality (I-3), see (Reference [18]).

Consequently

$$\iiint_D \{Xh_x \phi_x + Yh_y \phi_y + Zh_z \phi_z - Gh\} dx dy dz + \iint_S h\{q + a\phi\} dS = 0 \quad (1-4)$$

and noting that

$$Xh_x\phi_x = (hX\phi_x)_x - h(X\phi_x)_x,$$

with similar results for  $Yh_y\phi_y$ , and  $Zh_z\phi_z$ , equation (1-4) reduces to

$$\begin{aligned} & \iiint_D -h[(X\phi_x)_x + (Y\phi_y)_y + (Z\phi_z)_z + G] dx dy dz + \\ & \iiint_D [(hX\phi_x)_x + (hY\phi_y)_y + (hZ\phi_z)_z] dx dy dz + \iint_S h[q + \alpha\phi] dS = 0, \quad (I-5) \end{aligned}$$

Since  $\phi$  has continuous second order derivatives in  $D$ , and  $h$  has piecewise continuous first derivatives in  $D$ , then Green's identity may be applied to the second term in equation (I-5), i.e.

$$\begin{aligned} \iiint_D [(hX\phi_x)_x + (hY\phi_y)_y + (hZ\phi_z)_z] dx dy dz &= \iint_S h[X\phi_x n_x + Y\phi_y n_y + Z\phi_z n_z] dS \\ &\dots\dots\dots (I-6) \end{aligned}$$

Substitution of relation (I-6) into equation (I-5) results in

$$\begin{aligned} & \iiint_D -h[(X\phi_x)_x + (Y\phi_y)_y + (Z\phi_z)_z + G] dx dy dz + \\ & \iint_S h[X\phi_x n_x + Y\phi_y n_y + Z\phi_z n_z + q + \alpha\phi] dS = 0 \quad (I-7) \end{aligned}$$

Since  $h$  is arbitrary, it can be chosen to be zero on the bounding surface  $S$  but otherwise arbitrary in  $D$ . Hence the surface integral in (I-7) vanishes, and consequently

$$\iiint_D -h[(X\phi_x)_x + (Y\phi_y)_y + (Z\phi_z)_z + G] dx dy dz = 0$$

which implies that

$$(X\phi_x)_x + (Y\phi_y)_y + (Z\phi_z)_z + G = 0$$

in the interior of  $D$ . However, this in turn implies that the integral over the domain  $D$  in equation (I-7) vanishes, and hence that

$$\iint_S h[X\phi_x n_x + Y\phi_y n_y + Z\phi_z n_z + q + a\phi] dS = 0 \quad (I.8)$$

To satisfy equation (I-8), the following choices of  $h$  are of particular interest:

(a)  $h = 0$  on  $S$  but otherwise arbitrary and non-zero in  $D$ .

This corresponds to the case where the boundary condition is prescribed as  $\phi = g(x,y,z)$  on  $S$ .

(b)  $h =$  arbitrary and non-zero on  $S$  and in  $D$ . This forces

$X\phi_x n_x + Y\phi_y n_y + Z\phi_z n_z + q + a\phi = 0$  on  $S$ , which is the natural boundary condition associated with the functional

(1).

(c) Conditions (a) or (b) on a separate or connected boundaries  $S_1, S_2, \dots, S_n$  in any combination where  $S = S_1 + S_2 + \dots + S_n$ .

Therefore, if  $\phi$  is not prescribed on  $S$ , then the solution to the variational problem is the solution of

$$(X\phi_x)_x + (Y\phi_y)_y + (Z\phi_z)_z + G = 0 \text{ in } D,$$

subject to

$$X\phi_x n_x + Y\phi_y n_y + Z\phi_z n_z + q + a\phi = 0 \text{ on } S,$$

which is indeed the same boundary-value problem, which was stated previously in this appendix. If, on the other hand,  $\phi$  is prescribed on part of the boundary  $S_D$  as

$$\phi = g \text{ on } S_D,$$

and furthermore, on the remaining part of  $S_C$

$$X\phi_x n_x + Y\phi_y n_y + Z\phi_z n_z + q + a\phi = 0 \text{ on } S_C,$$

where

$$S = S_D + S_C$$

and, as before,  $\phi$  satisfies

$$\frac{\partial}{\partial x} \left( X \frac{\partial \phi}{\partial x} \right) + \frac{\partial}{\partial y} \left( Y \frac{\partial \phi}{\partial y} \right) + \frac{\partial}{\partial z} \left( Z \frac{\partial \phi}{\partial z} \right) + G = 0 \text{ in } D,$$

then it is clear from the discussion of equation (I-8) that the function  $\phi$  which minimizes the functional (I-1) is indeed the solution to the problem posed above.

It is noted that for the special case when  $X = Y = Z = 1$ , there obtains

$$\nabla^2 \phi + G = Q \text{ in } D,$$

with

$$\phi = g \text{ on } S_D$$

where  $g$  is the prescribed value of  $\phi$  on  $S_D$ , and

$$\frac{d\phi}{dn} + q + a\phi = 0 \text{ on } S_C$$

where

$$S = S_D + S_C$$

which is a boundary-value problem of a type frequently encountered in potential problems.

## APPENDIX II

## FLOW CHART OF THE COMPUTER PROGRAM OF THE FINITE ELEMENT SOLUTION

